JOURNAL OF THE AERONAUTICAL SCIENCES

VOLUME 7 MAY, 1940 NUMBER 7

Reversible Pitch Propellers as Applied to Water Handling of Multi-Engine Flying Boats

C. W. CHILLSON

Curtiss Propeller Division, Curtiss-Wright Corporation

ABSTRACT

Brief mention is made of several reversible pitch propeller applications. Some of the problems encountered in the water handling of multi-engine flying boats are discussed. The use of reversible propellers is proposed as an aid to maneuvering, and tests are cited in which it was found possible to turn a four-engine flying boat in as small a radius as desired and to stop or to back against the wind. Adaptation of a conventional electrically controllable propeller for reverse pitch operation is illustrated schematically and described briefly. While engine cooling imposes limitations to protracted high power operation in reverse pitch, experience to date indicates that these limitations need not be exceeded in normal operation. Engine overspeeding while the blades are going through zero angle is prevented by engine and propeller inertia at moderate throttle settings and with available rates of pitch change. Limitations imposed by propeller blade and retention stresses and the effect of forward tilt thereon are discussed. No ill effects of negative thrust are to be expected on either engines or engine mounts.

INTRODUCTION

MANY of the early inventors of propeller pitch controlling mechanisms considered that ability to reverse pitch to obtain negative thrust was of primary importance, with a result that most early controllable propellers were referred to as "reversible propellers." This appellation persisted for some time after the much greater importance of having a selection of positive blade angles became generally recognized. The use of negative blade angles has been proposed to reduce airplane landing speeds and landing runs. However, although numerous experiments have been conducted, the hazards and difficulties involved have prevented general application. Reverse pitch has also been proposed as an aid in the maneuvering of lighter-than-air craft near the ground.

More recently with the advent of dive bombing and relatively aerodynamically clean aircraft, the use of modern controllable propellers to limit the terminal velocity of diving aircraft by the use of a negative pitch setting has been proposed and tested. At high air speeds such as are encountered in diving, pitch reversal must, however, be almost instantaneous or the wind-milling speed of the propeller will become excessive while the blades are passing through the lower positive angles. The use of reversible propellers in other flight maneuvers has also been suggested. No data are available to indicate all of the practical difficulties which might be encountered if the propeller of a single engine airplane were reversed in normal flight. It would appear that they might prove to be considerable.

The application indicated in the title of this article was proposed and successfully tested during the past year on a large four-engine flying boat with the assistance and cooperation of the Bureau of Aeronautics, Navy Department.

WATER HANDLING

In the water handling of flying boats with conventional propellers, as in the case of land planes, little or no control is available from aerodynamic surfaces during low speed taxiing. In addition to wind, flying boats must at times maneuver in adverse currents without assistance from brakes or other source of negative thrust or directional control from the supporting element. Water rudders and sea anchors are sometimes employed but certainly do not represent the ultimately desirable means of control. Without reversible propellers, the only other source of directional control is a variation in the forward propeller thrust between the various engines. This forward thrust also causes varying rates of forward motion. In most situations, a skilled pilot is able to take advantage of the wind conditions and to allow for currents and tides,

Presented at the Power Plants Session, Eighth Annual Meeting, I.Ae.S., New York, January 24, 1940.

although cross or tail winds and adverse currents may, in restricted areas, make the desired approach or other maneuver hazardous or impossible. Also, with no wind the problem of water handling is one requiring the most skillful manipulation. Although normally only outboard propellers are used, the thrust of these even at idling speeds, added to the momentum of the ship remaining from the taxiing run, make it necessary to reduce speed to a point where steerage-way may be lost some distance from the buoy to prevent overshooting the mark. If the buoy is approached at too great a speed, it does not permit sufficient opportunity to make fast a line, and a reapproach must be made. If, in reducing the possibility of overshooting, speed is reduced some distance from the buoy, a small error in judgment or slight current shift may result in the buoy being passed out of reach.

Care must also be exercised in areas restricted by docks, breakwaters, or by other moored craft to allow sufficient room for a turn and reapproach. With no wind it is not possible to turn a flying boat in the water in much less than a radius of approximately one wing span. On some flying boats, the minimum turning radius in still air may be several times the wing span. Fig. 1 illustrates a typical down-wind approach using conventional propellers to a buoy moored close to land. Arrows extending from the centerlines of the engines indicate the direction of propeller thrust on the airplane. The length of the arrows is intended to give a rough quantitative comparison of the magnitude of these thrusts. Three approaches are illustrated, the correct one being shown by the middle line. The ship drifts down wind with a very slight propeller thrust until the nose of the ship comes to the buoy. The results of underestimating the forward motion of the ship and of opening the throttles at the last minute in order to reach the buoy is shown by the upper path. The buoy is passed with too great forward speed to permit securing a line. The lower path is the result of overshooting. The buoy passes under the ship or drags along the side, and a reapproach is necessary.

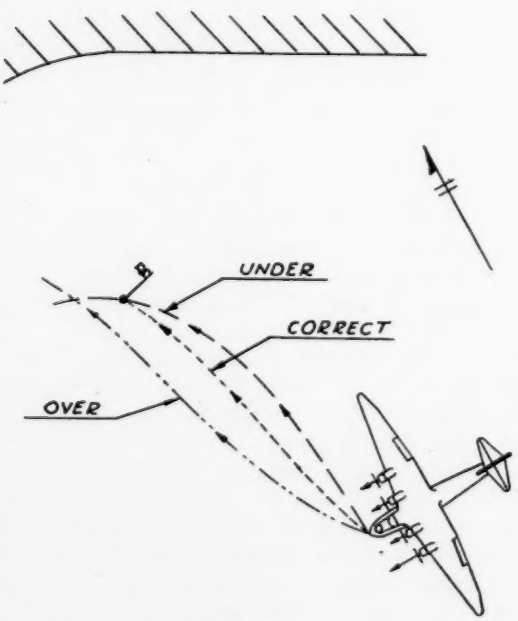

FIG. 1.

WATER HANDLING WITH REVERSIBLE PROPELLERS

The addition of controllable negative thrust to the normally available thrust in the forward direction makes it possible to turn on as small a radius as is desired and to stop or to back, maintaining the orientation of the boat in the water in almost any combination of wind and current. Controllable negative thrust also makes it possible to approach close to a buoy at a speed where relatively good control can be maintained, and to stop in a short distance. Any combination of negative and positive thrusts can be applied by manipulation of the throttles. As soon as the ship is well in the water, the inboard propellers may be reversed, making negative thrust available by use of the throttles at any time it is desired during the taxiing run. Obstacles in the water not visible at a distance may be avoided by a sudden application of this force. It is also possible to maintain steerage-way at very low speeds. This is of particular importance in taxiing through broken ice. It appears at present that it is more desirable to reverse the inboard than the outboard propellers inasmuch as water operation is normally accomplished with the outboards. Tests also indicate that less spray is caused by this arrangement. Figs. 2 and 3 show two methods of approaching a buoy under circumstances similar to those shown in Fig. 1. Fig. 2 shows a direct down-wind approach where a negative thrust is applied just before reaching the buoy. Fig. 3 is probably a preferable method of approach under the conditions shown. The boat is taxied until the hull is opposite the buoy, and turned sharply into the wind by applying power to one outboard and one inboard engine. This assists the ship to weathercock into the wind and places the nose close to the buoy.

The maneuvers illustrated were duplicated recently on a 25 ton four-engine flying boat without difficulty by pilots with no previous experience in the use of reversible propellers. With very little practice, it was possible to make several complete turns keeping the buoy between the wing tip float and the hull in moderate winds and seas. The importance of being able to make extremely short turns was demonstrated. In the event of an error on the first attempt, it was not found necessary to make a wide circle to reapproach.

PROPELLER MECHANISM

A recent development of the conventional electric propeller permits the pitch to be reversed in a matter of

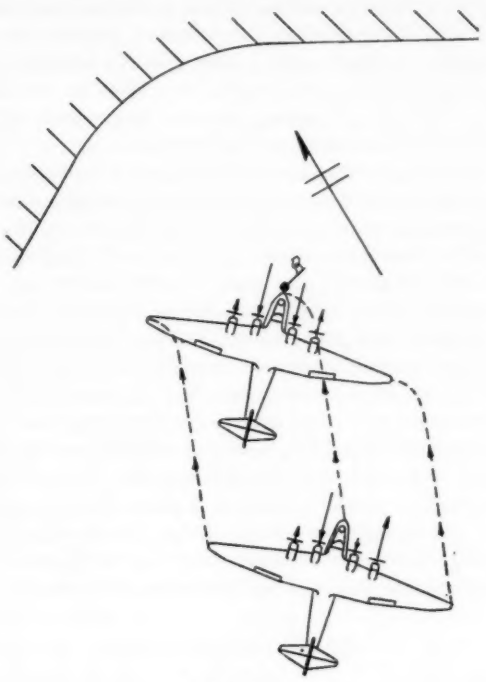

FIG. 2.

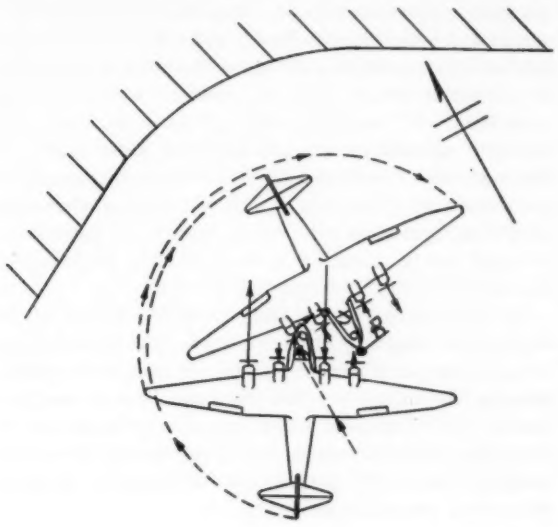

FIG. 3.

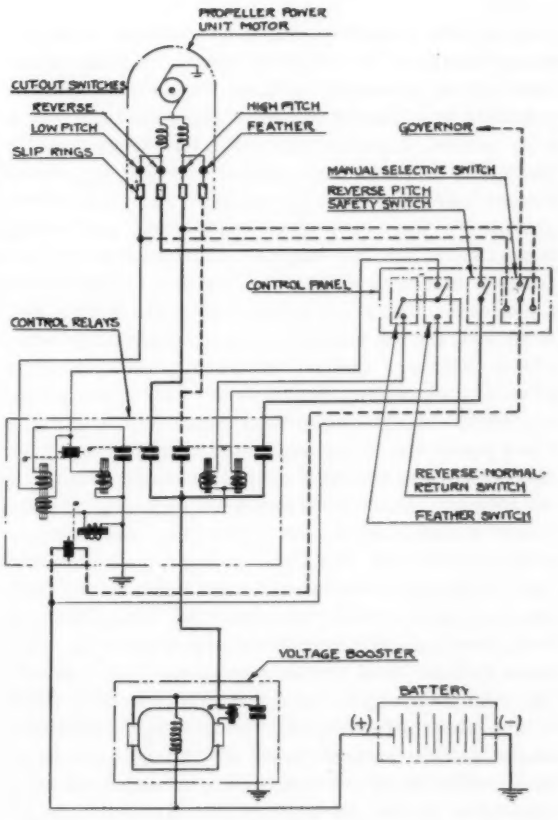

FIG. 4.

seconds (Fig. 4). In this type of propeller a series-wound double-field direct-current motor is mounted on a gear reduction unit on the front of the hub. A bevel gear on the back of this so-called "power unit" engages with a bevel gear on the shank end of each blade. A set of cams in the back of the power unit actuate cut-out switches to selectively open the appropriate circuit to halt pitch change at preselected limits. To the normally used low, high, and feather angle cut-out switches, a fourth was added to stop pitch change when the desired negative angle is reached. Normal propeller operation between high and low pitch utilizes the plane's battery voltage directly. When, some time ago, it appeared advisable to speed up the normal rate of pitch change for emergency feathering, an auxiliary voltage booster was developed which provides approximately four times battery voltage. This increases the rate of pitch change approximately four-fold and has become more or less standard equipment on multi-engine aircraft using electric propellers. Advantage was taken of the presence of this unit to also provide an accelerated pitch change during reversal and return to low pitch. The action during reversal is much the same as during fast feathering. Switches operated by the pilot act to simultaneously start the booster and pitch change motor. When the predetermined negative angle is reached, a cut-out switch in the hub opens, stopping both the pitch change motor and the booster. When it is desired to return to flight pitch, operation of a switch by the pilot starts the voltage booster and causes the pitch change motor to run in the opposite direction. A system of relays is provided which again brings the operation to a stop when the low pitch cut-out switch opens. It is then merely necessary to return the switches to a normal operating position for conventional constant speed or

selective pitch control. A refinement has been incorporated which it is believed will effectively prevent inadvertent operation. It takes the form of an additional switch which must be operated to reverse the propellers. By requiring the pilot to perform two separate operations, an attempt has been made to eliminate the possibility of this extremely hazardous occurrence in flight. It is not anticipated that this additional operation will unduly burden the pilot since it would not be normally made until after alighting on the water.

No increase in the rotating propeller weight is involved in adapting it for reverse pitch operation. By making use, wherever possible, of existing units the increase in control weights has been kept to a minimum. Including relays and switches, the increase is less than approximately four pounds per reversible propeller, or eight pounds per four-engine airplane where two propellers are reversible.

Cooling Problems

While the engine cooling characterisics of a propeller of which the blade sections inside the engine cowl are set at substantially zero angle cannot be expected to be adequate to permit protracted running at high powers, experience to date has been that the limitations imposed may not be exceeded by normal surface maneuvering requirements. Fig. 5 illustrates graphically the effect on cylinder head and oil-out temperatures on all engines of maneuvering continually around and approaching and reapproaching a buoy over a period of 30 minutes. These tests were conducted for the purpose of determining temperature effects and in a manner intended to bring out the existence of cooling limitations. The engines were repeatedly brought up to approximately 40 per cent rated power and 75 per cent rated r.p.m. The outside air temperature was 95°F. It is estimated that the 30 minutes of operation represented between ten and fifteen normal approaches. The ship was equipped with conventional N.A.C.A. cowlings. Cowling flaps were kept open. No measurement was made of baffle pressure drop but it is apparent that some flow must have been induced through the engine since the maximum cylinder head temperature seemed to be stabilizing toward the end of the run at approximately 450°F.

The effect of this type of operation on "submerged" engine installations, airplanes with wing entry reverse flow cooling ducts or other cowling arrangement where cooling in reverse pitch might be expected to be less favorable, have not as yet been directly determined. However, test stand results have been obtained which are believed to be indicative to some extent. On one occasion after 11 minutes of operation of a Cyclone engine during which the power was increased approximately uniformly from 25 per cent to 50 per cent rated power, the maximum head temperature was less than 400°F. This test, conducted on an indoor test stand, was not, however, for the primary purpose of determining temperatures. Except for a narrow ring over the cylinders, the engine was open on all sides, so no definite conclusions may be drawn with regard to an actual installation in an airplane.

Cooling tests were conducted with zero baffle pressure drop on a large double-row radial air-cooled engine on a dynamometer stand. By leaving the cooling fan off, an effort was made to simulate the worst cooling conditions. However, the back of the engine was not enclosed. With this arrangement, three minutes of one-quarter power operation at 60 per cent rated r.p.m. brought the temperature from 300 to 450°F. Idling for 10 minutes gave approximately the same result.

Inasmuch as normal reverse pitch operation will only require short bursts of power, it appears on the basis of the tests reported that the problem of cooling for this type of operation may not prove to be a serious one. However, the effect of less favorable cooling arrangements may be appreciable and additional tests on other installations should be watched carefully.

Engine Overspeeding

The torque absorbed by the propeller aerodynamically is very low at blade angles in the neighborhood of zero degrees. Hence as the propeller pitch is reduced during the pitch reversal the engine will tend to accelerate. The inertia of the engine and propeller must

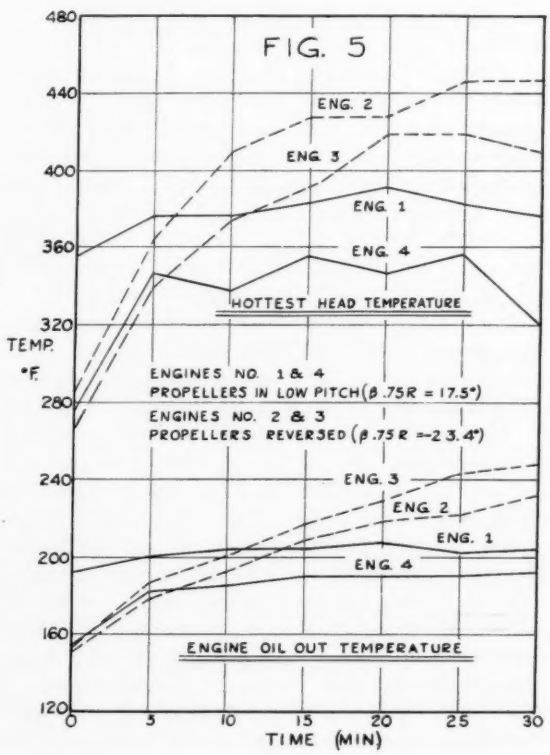

absorb the excess torque of the engine as the aerodynamic propeller torque requirements drop off. By making the rate of pitch change reasonably rapid, it is possible to absorb this excess torque without objectionable overspeeding even at appreciable throttle settings. Measurements have been made on a Cyclone engine with an 11 ft. 6 in. three-blade aluminum alloy propeller with a rate of pitch change of 3° per sec. Starting with a low pitch of 15° at the 42-inch station and an engine speed of 1680 r.p.m. (approximately 250 hp.), the engine speed did not exceed a maximum of 2000 r.p.m. as the pitch was reversed to −15°. The same maximum was obtained as the pitch was returned from −15° to +15°, at the same rate. Inasmuch as somewhat higher rates of pitch change could be expected for normal installations, it is estimated that the pitch might be safely reversed with the throttle set for approximately half power with the propeller in low pitch. The safe initial throttle setting for each installation should, however, be checked by running through a few trial cycles.

The use of a throttle lock in conjunction with the reverse pitch control is not thought to be essential if adequate means are taken to prevent inadvertent operation of the reversing control. This should, of course, be done in any event to prevent accidental pitch reversal during flight. This was accomplished on the test installation by the use of two separate switches so arranged that it was necessary to operate both as was described in an earlier section.

Propeller Stresses

In order to make certain that safe operating limits cannot be exceeded under any circumstances, it is necessary to make propeller stress calculations at the full throttle speeds dictated by the negative pitch angle setting selected. Stresses at the front surfaces of the propeller shank are the most critical in reverse pitch operation. Except in the case of aluminum blades, it is common practice to machine the hub barrels so that an initial forward tilt of from $\frac{1}{2}°$ to $2\frac{1}{2}°$ is imparted to the propeller blades. This practice was adopted because it causes an appreciable reduction in blade stresses due to thrust bending moments by introducing a "centrifugal restoring moment" tending to counteract the thrust moments. This initial forward tilt, however, ceases to be an advantage as soon as conditions of negative thrust are encountered inasmuch as the centrifugal and thrust moments then act in the same direction. The other design condition under which stresses at this point in the blades are a maximum is during overspeed operation at zero thrust. For reverse pitch operation, stresses on the front surface of the blade shank due to a combination of the centrifugal force, thrust bending moment, and centrifugal bending moment should not exceed those for the condition of overspeed at zero thrust for which the propeller is designed. The selection of a negative operating angle should be subject to the restriction that full throttle operation will not cause blade stresses to exceed those so determined, although operating instructions should restrict normal use somewhat below this limit.

By limiting propeller blade shank stresses as described above, the stresses in the hub and blade retaining components are also limited to previously determined safe values.

Engines and Engine Mounts

Modern aircraft engines, so constructed that they may be applied to either tractor or pusher type installations, should withstand negative thrusts incident to reverse pitch operation without difficulty. Nor does it appear that either conventional or "dynamic" engine mounts will suffer from this type of propeller operation.

Thrust Requirements

An analysis of the various factors acting on a flying boat in the water will serve to establish certain minimum thrust requirements. However, actual practice indicates that rapid handling is facilitated if ample excess negative thrust is available.

In general the requirements may be divided into three sections. It should first be possible to prevent the ship from weather-cocking in the highest relative cross wind in which it is expected that it may be required to maneuver. This will probably be in the neighborhood of from 30 to 35 m.p.h. The moment exerted on the ship by the wind will depend on the effective side area including hull, rudder, and wing undersurface at the maximum angle of heel, and an estimate of the location of the effective center of pressure with relation to the effective center of hull resistance in the water to side slip at zero forward velocity. This weather-cocking moment must be resisted by a combination of negative and positive thrusts from the inboard down-wind engine and outboard windward engine, respectively. The required thrust is determined when the distance between these engines is known. Available negative thrusts in excess of this amount will make it possible to turn the ship against the effect of the wind. An analysis of the four-engine boat tested indicates that the maximum weather-cocking moment with a relative wind of 35 m.p.h. and the ship heeled over 7° is in the neighborhood of 12,000 lbs. ft., and that the negative thrust necessary to balance this moment is approximately 400 lbs.

The negative thrust necessary to decelerate the forward motion of the mass of the ship will depend upon the weight of the ship, the drag velocity relation of the hull in the water, and the rapidity of deceleration desired. Negative thrust from both reversible propellers is available for this purpose.

The third requirement is that of turning the ship in the water. The principal forces to be overcome are the water resistance of the hull and one wing float or "hydro-stabilizer" and the moment required to accelerate the ship angularly against its polar moment of inertia about a line through its center of gravity.

The above factors, while tending to establish rough minimum thrust requirements, are not to be taken to represent the maximum values. The negative thrust available on each of the inboard engines of the test installation with the negative pitch angle selected and an operating engine speed limitation of 2000 r.p.m. was equivalent to approximately 30 per cent of the forward static take-off thrust. While this thrust was found to be more than adequate in all situations encountered, higher thrusts would probably have been used to obtain more rapid maneuvering had they become necessary. Hence, the maximum thrust is limited only by the thrust available in the face of various engine and propeller limitations which are determined by the selection of the operating reverse pitch setting.

Negative Blade Angle Setting

The selection of the optimum negative blade angle setting is at present somewhat hampered because of the lack of complete aerodynamic data covering power and thrust coefficients at negative blade angles for the various propeller airfoil sections and planforms. Data for an R.A.F.-6 Blade is given in reference 1. A replot of power coefficients *versus* blade angle under static thrust conditions ($V/nD = 0$) is shown in Fig. 6, Curve 1. Curve 2 shows the results of a test stand

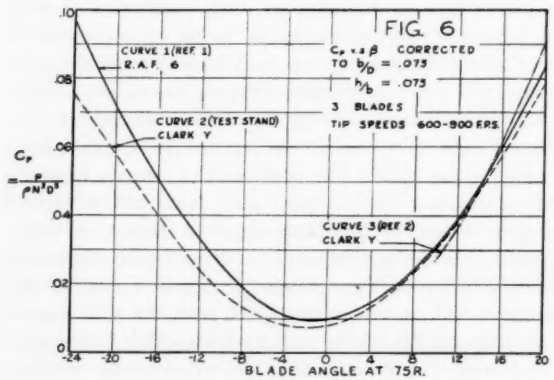

run on an engine with a torque meter nose of a 13 ft. aluminum blade with a Clark Y airfoil. In order to check the Clark Y blade curve, points in the positive pitch angle range are shown in Curve 3, as taken from a large number of whirl tests on blades of various planforms and diameters. In order to reduce the data as far as possible to a form in which it is more or less directly comparable, corrections for thickness ratio and activity factor have been applied to the data from which the several curves were obtained, all being figured on the basis of a blade with a thickness-width ratio of 0.075, and width-diameter ratio of 0.075. (See reference 2.) Tip speed corrections have not been applied, but all tip speeds are in the range of 600 to 900 ft. per sec. That the combination of corrections usually applied to power coefficient calculations in the positive angle range may be applied to negative blade angle settings with equal accuracy may be somewhat questionable. While the effect of variations in pitch distribution has not been found to be great in the positive angle range, it is possible that the inverse pitch distribution encountered in reverse pitch operation may appreciably modify the relative effectiveness or activity of various portions of the blade.

Data on negative thrust are even more meager. In plotting the thrust coefficient curves in Fig. 7, thrust data were available for only two of the three curves shown for power coefficients. When more data become available, the preselection of angles will be greatly facilitated.

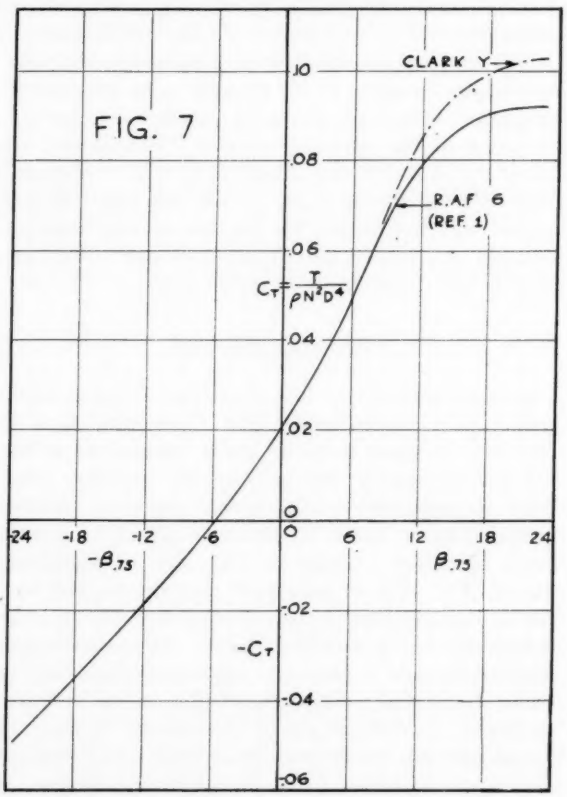

With torque and thrust coefficients known, it is possible to plot thrust *versus* r.p.m. for various horsepowers, cross plotting lines of constant blade angle. In the selection of positive pitch angles for best static thrust, curves constructed in this fashion generally make it possible to select a blade angle which will give the best thrust and thrust-per-horsepower over a fairly

wide range of r.p.m. This does not, however, seem to be the case for negative blade angles from the data available over the range of negative angles covered. In this range, it appears that increased thrust-per-horsepower is obtained at increased blade angles. By the addition of a curve of the limiting sea level operating engine characteristics at full throttle, the point of maximum thrust with the given engine-propeller combination may be determined. A further limitation may be imposed by propeller stresses. If it is not apparent by inspection that these stresses are well within safe limits, it will be necessary to calculate them for the particular conditions which are to be met, as outlined earlier in this paper.

At idling speeds, a very high negative angle may prevent the engine from idling properly during low speed taxiing with the throttle closed and may produce excess negative thrust as well. However, because of the very low power absorbed by the blades at low speeds, it is not believed that this will become a problem. For operation at a given horsepower where maximum negative thrust is desired, lower engine speeds will favor cooling inasmuch as the heat to be dissipated is based on indicated horsepower.

An illustration of the recommended procedure for the determination of negative blade angle settings is shown in Fig. 8, which presents the results of an analysis made for the four-engine flying boat installation previously referred to. Because of the lack of data, some simplifying liberties have been taken in applying the values for propeller coefficients presented above in Figs. 6 and 7. On a plot of thrust *versus* propeller r.p.m., lines of constant horsepower have been cross-connected by constant pitch lines. The limitations imposed by maximum permissible engine speed and the maximum obtainable engine speed at full throttle are shown. In the case investigated, propeller stresses did not impose operating limitations, as may be seen from the limiting line on the chart which falls outside of the permissible engine operating area. The pitch selected was minus $23^1/_2°$. It will be seen that this selection will prevent engine overspeeding at full throttle and that maximum negative thrust is available for use in an emergency. The "check-point" was obtained by interpolating between horsepower curves at a measured r.p.m. from engine data obtained on the test installation. It seems to confirm propeller power coefficient data although the thrust was not checked. As a matter of interest, it was not found necessary at any time to operate the reversed propellers at a greater horsepower than that indicated by the "check-point" which was roughly 40 per cent of the take-off horsepower for which the engines were rated. Where propeller stresses are not a limiting factor it is suggested that limiting conditions of 75 per cent to 80 per cent speed

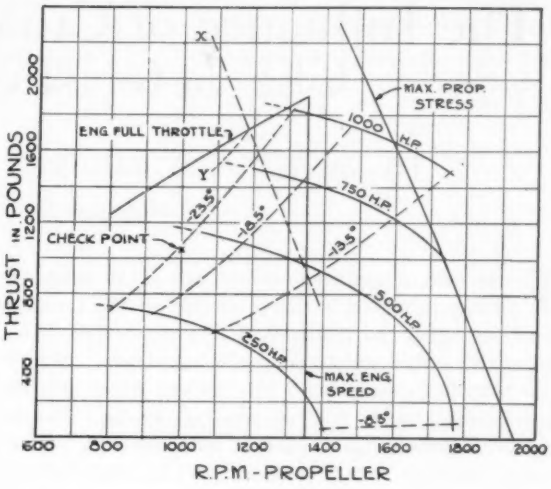

FIG. 8.

and 50 per cent power (based on take-off rating) be imposed for normal operation inasmuch as they should provide adequate thrust and at the same time permit reasonably prolonged operation without engine overheating. If the pitch is selected on this basis, engine operating limitations at full throttle will also be met.

In order to illustrate the possible effect of propeller stress limitations, the dotted line X has been arbitrarily added. If this hypothetical limitation had actually existed it would have been desirable to modify the selection of a negative angle to Y, a somewhat greater negative angle than the one which was selected.

SYMBOLS

C_P = Propeller power coefficient = $P/(\rho N^3 D^5)$.
C_T = Propeller thrust coefficient = $T/(\rho N^2 D^4)$.
N = Propeller rotational speed.
D = Propeller diameter.
R = Propeller radius.
P = Power absorbed by propeller.
T = Effective propeller thrust.
V = Forward airplane velocity.
b = Blade airfoil chord at 0.75 R. station.
h = Blade airfoil thickness at 0.75 R. station.
β = Blade pitch angle at 0.75 R. station.
ρ = Mass density of air.

REFERENCES

[1] Hartman, E. P., *Thrust and Torque Characteristics of an Adjustable Pitch Metal Propeller*, N.A.C.A. Technical Report No. 464, 1933.

[2] Thomas, F. M., Caldwell, F. W., and Rhines, T. B., *Practical Airscrew Performance Calculations*, Journal of the Royal Aeronautical Society, Vol. 42, No. 325, page 1, January, 1938.

The Influence of Curvature on the Buckling Characteristics of Structures

TH. VON KÁRMÁN, LOUIS G. DUNN, AND HSUE-SHEN TSIEN
California Institute of Technology

IN the field of applied elasticity, one of the most perplexing problems is the prediction of the buckling load, or rather the failing load of a thin-walled structure with either simple or double curvature. Everyone who has contact with this subject will notice the gap between theory and experimental results. The designer, however, has to proceed with his work regardless of whether or not the theory of elasticity can give him the correction solution of his problem. Hence, in this case he has to resort to empirical relations determined by experimental methods. But such an empirical approach to a complex subject without solid physical basis has its definite limitations. Therefore, a correct picture of the interactions of the different factors which determine the failing load and the mechanism of the failing process will be always useful to the designer.

In this paper the authors do not present a new theory, but certain considerations which they believe bring out the crucial point of the subject. In Section I, a comparison is made between the buckling of one dimensional and two dimensional structures with and without curvature. Section II contains a critical examination of the discrepancies between the classical buckling theory of cylindrical shells and the experimental evidence together with a description of various investigations which have been made to reveal the true character of the mechanism of failure. In Section III, the buckling phenomena observed in the laboratory for different structures are discussed from the point of view developed in the previous sections.

SECTION I

Columns

One of the earliest problems of Applied Elasticity is that of a uniform column subjected to axial thrust, generally referred to as Euler's problem. This problem was first investigated by Euler in 1744 and has since occupied the attention of numerous investigators. The exact solution of the problem requires a solution of a non-linear differential equation which determines the shape of the deflected central line of the column. Using a rectangular coordinate system x, y, such that the x axis coincides with the line of thrust, then the differential equation for the displacement w in the y direction may be written in the form:

$$\frac{d^2w}{dx^2} + \frac{Pw}{EI}\left[1 + \left(\frac{dw}{dx}\right)^2\right]^{3/2} = 0 \tag{1}$$

An approximate solution can be readily obtained by assuming small deflections and neglecting the second order term $(dw/dx)^2$ in the bracket. This simplification leads to a simple second order linear differential equation of the form:

$$\frac{d^2w}{dx^2} + \frac{P}{EI}w = 0 \tag{2}$$

The boundary conditions for a simple supported column are $w = 0$ for $x = 0$ and $x = l$, where l is the length of the column. The expression

$$w = A \sin \sqrt{P/EI}\, x \tag{3}$$

is the solution of Eq. (2), which satisfies the boundary condition at $x = 0$. In order to satisfy the boundary condition for $x = l$, $\sqrt{P/EI}\, l$ must be equal to $n\pi$, where n is an integer. Hence the "critical" values of P are

$$P_n = n^2\pi^2 EI/l^2 \ (n = 1, 2, 3, \ldots .) \tag{4}$$

Thus for a thrust corresponding to any one of the critical values of P, a state of equilibrium exists in which the deflection form is given by

$$w = A_n \sin n\pi x/l \tag{5}$$

It is seen that the amplitude remains undetermined. The first critical load, *i.e.*, $n = 1$, corresponds to the "Euler buckling load."

If $P \neq P_n$, the linear theory gives $w = 0$ as the only equilibrium shape. If it is desired to obtain the force-deflection relation beyond the first buckling load P_E it is necessary to integrate the non-linear Eq. (1). The integration of this equation by the use of elliptic integrals is well known and only the final results will be given here. A relation between the thrust P and the deflection δ at the center is obtained in the parametric form:

$$Pl^2/EI = 4[K(\sin \alpha/2)]^2 \tag{6}$$

$$\frac{\delta}{l} = \frac{\sin \alpha/2}{K(\sin \alpha/2)} \tag{7}$$

Here $K(\sin \alpha/2)$ denotes the complete elliptic integral of the first kind of the modulus $\sin \alpha/2$, where α is the angle between the line of thrust and the tangent to the centroidal axis at its end points. From these two equations it is a relatively simple matter to obtain the

Presented at the Structures Session, Eighth Annual Meeting, I.Ae.S., New York, January 25, 1940.

relation between P and δ illustrated in Fig. 1. It is seen that with a steadily increasing thrust the deflection δ will increase and then slowly decrease. The decrease in deflection is easily understood by considering the physical process illustrated in Fig. 2. It is seen that the deflection will increase to a maximum

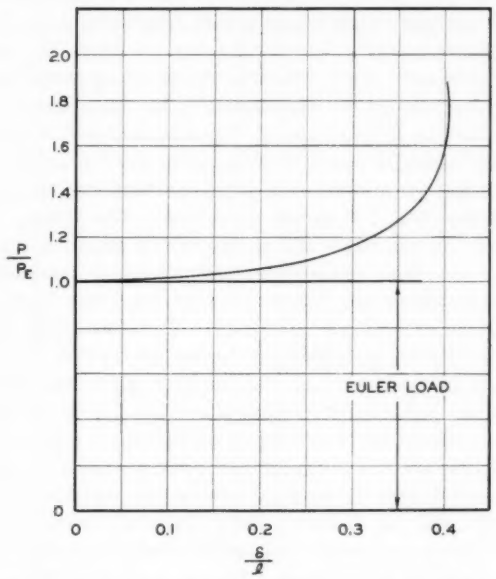

FIG. 1. Theoretical load-deflection curve for a slender column.

FIG. 2. Progressive deformations of an elastic strut.

when the two end points are close together and as they pass each other a point will be reached at which the deflection starts to decrease. It is of course assumed in this discussion, which is generally referred to as the theory of the "Elastica," that no plastic deformation takes place. This would only apply to extremely slender columns.

Another interesting aspect of the problem which seems to appeal particularly to the practical mind of the engineer, is the effect of small initial irregularities. This can be done quite readily by either assuming a small initial curvature, or a bending moment. If all deflections are considered small; the effect of an initial curvature or bending moment can be taken into account by an additional term in Eq. (2), which in this case also remains linear. The practical significance of the equation thus obtained is that it yields a solution in which the deflection δ appears explicitly, namely:

$$\frac{P}{P_E} = \frac{1}{1 + a_1/\delta} \tag{8}$$

where P is the column load, P_E the Euler buckling load and a_1 is a constant proportional to the initial deflection. It is evident that as δ becomes large compared to a_1 the load P always approaches Euler's load, as indicated by curve A in Fig. 3.

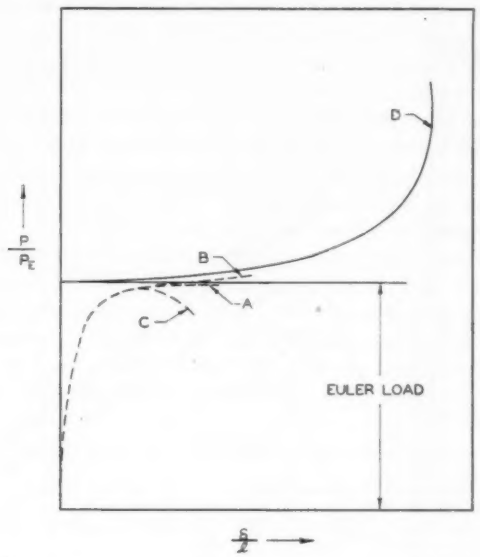

FIG. 3. Actual load-deflection curves of slender columns.

In engineering practice it is commonly considered that the approximate solution is sufficient to describe the collapsing of slender columns. A detailed consideration will show this to be generally true. It was shown that for the strut with a small initial displacement the thrust, P, according to the linear theory approaches asymptotically a horizontal line corresponding to the Euler load. The exact solution for this problem would yield a line B, Fig. 3, which follows in general trend the curve D, obtained for an initially straight column, *i.e.*, an increase in deflection is also accompanied by a steadily increasing thrust. However, there still remains to be considered the effect of the physical properties of the material. The column will, after deflection, be subjected to combined compression and flexural stresses. Since at first δ increases much faster than P, the flexural stress will predominate. For a slender column in which the compression stress is well below the yield stress it may then be concluded that during the loading process the deflection will follow the curve B until the combined compression and flexural stress reaches the yield stress. When this point, which will in general be close to the Euler load, is reached the load deflection curve follows a curve similar to C. Therefore, it can be said, that for slender columns in which the compression stress is well below the yield stress, the collapsing load will always be very near to the Euler buckling load.

However, if the column is short so that the stress in

the column at buckling is very near the yield stress, the effect of plastic deformation on the load will be felt immediately after buckling starts. This would cause a drop in the load-deflection curve as shown in Fig. 4. This phenomenon was shown by the senior

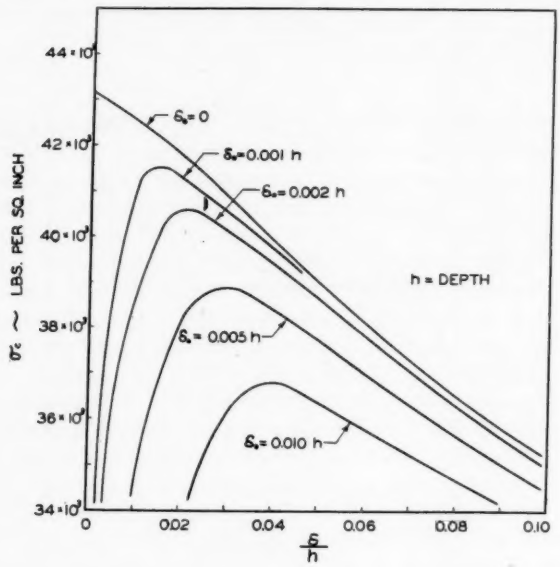

FIG. 4. Calculated load-deflection curves for short columns ($l/\rho = 75$) with various amounts of initial deflection for mild steel with a yield point = 45,000 lbs. per in.² (cf. von Kármán[1]).

author in 1909.[1] An essential difference between this case and the case of a slender column is that the presence of initial deflection will make the failing load of a short column much lower than the Euler load (cf. Fig. 4).

Flat Plates

In the previous section it was noted, that in general the buckling load calculated by the linear theory was sufficient for determining the failing load of columns. However, the buckling load is in many cases not sufficient as a design criterion, as for instance, in the design of airplane structures of the semi-monocoque type where advantage is taken of the fact that the thin metal sheet covering of wings, fuselages, etc., although buckling at a low load, has an ultimate strength or load-carrying ability which is in some cases a large multiple of the buckling load. For an efficient design it is then necessary that the designer be able to calculate with a fair degree of accuracy the amount of load which can be transferred through the metal sheet covering, apart from that which is carried by the longitudinal stiffening members.

For purposes of analysis the sheet between the longitudinal members may be considered as a flat plate. This problem is much more complicated than the analogous problem of the "Elastica" for, in the case of the deflected column the resultant of the normal stresses in any arbitrary cross-section is determined statically by the end thrust P, whereas in the case of the deflected plate the distribution of the resultant stresses acting in the median surface of the plate depends on the distribution of the normal deflection.

An exact solution of the problem is quite difficult as the amplitude is a non-linear function of the end thrust, and the wave form changes with increasing deflection. Approximate solutions for the case in which the edge stress is not very far beyond the buckling stress have been given by S. Timoshenko[2], K. Marguerre[3], E. Trefftz[4], H. L. Cox[5], and M. Yamamoto and K. Kondo.[6] They assumed either a wave form very near to the buckling wave form or an average extentional strain to simplify the differential equations. The former assumption precludes the possibility of multiple waves near the edges of the plate and the latter assumption oversimplifies the interaction between the bending and the extensional stiffnesses. Therefore, both tend to limit their usefulness for higher edge stresses. For loads far in excess of the buckling load, the senior author[7] of this paper developed an approximate method, based upon the following considerations: If a rectangular plate freely supported along two edges is compressed between two rigid plates, the distribution of stress will be uniform until buckling takes place. Further compression will cause buckling across the plate except at the edges. Hence, as the end plates are brought still further together the stress along the edges will increase to a large multiple of the buckling stress, whereas the stress in the center of the plate remains substantially of the order of the buckling stress.

To simplify the calculations it was then assumed that near failure the entire load is carried by two narrow strips adjacent to the edges. An analysis based on these simplifying assumptions leads to a simple and convenient expression for the total load carried by the plate, namely:

$$P = C\sqrt{E\sigma}\, t^2 \tag{9}$$

This equation is only valid below the elastic limit; beyond the elastic limit it is necessary to correct for the change in E. On the other hand if σ is replaced by σ_y, the yield point stress, the resulting value of P will differ but slightly from the maximum value of P. Hence for calculating the maximum load that can be sustained by the plate, Eq. (9) is replaced by

$$P_{max.} = C\sqrt{E\sigma_y}\, t^2 \tag{10}$$

where E = Young's modulus of elasticity in lbs. per sq.in.
σ_y = Yield point stress in lbs. per sq.in.
t = The plate thickness in inches.

The value of the constant could be either calculated in accordance with the assumptions or experimentally determined.

It is of interest to note that the experimental load

deflection curve, Fig. 5, of a sheet attached to longitudinal stiffeners is, in the elastic range, analogous to that of the "Elastica." A non-dimensional plot is obtained by plotting the ratio of the applied load to the buckling load as a function of the ratio of the maximum

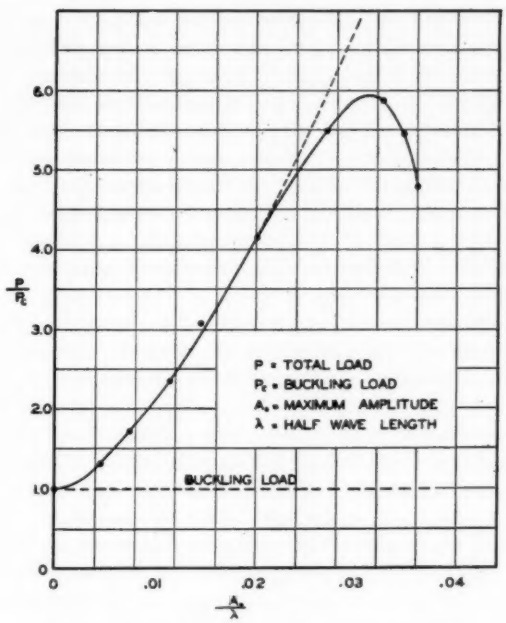

FIG. 5. Load-deflection curve for a thin dural sheet (t = 0.025 in.; b = 5 in.) riveted to strong stiffeners. (I_{st} = 0.0094 in.^{4}).

amplitude to the half-wave length. As certain portions of the sheet are stressed beyond the elastic limit, the curve tends to flatten until finally the load decreases with increasing deflection. A characteristic behavior of the plate, of which a clear understanding is essential in design work, is, that the load carried by the plate is a non-linear function of the edge stress. This fact is clearly demonstrated by the experimental curve of Fig. 6.

Curved Bars

So far, the discussion has dealt with structures in which there is no curvature in the undeformed state. If the undeformed structure is curved an entirely new phenomenon is revealed. This new phenomenon will be the central interest of the present paper.

To simplify the problem, consider first the case of a curved bar under the action of a single concentrated load P at the center (Fig. 7). The ends of the bar are assumed to be laterally restrained. Now, starting from the undeformed position assume the load P is gradually increased and consider for the time being only the symmetrical type of deflection. During the initial stage of loading, the bar behaves in a manner similar to that of a straight beam under the action of a concentrated load, *i.e.*, the load P increases with the deflection δ at the center of the bar. However, large deflections in a curved bar with fixed ends produce a shortening of the centroidal axis and consequently an increasing compression. This is contrary to the case of a straight beam with fixed ends where large deflections will produce tension. It is a well known fact that a beam under end compression is much weaker in sustaining a lateral load than one without end compression. In fact for the case of a straight beam, when the end compression reaches the Euler load, the beam loses all its ability to sustain a lateral load. This general property of beams applies also to the case of the curved bar under consideration. Thus, with increasing compression in the bar due to an increasing deflection δ at the center, the effective rigidity of the bar to sustain the lateral load P is gradually reduced. In other words, the slope of the P *vs.* δ curve decreases with increasing δ. Thus as the load P is increased, a point will be soon reached where the slope is decreased to zero. Therefore a maximum load P is reached.

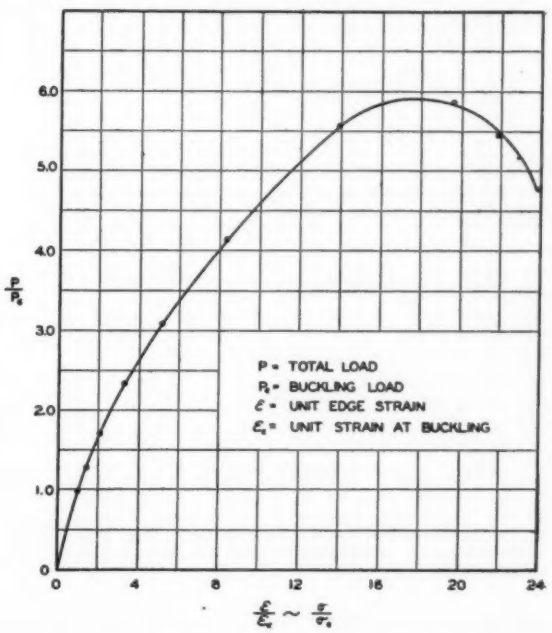

FIG. 6. The relation between the total load, P on the sheet and its edge strain ϵ. (The same specimen as for Fig. 5.)

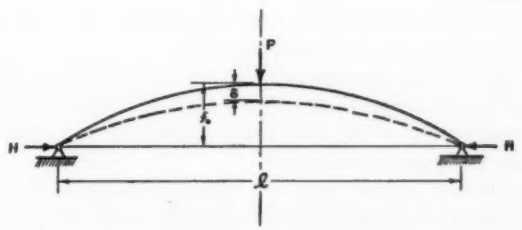

FIG. 7. A curved bar under a concentrated load P applied at the center of the bar.

Beyond this point, the load P will decrease with increasing deflection δ. That is, this part of the P *vs.* δ curve is highly unstable. This instability will continue until the actual shape of the bar has a curvature opposite to that of the undeformed bar. In other words, if the undeformed bar is curved downward, the bar has to be deformed so far as to curve upward before the decreasing process of the load P stops. If the deflection δ is further increased, then the load P again increases. The reason for this phenomenon can be again sought in the change of the end compression in the bar. Once the curvature of the bar is reversed, then the increase of deflection will decrease the compression in the bar, as shown in Fig. 8. This decrease in the

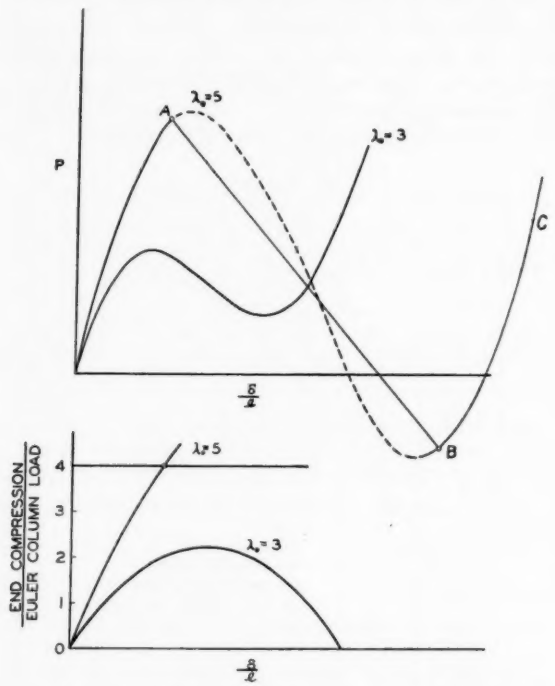

FIG. 8. Load-deflection relations for curved bars ($\lambda_0 = f_0/\rho$ where ρ = radius of gyration of the bar, cf. Fig. 7) (see reference 8).

end compression will, of course, increase its ability to carry lateral load. Finally the compression in the bar is changed into tension and its magnitude increases with further increase in the deflection δ. Thus increasing δ will further increase the ability of the bar to carry a lateral load P, *i.e.*, the slope of the P *vs.* δ curve will now increase with an increase in δ.

The process described in the preceding paragraphs has been demonstrated very clearly by a mathematical investigation of K. Marguerre.[8] Fig. 8 was taken from K. Marguerre's paper.

However, so far only the symmetrical type of deflection has been considered. Actually for slender bars, the situation is further complicated by the appearance of an anti-symmetrical type of deflection. It was shown by K. Marguerre that when the end compression in the bar reaches a value which is four times the Euler load, an anti-symmetrical type of deflection appears together with the symmetrical type of deflection discussed. This new component of deflection gives a P *vs.* δ curve as shown by the light straight line in Fig. 8. It is thus evident that the actual loading will start from the origin along the curve corresponding to a symmetrical deflection up to point A. Then, the anti-symmetrical component of deflection sets in and the bar will follow the light straight line to point B. From then on the deflection of the bar is again purely symmetrical and follows the heavy curve with increasing load. In a testing machine, the bar will actually "jump" from point A to some point C, depending upon the rigidity of the machine, with violent vibration due to a sudden release of elastic energy.

It is thus shown, in the case of a curved bar with laterally restrained ends and a load at the center, that the load-deflection relation is not linear but highly complicated. Moreover, the phenomenon occurs completely within the elastic range. Hence, the linear stress-strain relation gives a non-linear load-deflection relation involving a region where the load decreases with increase in deflection. This phenomenon is different from that of the plastic buckling of an Euler column in that it is purely elastic. It is again different from the case of a flat plate in that an increase in deflection can cause a decrease in load.

Spherical Shells

The buckling of a spherical shell under uniform external pressure is quite similar to the case of the curved bar just discussed. Consider a segment of an extremely thin spherical shell as shown in Fig. 9, and assume that the bending stiffness, which is proportional to t^3 can be

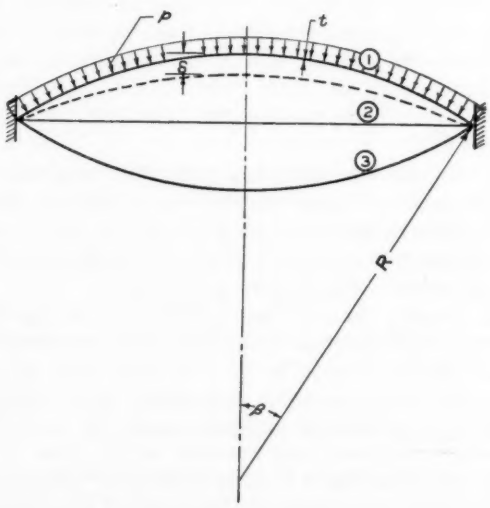

FIG. 9. Spherical shell segment under a uniform external pressure p.

completely neglected. Under this assumption the strain energy consists only of the energy due to extension or compression of the median surface of the shell, and it is equal to zero in the deflected position (3) provided it is zero in the undeflected position (1), Fig. 9. It is thus evident that it will be in equilibrium in position (3) without the aid of external pressure.

On the other hand, the intermediate positions between (1) and (3) do involve compression of the shell elements, and, therefore, the shell can be held in equilibrium in these positions only by an external pressure. However, just as in the case of the curved bar, the compression in the shell elements tends to reduce its pressure-carrying ability. Thus, if only a rotationally symmetric type of deflection is considered, the initial part of the pressure p *vs.* maximum deflection δ curve again has a decreasing slope with increasing δ. When the deflection δ of the shell goes beyond the position (2) and above position (3), a negative external pressure is necessary to maintain equilibrium as the compressed elements tend to force the shell to take the equilibrium position (3). The pressure-deflection curve under the assumption of negligible bending stiffness and symmetrical deflection is, therefore, of the form of curve A_1, shown in Fig. 10.

The effect of the bending stiffness is to increase the positive external pressure necessary to hold the shell in equilibrium. In other words, the pressure-deflection curves with increasing bending stiffnesses should be of the form of curves A_2, A_3, . . . in Fig. 10.

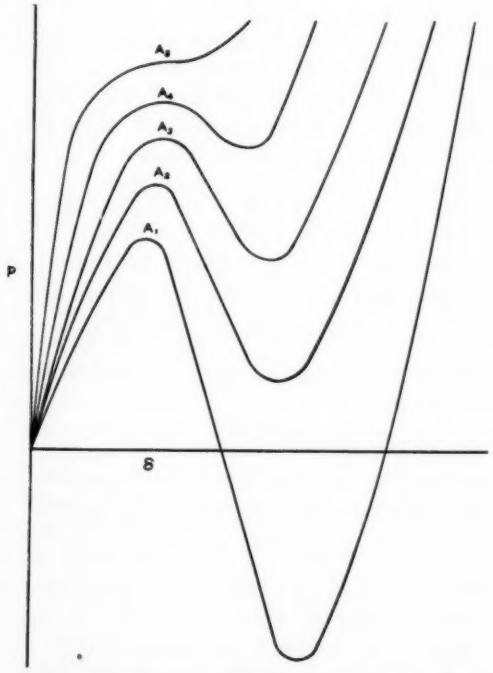

FIG. 10. Pressure-deflection curves for spherical shell segment with increasing thickness—radius ratios (A_1, A_2, A_3, —) (cf. Fig. 9).

The calculation of a spherical shell segment under uniform external pressure with clamped and laterally restrained edges was carried out by two of the present authors[9] under several simplifying assumptions. Fig. 11 is taken from this investigation. However, it should be noted that this load-deflection curve was obtained without the consideration of the anti-symmetrical type of deflection. Thus, it is possible that instability might occur before the point A is reached (Fig. 11) due to the anti-symmetrical type of deflection as in the case of a curved bar.

Hence, a segment of a spherical shell under a uniform external pressure behaves similarly to a curved bar under a lateral load. In both cases, the load-deflection curve is not a straight line and has an unstable portion within the elastic regime.

With this non-linear relation between the load and the deflection of a spherical segment the problem of buckling of spherical shells in general takes on an aspect quite different from that of the classical theory. The latter assumes that the shell buckles into a field of rotationally symmetrical waves of infinitesimal amplitude and gives a critical value for the external pressure as

$$pR/2t = 0.606\, E(t/R) \qquad (11)$$

As this value is much higher than observed, the following calculations were carried out. It was assumed that the deflection is restricted to a small segment whose vertex angle is undetermined. The load-deflection

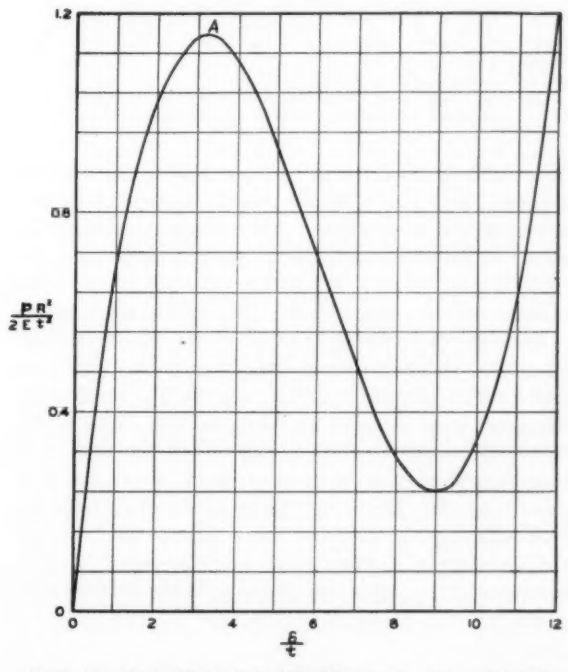

FIG. 11. Calculated load-deflection curve for a spherical shell segment with $\beta^2 R/t = 14$ where β is the semi-vertex angle of the segment (cf. Fig. 9). (The edge is clamped and laterally restrained.)

curve was then calculated for various fixed values of the vertex angle. The minimum loads obtained in this way give an envelope as shown in Fig. 12. The significance of this envelope is that it shows corresponding values of minimum pressure and deflections, for which the deflected shell is in equilibrium. For very small

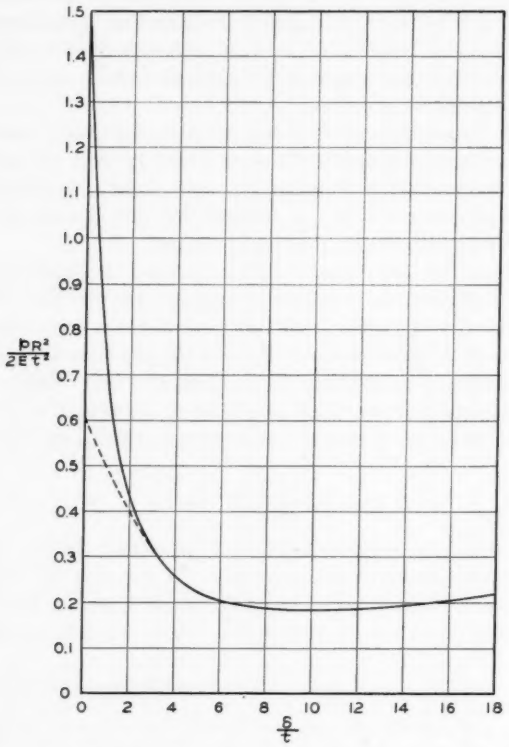

FIG. 12. Calculated buckling load-deflection curve for a spherical shell under uniform external pressure p.

deflections this calculation does not give the smallest possible loads due to the restrictions imposed by the assumed deflection shape. The correct location of the point of intersection between the envelope and the vertical axis ($\delta/t = 0$) is given by Eq. (11). The probable correct shape of the envelope for small values of δ/t is shown by the dotted line in Fig. 12. The most important point of this investigation is that the pressure which is necessary to keep the shell in equilibrium decreases once the shell starts to buckle. This is due to the decrease in effective stiffness of the shell with increasing deflection as in the case of curved bars discussed in the preceding paragraphs. The buckling load given by the new non-linear theory will be called the "minimum buckling load" and the point of intersection of the equilibrium curve with the vertical axis, given by the classical theory, the "initial buckling load."

The decrease in load after buckling appears superficially to be similar to the case of a short column (cf. Fig. 4). But there is one fundamental difference between these two cases: While the decrease in load carried by a short column after buckling is due to plastic yielding of the material, the decrease of load on the spherical shell after buckling occurs completely within the elastic regime.

The only experimental data known to the authors are those obtained by E. E. Sechler and W. Bollay on a copper hemisphere of 18 inches radius and a thickness of 0.02 inch. Their results are compared with the theoretical values in the following table:

	σ	Maximum Deflection	Angular Extension of Buckle
Experiments	$0.154\ E(t/R)$	$\approx 12.5\ t$	16°
Minimum Buckling Load (Theoretical)	$0.1826\ E(t/R)$	$\approx 10\ \ t$	14.8°
Initial Buckling Load (Theoretical)	$0.606\ E(t/R)$		6.6° (First nodal line)

It is seen that the theoretical "minimum buckling load" agrees closely with the experimental value whereas the "initial buckling load" does not. Thus, the shell actually does not reach the classical buckling load but "jumps" to an equilibrium position involving a large deflection at a considerably lower load.

SECTION II

The Inadequacy of the Classical Theory of Cylindrical Shells

It appears from the results of the first section that any buckling theory of thin shells based upon considerations of small deflections alone will only give the "initial" buckling load and will not be able to explain the failing load experimentally obtained, which is much more important in practical applications. One example of this general inadequacy of the small deflection theory is the classical investigations of buckling of cylindrical shells.

The buckling load of cylindrical shells under axial compression, based on the classical theory, was calculated by R. Lorentz, R. V. Southwell, S. Timoshenko, W. Flügge, L. H. Donnell, and others. The buckling stress obtained by these calculations is given by the equation

$$\sigma_{cr} = 0.606\ E(t/R) \tag{12}$$

The same problem was also investigated experimentally by many authors, especially by E. E. Lundquist[10] and L. H. Donnell.[11] In comparing the theoretical with the experimental results, it is found that the theoretical buckling load is about 3 to 5 times higher than the experimental value, as shown in Fig. 13. To remedy this situation W. Flügge[12] first considered the deviation of the assumed end conditions of the cylindrical shell from that realized in the laboratory. However, as was indicated previously[9] neither this effect nor the

assumption of initial deviations made by W. Flügge[12] and later by L. H. Donnell[11] are sufficient to explain the discrepancies.

The classical theory also gives a wave form which differs from those experimentally observed. The theory indicates that the shell will buckle into a series of rectangular waves whose nodal lines are parallel and perpendicular to the axis of the cylinder and that the amplitudes of the waves which buckle outward and those which buckle inward are equal. However, experiments indicate that the wave pattern, instead of being rectangular, is diamond-shaped, as shown in Fig. 17. Moreover, the outward radial deflections are much smaller than those inward. In other words, the shell definitely prefers to buckle inward.

If the exponent of (t/R) in Eq. (12) is correct, then when $\sigma_{cr}R/Et$ is plotted against (R/t) (Fig. 13) the points should lie on a horizontal line. This is evidently not the case. In fact by plotting the experimental buckling stress against (t/R) on a log-log-scale, it is found that the following expression is more correct:

$$\sigma_{cr} = \text{constant } E(t/R)^{1.4} \tag{13}$$

By considering each element of the shell as a small Euler column, the dimensional relation

$$\sigma_{cr} = \text{constant } E(t/l)^2$$

should be correct where l is the half wave length of this element. Comparing this relation with Eq. (12), it is evident that according to the theory the following relation should hold

$$l/t = \text{constant } (R/t)^{1/2} \tag{14}$$

Using the experimental data obtained by L. H. Donnell[11] it is found that

$$l/t = \text{constant } (R/t)^{0.7} \tag{15}$$

which is consistent with Eq. (13) but disagrees with Eq. (14) given by the classical theory. A strip of the cylindrical shell in an axial direction can also be considered as an elastically supported column, the supporting force being derived from the circumferential stress in the shell. It is well known that for such a column, the wave length decreases with increase in the elastic support, *i.e.*, a stronger elastic support gives a shorter wave length. Therefore, by comparing Eqs. (14) and (15), it is evident that in the case of thin shells with large values of R/t the classical theory has overestimated the elastic support and thus arrived at a higher buckling load.

If the total length L of the cylinder is of the order of one wave length or less, then it can be expected that the length will have an effect on the buckling load. In this case the natural extension of the wave is restricted by the length of the shell and the buckling load will increase with decreasing length. As shown in the preceding paragraph, the classical theory has underestimated the natural wave length, and thus the theory would predict that the length effect is negligible at much lower values of L/R than experiments would indicate. This expectation is verified through tests made by N. Nojima and S. Kanemitsu at the California Institute of Technology under the direction of E. E. Sechler. Their results are shown in Fig. 14 together with the theoretical values based on small deflections. It appears that while the classical theory predicts a length effect only at $L/R \approx 0.1$, the test data show an increase of buckling load at a L/R ratio of about 15 times this value. Thus it is evident that the natural wave length of the classical theory is very much under-

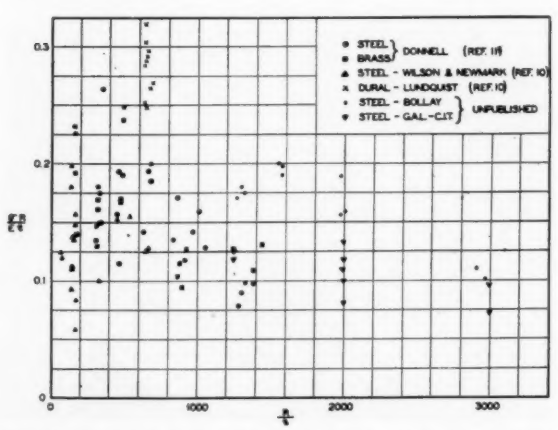

FIG. 13. Experimental buckling stress σ of cylindrical shells of different radius—thickness ratios, R/t. $(L/R > 1.5.)$

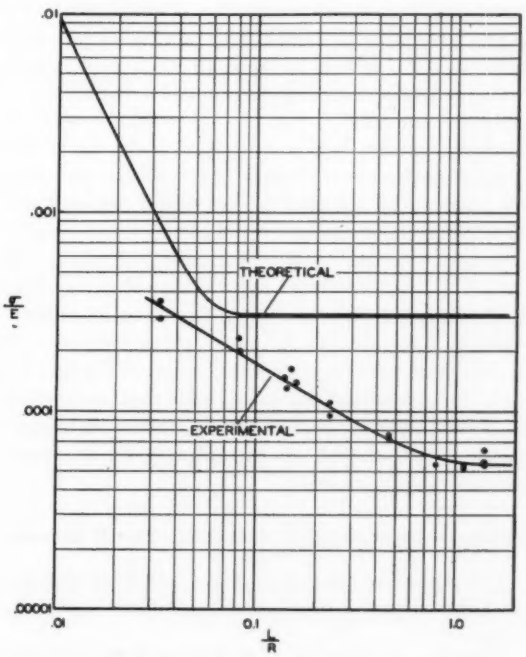

FIG. 14. The effect of the total length L of a cylindrical shell $(R/t = 2000)$ on its buckling stress.

estimated. However, the meaning of the large difference in the slopes of the theoretical and the experimental curves (Fig. 14) cannot be definitely stated; since, for most of the shorter specimens, failure is accompanied by a rotation around the axis of the cylindrical shell, due to the fact that the particular loading mechanism used is free to rotate in this manner. This type of failure is entirely different from that predicted by the classical theory.

Visual Study of the Buckling Phenomena of Cylindrical Shells

To obtain a better understanding of the mechanism involved in the failure of thin wall cylinders it was felt that it would be desirable to determine the exact shape of the initial waves which actually appear on the cylindrical surface during a test. This was accomplished by restraining the loading mechanism so that every stage of the buckling process could be maintained for an arbitrary length of time.* Thus photographs could be taken which show the intermediate phases of the buckling process.

The test apparatus is shown in Figs. 15 and 16. The three upper set screws afford adjustment of the loading head and rest on a $^3/_4$ inch plate. This plate in turn is held in position by three $^1/_2$ inch screws resting on the base plate. These latter screws are turned by means of the gear system shown and lowers or raises the $^3/_4$ inch plate as desired. The small 2 inch central gear, which turns the three 5 inch gears, can be externally operated. In this manner the motion of the loading head can be arrested at any desired position during loading of the specimen. The specimen was 9 inches long with a 0.0034 inch wall thickness and a radius of 6.375 inches, clamped between the end plates.

The progressive change in the wave shape and wave pattern is indicated in Fig. 17. It should be noted that the wave pattern does not agree with the uniform rectangular pattern which has been previously assumed for the theoretical solution. The initial wave form is elliptical in shape and scattered at random through the specimen. As the load is increased the waves tend toward a diamond shape and take on a more uniform configuration. This change in the wave form may be taken as an indication of the varying interaction between the bending and the extensional stiffnesses of the shell. If a longitudinal strip of the shell is considered as an elastically supported column, the increase in wave length indicates that the elastic support decreases as the deflection increases.

A Column Supported by a Non-Linear Elastic Element

The preceding discussion of the buckling of cylindrical shells suggested that a longitudinal strip of a cylindrical shell may be considered as an elastically supported column. However, it follows both from the physical considerations discussed in Section I and from the experimental observations of the different wave patterns described in the preceding paragraphs that the actual elastic support cannot be linear. Therefore, the explanation for the discrepancies observed between the theoretical and experimental values of the buckling load must be found in some characteristic property of a non-linear elastic support.

The problem of a column elastically supported has been discussed by H. Zimmerman for the case of concentrated supports, and by F. Engesser and others for the case of a uniformly distributed support.[13] In all cases the investigations have been confined to elastic supports exhibiting a linear force-deflection relation.

It was, therefore, felt that it would be of general interest to investigate the effect on the load-deflection relation of a column supported by a non-linear elastic element. Since rings are commonly used in structural design and are known to have the desired non-linear properties, a thin semi-circular steel ring, as shown in Fig. 18, was used as the elastic support. It may be of some interest to consider first the elastic behavior of a semi-circular ring. Designating the radial load by P

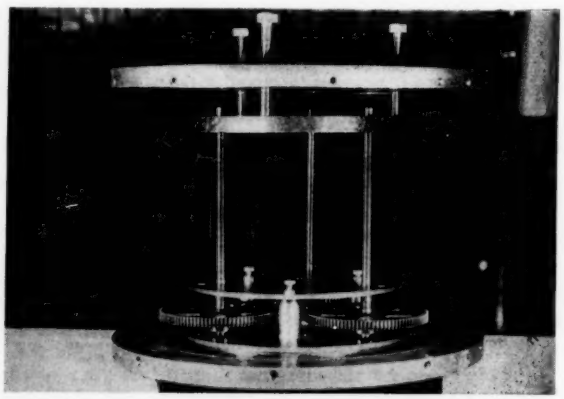

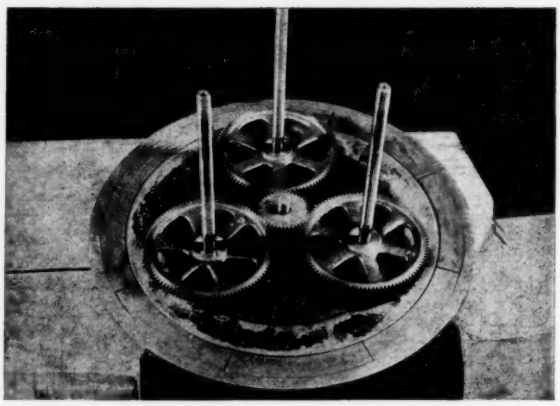

FIG. 15 and FIG. 16. Loading mechanism for visual study of the buckling of a cylindrical shell.

* This was carried out by N. Nojima and S. Kanemitsu under the direction of E. E. Sechler at the California Institute of Technology.

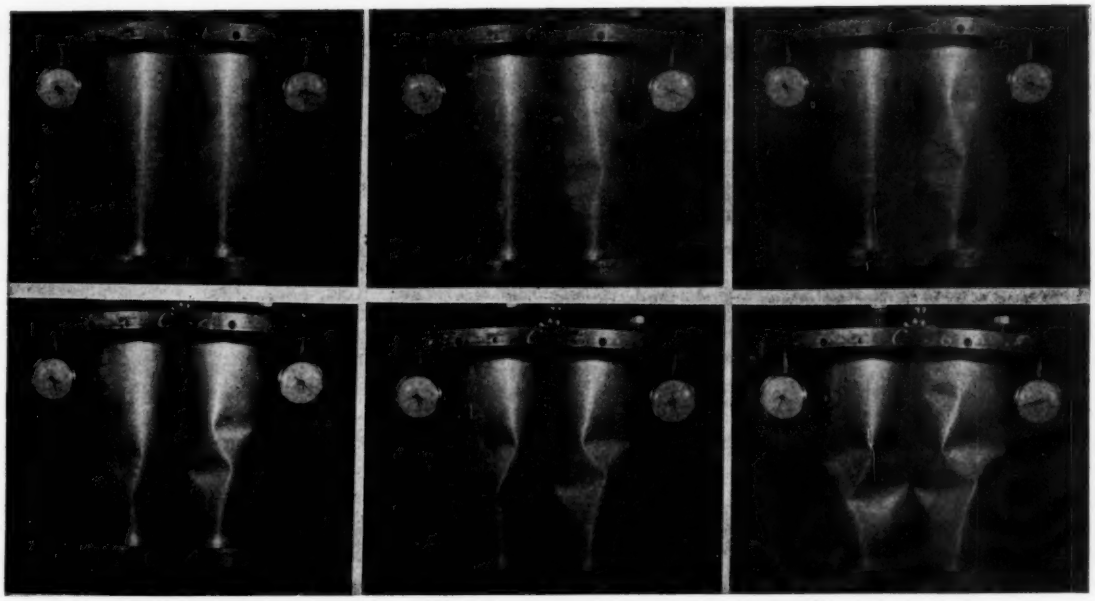

FIG. 17. Various stages during the buckling of a cylindrical shell under axial compression. ($R/t = 1875$.)

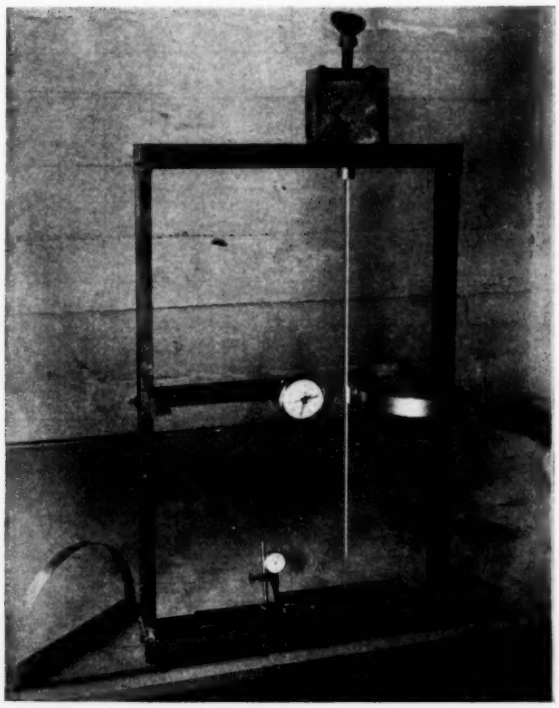

FIG. 18. Test apparatus for columns supported by a semi-circular ring.

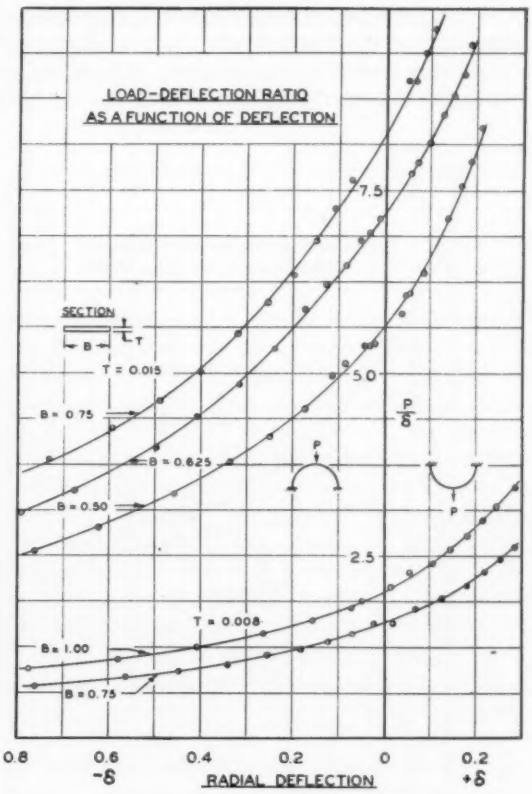

FIG. 19. Load-deflection ratio P/δ for semi-circular rings plotted as a function of deflection.

and the corresponding radial deflection by δ, the curves of Fig. 19 indicate that if the load is applied radially inward, the value of P/δ, the elastic constant, decreases with increasing deflection. When the load is directed radially outward the value of P/δ increases with increasing deflection. Obviously then, if an initially straight column is supported by such an element, or

elements, it may be expected that it would have a preference for buckling in the direction of decreasing P/δ, or, if due to an initial deformation in the direction of increasing P/δ, the buckling starts in that direction, then at some stage of the deflection a sudden "jump" may occur in the direction of decreasing P/δ.

Tests were conducted on columns 0.090 inch thick by 0.375 wide and 19 inches long. These columns were cut from 24SRT Alclad sheet stock. The steel rings were in all cases 8 inches in diameter with thicknesses of 0.008 and 0.015 inches; the width was varied between $^1/_2$ to 1 inch. The test apparatus and method of testing is illustrated in Fig. 18.

The results of these tests are indicated in Figs. 20 and 21, where the ratio of the column load to the Euler load is plotted as a function of the ratio of the normal deflection, δ, at the center of the column, to the column length l.

Considering first the results of Fig. 20, it is seen that the elastic support increases the buckling load of the "straight" column (upper curve) to nearly 3.5 times the Euler load. This load is reached at a relatively small deflection. Now, as the deflection δ increases, the decrease in load is at first quite rapid, then more gradual as the deflection becomes larger and may approach a minimum at large deflections. It was not possible to reach very large deflections because of plastic failure of both the rings and columns. The lower curves, in the same figure, indicate the effect of initial deflections, in which the column was rolled to approximately the form of a half-sine-wave, the maximum initial deflection being designated by δ_0. These curves show that with increasing initial deflection the maximum load decreases and occurs at increasingly larger deflections. In all cases the load sustained by the column tends to approach at large deflections the "minimum load" of the "straight" column. Thus in case of a non-linear support, any initial imperfections of the specimen will appreciably lower its buckling load. To illustrate the contrast between the column with a linear, and a column with non-linear elastic support, a number of tests were conducted on the same type of column, but with a linear elastic support (a coiled spring). As may be seen from the curves of Fig. 22 the columns with initial deflection in all cases approach the maximum load of the "straight" column.

A number of tests were made in which the width and thickness of the ring was varied. The results are shown in Fig. 21. As may be expected the maximum load increases as the ring stiffness increases, while the decrease in load at large deflections is correspondingly larger for the stiffer rings.

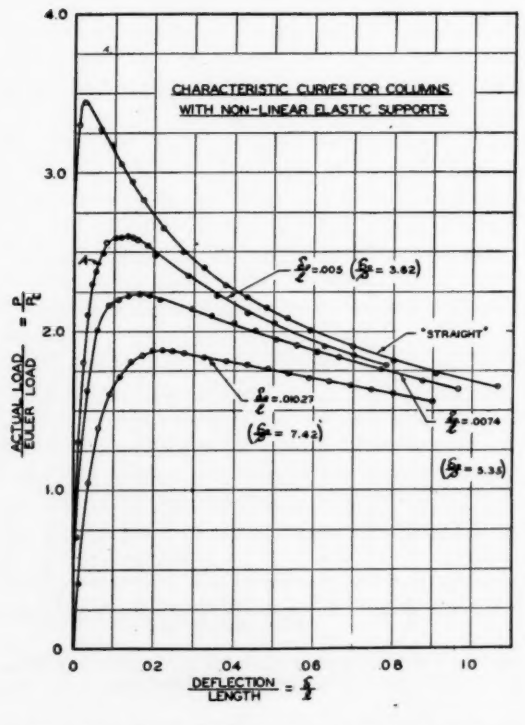

FIG. 20. Characteristic curves for columns with a non-linear elastic support (cf. Fig. 18) and different amounts of initial deflection.

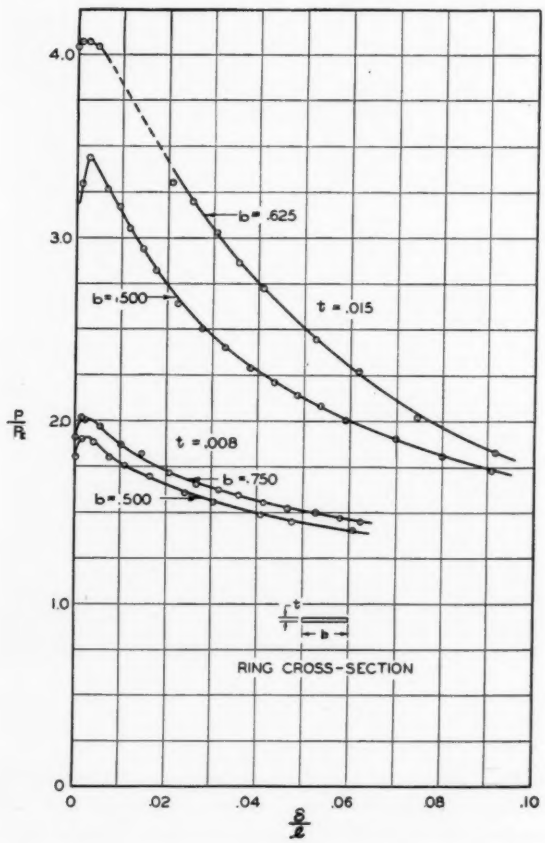

FIG. 21. Characteristic curves for columns with non-linear elastic supports of different stiffnesses.

The most striking features of the column supported by a non-linear elastic element are, first, that as the deflection increases the load decreases, and secondly, that there are two or three possible configurations of equilibrium for the same load; one corresponds to $\delta = 0$, the others to $\delta \lesssim 0$. Also in this case the decrease of the load with increasing deflection shows superficially a similarity to the behavior of a short

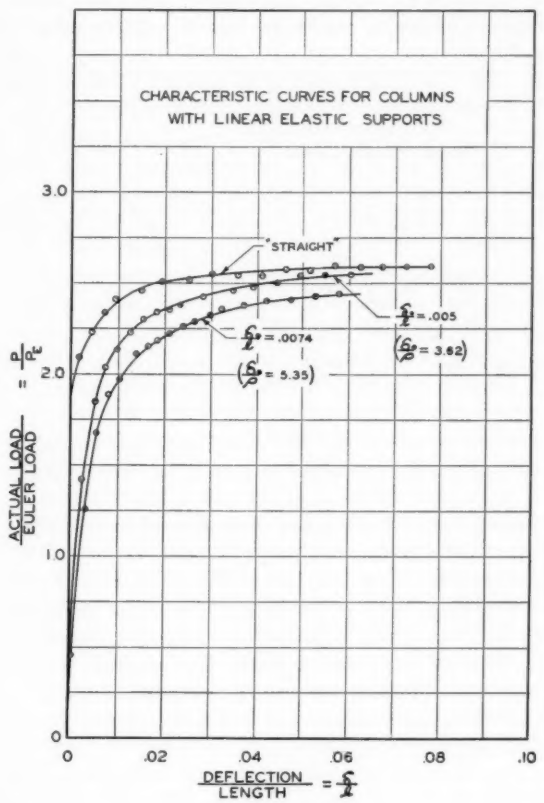

FIG. 22. Characteristic curves for columns with a linear elastic support and different amounts of initial deflection.

column in the plastic state as discussed in Section I. However, in the case of the column with the non-linear elastic support this phenomenon is entirely elastic in character.

These tests were conducted for the purpose of illustrating the buckling characteristics of a structure involving a non-linear elastic element. This particular experimental setup, as used, was chosen for the reason that the load P corresponding to any value of the deflection δ can be calculated analytically. Due to the complexity of the buckling phenomena of curved panels and cylindrical shells the authors are not yet able to give a thorough theoretical analysis. However, in the following section the phenomena will be discussed in the light of the above experimental observations.

SECTION III

Curved Panels

A curved panel can be primarily considered as being intermediate between a flat panel and a cylindrical shell. From the previous discussion, it may be expected that for a panel with very small curvature, the load carried will increase even after buckling; while for a panel with large curvature, the load carried will decrease after buckling. This is verified by the experimental work of W. A. Wenzek.[14] His results are shown in Fig. 23, where the ratio of the actual load carried by the specimen to the observed buckling load is plotted as a function of the ratio of the axial shortening of the specimens to the shortening at buckling. These results indicate that for a panel with a b/R ratio of 0.4 the load carried will be constant after buckling.

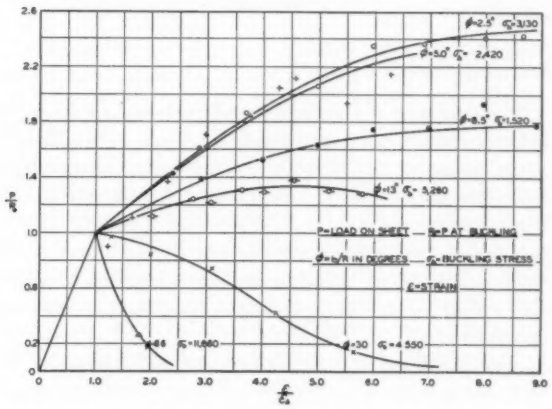

FIG. 23. The relation between the total load P and end strain ϵ for curved sheet of width b and radius R.

Hence, panels whose b/R ratio is less than 0.4 will fall in the flat plate category, *i.e.*, the load increases after buckling, while those for which the b/R ratio is greater than 0.4 will fall in the curved shell category, *i.e.*, the load decreases after buckling. Thus the value of $b/R = 0.4$ may be considered as a line of demarcation between these two categories of buckling phenomena.

However, a deeper understanding of these phenomena has to be sought in the concept of an elastically supported column developed in Section II. It is found that the increase or decrease of load after buckling depends entirely on the characteristics of the supporting element. Thus, if an elementary strip in the direction of the axis of curvature is considered as a column elastically supported by strips of material in planes normal to the column axis, then the behavior of the panel after buckling depends entirely on the load-deflection characteristics of these supporting strips of material. These strips or elements can, of course, be considered as curved bars. If the panel is flat these bars are without curvature and the elastic support derived from them increases with deflection. In other words, the elastic support given to the elementary

column concerned increases with an increase in wave amplitude. This results in a rising load-deflecting curve. By increasing the panel curvature, the curvature of the supporting bars is also increased resulting in a decrease of the load-carrying ability of these bars, *i.e.*, the elastic support given to the elementary column concerned decreases. This is revealed by a drop in the rate of increase of the load carried by the buckled panel. It is thus clear that an increase in curvature of the panel will decrease its load-carrying ability after buckling. Hence, by increasing the curvature of the panel, one soon reaches a point where the panel is no longer able to carry more load after buckling and a further increase in curvature of the panel causes the load carried by the panel to drop, just as the ring supported column discussed in Section II. The panel has thus passed from the flat-plate category to the curved-shell category.

Stiffened Shell Structures

The elements of a stiffened shell such as used in metal aircraft construction may be divided into three distinct parts, namely, the sheet metal covering, longitudinal stiffeners and frames or bulkheads. A structure of this type if subjected to, say, compression loads parallel to the axis of the cylinder may fail in one of four distinct ways. The types of failure may be classified as material failure, local failure, panel failure, and general instability.

The first three types of failure are well known to the designer and are those for which present-day airplanes are analyzed. These types of failure may occur regardless of the size of the airplane. However, general instability, defined as a simultaneous buckling of both longitudinal stiffeners and frames, is a function of the stiffness of the structure as a whole. In small airplanes the frame sizes are determined by practical considerations rather than from a standpoint of stability. It is fortunate that these considerations have led to sufficiently rigid frames to minimize the danger of general instability. It is felt that general instability is more likely to occur in large airplanes, as it seems customary to increase the overall dimensions of the airplane while the frame dimensions are kept nearly constant. An investigation is now being conducted at the California Institute of Technology on stiffened circular cylinders for the purpose of determining when general instability may occur.*

At present very little is known about the phenomena of general instability. Considering the shell as a whole it is immediately evident that it is anisotropic and the influence of one member upon the other is extremely difficult to determine. The most elementary concept of the problem would be that of a column supported by continuous and concentrated elastic supports, a longitudinal stiffener being the column, the sheet covering providing the continuous elastic support and the frames the concentrated elastic supports. Since the frames and the sheet have the characteristics of a non-linear elastic support it may be expected that the longitudinal members under compression will behave in a manner similar to the column with a non-linear elastic support as discussed in Section II. This expectation is verified by the results shown in Fig. 24. The abscissa is

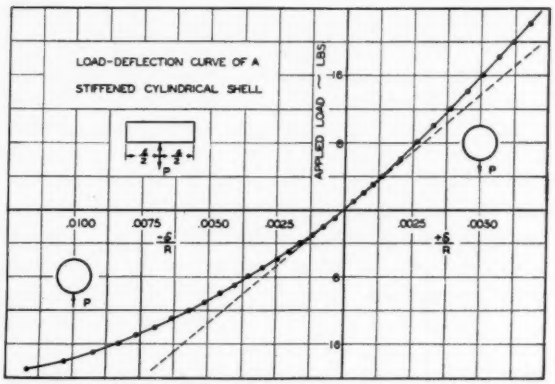

FIG. 24. Load-deflection curve of a stiffened cylindrical shell.

the deflection δ caused by a concentrated load P applied in a radial direction at the intersection of a longitudinal stiffener and frame (Fig. 24). The ordinate is the load P necessary for this deflection. It is thus evident that the stiffened shell is much less stiff when the load is applied radially inward than when applied radially outward. Furthermore, as the inward deflection is increased, the stiffness of the shell decreases. In this particular case, the slope of the P *vs.* δ curve at $\delta/R = -0.010$ is equal to only $^1/_3$ of that at $\delta/R = 0$. Therefore, the buckling characteristics of a stiffened shell must be similar to that of the non-linearly supported column. Any theory which is based on the assumption of small deflections will probably give a much higher buckling load than that actually observed. This may be considered as an explanation of the inadequacy of the theory developed by D. D. Dschou,[16] J. L. Taylor,[16] and others. E. I. Ryder[17] has solved the difficulty by resorting to empirical coefficients to obtain agreement with experimental results.

Concluding Remarks

In Section I, it was shown that while the load on thin-walled structures without curvature increases after buckling, the load on structures with curvature decreases after buckling. In Section II, this fact is demonstrated by experiments on columns with a non-linear elastic support. It is thus clear that for the buckling of structures with curvature there are two important values of the applied load. First, the

* This investigation was made possible through a grant from the Civil Aeronautics Authority. The discussions presented in this paper have been stimulated to a large extent by this particular research project.

"initial" or "upper" buckling load given by the classical linear theory and then a "minimum" or "lower" buckling load which is equal to the minimum load necessary to keep the shell in a buckled shape with finite deformations. If the specimen is geometrically perfect, it will start to buckle only when the "initial" buckling load is reached. Once the shell starts to buckle, the load will decrease with increasing deflection. The elastic energy thus released will accelerate the buckling process until the "minimum" buckling load is passed. Actually the increase in deflection is so rapid that the shell appears to "jump" to a position involving large deflections. The kinetic energy associated with the rapid increase in deflection will cause the shell to vibrate around the equilibrium position corresponding to the "minimum" buckling load. This vibration will be rapidly damped by both the intrinsic friction of the material and the forces exerted by the testing machine.

It is a common engineering practice to record the maximum load which the structure can sustain as the failing load of the structure. Therefore, in the case of the perfect specimen, the "initial" buckling load will be the failing load. However, similar to the column with a non-linear elastic support shown in Section II, the maximum load which the shell can sustain is very sensitive to the amount of initial deflection of the shell. Larger deviations from the perfect geometrical shape will give a lower maximum load, without, perhaps, an appreciable effect on the "minimum" buckling load. Therefore, without extreme precautions, both in the manufacture of the specimen and in the testing, the failing load obtained will be invariably lower than the theoretical maximum given by the classical linear theory. But, this consideration also shows that by striving to make the test specimen geometrically perfect, as has been done by certain investigators, it is possible to obtain higher failing loads than usual, approaching the value given by the classical theory as an upper limit. The particular value of the failing load of a specimen is, therefore, determined by the degree of its geometrical perfection. This, perhaps, is one of the reasons for the bad scattering of the experimental points shown in Fig. 13. However, there seems to be a lower limit which corresponds to the "minimum" buckling load.

This explanation of the large difference between the failing load obtained by the classical theory and in experiments has a similarity with Donnell's theory for thin cylindrical shells[11] in that the initial deflection is a controlling factor in determining the failing load. However it should be clearly understood that whereas Donnell assumed that failure was caused by yielding of the material, the present explanation is based on the non-linear characteristics of certain elements of the structure without exceeding the elastic limit of the material.

Besides the effect of the initial deflection on the failing load of a thin shell, the effect of vibration occurring in the surroundings during the testing of the specimen should be considered. If a specimen with slight geometrical imperfections is loaded up to, say, the point A in Fig. 20, the vibrations occurring in the surroundings will impart a certain amount of kinetic energy to the specimen. This additional amount of kinetic energy when transformed into potential energy might be sufficient to help the specimen to pass the "hump" in the load-deflection curve and thus fail the specimen. The failing load recorded by the testing machine is, however, only that corresponding to the point A and not the maximum load. Therefore, the vibrations occurring in the testing surroundings can further reduce the failing load of a curved shell, besides the effect of initial deflections.

References

[1] von Kármán, Th., *Untersuchungen über Knickfestigkeit*, Forschungsarbeiten, No. 81, Berlin, 1910.

[2] Timoshenko, S., *Theory of Elastic Stability*, pages 390–393; McGraw-Hill, New York, 1936.

[3] Marguerre, K., *Die mittragende Breite der gedrückten Platte*, Luftfahrtforschung, Vol. 14, pages 121–128, 1937.

[4] Marguerre, K., and Trefftz, E., *Über die Tragfähigkeit eines Plattenstreifens nach Überschreiten der Beullast*, Z.A.M.M., Vol. 17, pages 85–100, 1937.

[5] Cox, H. L., *The Buckling of Thin Plates in Compression*, British A.R.C. Reports and Memoranda, No. 1554, 1933.

[6] Yamamoto, M., and Kondo, K., *Buckling and Failure of Thin Rectangular Plates in Compression*, Rep. of Aero. Res. Inst., Tokyo, No. 119, 1935.

[7] von Kármán, Th., Sechler, E. E., and Donnell, L. H., *The Strength of Thin Plates in Compression*, Transactions A.S.M.E., Vol. 54, pages 53–57, 1932.

[8] Marguerre, K., *Die Durchschlagskraft eines schwach gekrümmten Balkens*, Sitzungsberichte der Berliner Mathematischen Gesellschaft, Vol. 37, pages 22–40, 1938. See also *über die Anwendung der energetischen Methode auf Stabilitätsprobleme*, Jahrbuch der Deutschen Versuchsanstalt für Luftfahrt, 1938, pages 252–262, by the same author.

[9] von Kármán, Th., and Tsien, Hsue-Shen, *The Buckling of Spherical Shells by External Pressure*, Journal of the Aeronautical Sciences, Vol. 7, pages 43–50, 1939.

[10] Lundquist, E. E., *Strength Tests of Thin-Walled Duralumin Cylinders in Compression*, N.A.C.A. Technical Report, No. 473, 1933.

[11] Donnell, L. H., *A New Theory for the Buckling of Thin Cylinders Under Axial Compression and Bending*, Transactions A.S.M.E., Vol. 56, pages 795–806, 1934.

[12] Flügge, W., *Die Stabilität der Kreiszylinderschale*, Ingenieur-Archiv, Vol. 3, pages 463–506, 1932.

[13] A review of these works together with references is given in S. Timoshenko's *Theory of Elastic Stability*, pages 100–112; McGraw-Hill, New York, 1936.

[14] Wenzek, W. A., *Die Mittragende Breite nach dem Ausknicken bei krummen Blechen*, Luftfahrtforschung, Vol. 15, pages 340–344, 1938.

[15] Dschou, D. D., *Die Druckfestigkeit versteifter zylindrischer Schalen*, Luftfahrtforschung, Vol. 11, pages 223–234, 1935.

[16] Taylor, J. L., *Stability of a Monocoque in Compression*, British A.R.C. Reports and Memoranda, No. 1679, 1935.

[17] Ryder, E. I., *General Instability of Semi-monocoque Cylinders*, Air Comm. Bulletin, Vol. 9, pages 241–246, 1938.

New Developments in the Theory of Airfoils of Infinite Span

R. VON MISES
Harvard University

ABSTRACT

This paper gives some supplementary developments and revisions of the two dimensional airfoil theory. (1) The chief results are reviewed and the concept of "second axis" of a profile is revised. (2) In discussing stability questions the theory of Hamilton's center is referred to. (3) The method of successive approximations is outlined in its relation to the so-called thin-wing theory. (4) The addition of two independent lift-force systems is explained. (5) The general theorem is proved that in any case of several airfoils with mutual interference the lift force follows the same laws in its dependency on the angle of attack as in the case of a single wing.

IN 1917 and 1920 the author published two papers[1] in which, for the first time, a general and complete solution of the lift problem for an airplane wing of infinite span was given. About the same time Prandtl developed his famous theory of vortex motion behind an airfoil which supplies a most valuable estimation of the influence of the finite ends. Both theories form today the basis of the practical computations in airfoil design and both are the subject matter of numerous papers continuously being published in almost all countries. In that which follows the author presents some supplementary developments and revisions to his former papers, suggested in part by recent publications.

1. THE CHIEF RESULTS OF THE THEORY

The principal results of the theory are the following. To any cross-section of an airfoil which has a sharp trailing edge (B in Fig. 1), there corresponds a point

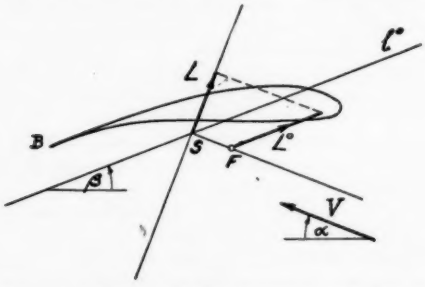

FIG. 1. Lift magnitude, direction, and line of action.

F, a straight line l° and a vector L° parallel to l°. These elements, depending on five parameters (two coordinates of F, direction and position of l°, magnitude of L°) entirely determine the lift force for every angle of attack α. It is only necessary to draw through F a parallel to the velocity V at infinity (at the angle α to the x axis). The lift L is perpendicular to V, its line of action passes through the point of intersection of the parallel to V with l° and its magnitude equals the projection of L° (see Fig. 1). It is easy to see that the lines of action so determined envelop a parabola with focus at F and with l° as vertex tangent. If the direction of the flow at infinity is normal to l°, then l° and L° immediately give the line of action and the magnitude of the lift.

The elements F, l°, L° are connected with the cross-section of the profile through the theory of conformal transformation. If z designates the complex number (or the vector) $x + iy$ corresponding to a point x,y of the profile or its surroundings, then a function $f(z) = z' = x' + iy'$ relates to the point x,y another point x',y' and this correspondence is called a conformal transformation. If the difference $z - z'$ vanishes for infinite values of z and z', the transformation leaves infinity unchanged. The decisive theorem is the following: There exists one and only one conformal transformation, leaving infinity unchanged, which transforms the outside of a given closed curve (the profile) into the outside of a circle. This circle, its center M and its radius a (Fig. 2), are uniquely

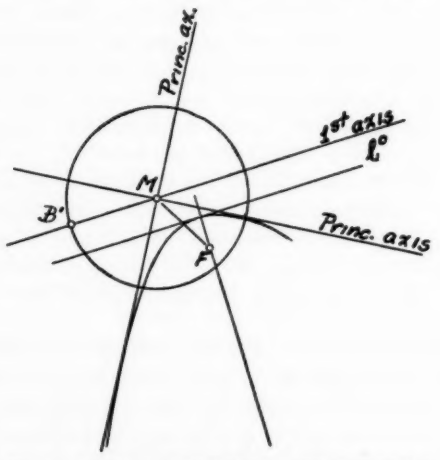

FIG. 2. First axis, principle axes, and metacentric parabola.

determined by the given profile and so is the first coefficient k in the expansion of $z - z'$:

$$z - z' = \frac{k}{z'} + \ldots = \frac{k}{z} + \ldots \qquad (1)$$

where the dotted terms are of higher order in z' or z. If B′ is the point of the circle into which the singular

Presented at an Aerodynamics Session, Eighth Annual Meeting, I.Ae.S., New York, January 25, 1940.

point B of the profile is mapped, then MB′ is the direction of l°. The point F is determined by the fact that the vector or the complex number MF equals the quotient $k/\overline{\text{MB}}'$. The straight line l° halves the distance between F and MB′ and L° is given by

$$L^\circ = 4\pi\rho V^2 a \tag{2}$$

where ρ is the density of the air. If h is the distance between F and l° (positive when F lies above l°) the moment of the lift with respect to F is $M_F = L^\circ h$, and is independent of the angle of attack α. From these geometrical facts follow immediately the usual formulas for lift L and moment M with respect to the center of the mapping circle:

$$L = L^\circ \sin(\alpha + \beta);\quad M = L^\circ \frac{c^2}{2a} \sin 2(\alpha + \gamma) \tag{3}$$

where β is the angle of the first axis, $c^2 = |k|$ and $2\gamma = \arg k$.

In his first publications the author introduced the name "first axis of the profile" for MB′ and "focus of the profile" for F. Moreover the word "second axis of the profile" was used for the straight line bisecting the angle between MF and MB′ which touches the parabola and is a line of action passing through M. But this latter definition is not correct, because there are two directions, perpendicular to each other, both of which have the same properties. The real meaning of these directions is the following: The conformal transformation which converts the circle of radius a into the given profile, transforms any circle with a very large radius R into an ellipse the semi-axes of which are of length $R \pm |k|R$ and run parallel to the bisectors of the angle B′MF. So it would be better to speak of the "pair of principal axes of the profile" instead of a second axis. It is obvious that one of these principal axes will be almost parallel to the longest diameter of the profile and the other perpendicular to it. The complex value k which determines both the lengths and the directions of the principal axes can be called the "deformation coefficient" of the transformation."

2. Stability Questions

The parabola enveloped by the lines of action l is the metacentric curve of the airfoil. The point P where the line of action touches the parabola and which can be obtained by FP′$\|l$, SP′ $\perp l^\circ$, P′P$\|$FS, is the metacenter.

A supporting system such as an airplane wing in itself is neither stable nor unstable. If the load which is to be supported has its center of gravity below the metacenter, the system can be called stable; in the opposite case it is unstable. This conception corresponds to the usual assumptions about the disturbances that may occur. In most cases h is negative and the parabola is directed downward as shown in Figs. 2 and 3. For $h > 0$ the parabola lies above the vertex tangent l° and then the condition that the center of gravity ought to lie below P can be more easily fulfilled. But there is no reason to call an airfoil profile "stable" when h is positive or of "indifferent equilibrium" in the case where $h = 0$ and all lines of action pass through F.

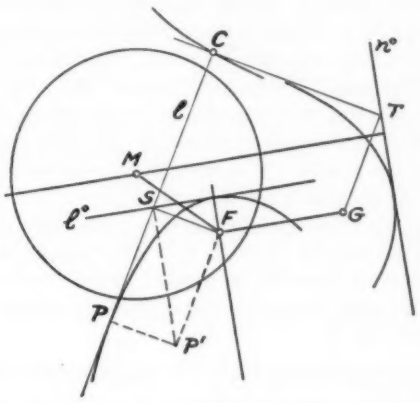

Fig. 3. First and second foci; Hamilton center C.

Another point of view for the discussion of stability is supplied by the so-called "astatic" theory or theory of Hamilton's center of a force system. If w designates the complex potential so that the derivative w' represents the (reflected) velocity vector, the moment of the air force with respect to the point z_0 is determined by

$$M + Ni = -(\rho/2)\oint w'^2(z - z_0)dz \tag{4}$$

The real part of the integral gives the moment, the imaginary part N the "virial" of the forces. The points z_0 for which M vanishes form the line of action of the resultant force. The points for which the imaginary part N equals zero lie on a straight line which is perpendicular to the resultant force and is called the Hamilton axis of the system. The point determined by

$$z_0 = \frac{\oint z w'^2 dz}{\oint w'^2 dz} \tag{5}$$

for which both M and N are zero is the Hamilton center. That is the point about which the line of action turns if all pressure elements turn about their respective points of application. If it is assumed that after a small accidental turning of the airfoil, in the very first instant, the pressures keep their original values, then the stability condition would require that the center of gravity lie below the Hamilton center.

It is easy to see that the axes $N = 0$ can be found in a similar way as the lines of action $M = 0$. There exists a second focus G and a straight line n° perpendicular to l°. By drawing GT normal to the velocity V and TC parallel to V, TC is the axis and C the Hamilton center. The straight lines $N = 0$ envelop a parabola with focus at G and with n° as vertex tan-

gent. The locus of the centers C is a curve of third order. The second focus G is determined by the facts that FG is parallel to the first axis and $\overline{FG} = a$. Furthermore the distance between the vertex tangent n° and the center M of the mapping circle equals $2a$.

In the case of $h < 0$, as Fig. 3 shows, the centers C lie above the metacenters P so that the new point of view adds nothing to the stability condition. But in the case $h > 0$ where the metacentric parabola lies above the first axis the Hamilton centers are found below this axis. This could impair the value of a positive h. But it is not the author's aim to recommend the unlimited application of this modified stability conception. It seemed, however, not without interest to present it for discussion.

The whole stability investigation gains more interest when it is realized (Section 4 of this paper) that all concepts used here can be applied to the combination of a supporting wing with a stabilization surface.

3. Determination of the Lift Parameters

All practical methods for computing the parameters for a given profile are based upon the fact that the cross-sections used in airplane design are very similar to each other: They are slender crescent shapes of slight curvature. In most cases a suitably chosen straight line (an infinitely narrow strip) can be considered as first approximation. Hence the so-called theory of thin wings which, however, involves an assumption which is almost never fulfilled: that the average thickness of the cross-section is of lower order of magnitude than the deviations of its border from the assumed middle straight line. A method avoiding this disadvantage and supplying a set of successive approximations for any required accuracy can be outlined as follows.[2]

If the given profile P is close to a profile P′ for which the mapping circle (center M′, radius a') and the mapping function $z = f(z')$ are known, then the inverse transformation applied to P will convert this profile into a curve C which is near to the circle M′, a'. It is, of course, necessary that the trailing edges of P and P′ coincide, that the tail angles are equal in both cases, and that no singular point of the transformation lies outside P. The equation in polar coordinates of the curve C may be $r = a'[1 + \eta(\phi)]$ where $\eta(\phi)$ is a small quantity.

Here, it is possible to apply a theorem about conformal transformations which states: If

$$\eta(\phi) = a_0 + a_1 \cos\phi + \ldots + b_1 \sin\phi + \ldots \quad (6)$$

is an absolutely convergent Fourier series (expansion of a twice differentiable function) then the transformation

$$z - z' = \lambda z'[a_0 + (a_1 + b_1 i)a'/z' + \ldots] \quad (7)$$

converts the circle of radius a' into a curve for the polar equation $r = r(\phi)$ of which

$$\lim_{\lambda = 0} \frac{r(\phi) - a'}{\lambda} = a'\eta(\phi) \quad (8)$$

This means that, if $\eta(\phi)$ is small enough, the transformation (7) with $\lambda = 1$ will transform approximately the circle M′,a' into the curve C. It follows from a short consideration how the coefficients of the Fourier series (6) or the function $\eta(\phi)$ itself can be used for correcting the first assumptions regarding the parameters. In the transformation corresponding to P′ (the auxiliary profile) let a' be the radius, m' the vector to the center M′, β' the angle of the first axis and k' the deformation coefficient. Then the corrected values will be

$$\left.\begin{aligned} a &= a'(1 + a_0) = a' + \frac{a'}{2\pi}\int_0^{2\pi} \eta(\phi)d\phi \\ m &= m' + a'(a_1 + b_1 i) = m' + \frac{a'}{\pi}\int_0^{2\pi} \eta(\phi)e^{\phi i}d\phi \\ k &= k' + aa'(a_2 + b_2 i) = k' + \frac{aa'}{\pi}\int_0^{2\pi} \eta(\phi)e^{2\phi i}d\phi \\ \beta &= \beta' + \frac{1}{2\pi}\int_0^{2\pi} \eta(\beta' + \phi)\tan\frac{\phi}{2}\,d\phi \end{aligned}\right\} \quad (9)$$

In this way the complete solution can be found to a second approximation by means of six integrations.

The thin wing theory uses a straight line of length $4c$ as a first approximation to the profile. Then the corresponding first transformation is given by $z = z' + c^2/z'$ if the straight line is assumed as x axis and its middle point as origin. Whence,

$$a' = c,\ m' = 0,\ \beta' = 0,\ k' = c^2$$

If, as usual, the computations are restricted to small values of the angle of attack α, disregarding all terms which are of higher order in α and in the corrections, only two of the six integrals mentioned above are needed:

$$\left.\begin{aligned} L &= 4\pi\rho V^2 c\left[\alpha + \frac{1}{2\pi}\int_0^{2\pi} \eta(\phi)\tan\frac{\phi}{2}\,d\phi\right] \\ M &= 4\pi\rho V^2 c^2\left[\alpha + \frac{1}{2\pi}\int_0^{2\pi} \eta(\phi)\sin 2\phi d\phi\right] \end{aligned}\right\} \quad (10)$$

These are, essentially, the formulas used in the thin wing theory. But this theory fails by assuming a too simple relation between the function $\eta(\phi)$ and the given boundary of the profile: The straight line is chosen as the chord of the middle line of the profile and the coordinates of this line are assumed to be $x = 2c\cos\phi$, $y = 2c\eta(\phi)\sin\phi$. This is an admissible approximation only for the points of the boundary which are sufficiently distant from the leading edge. The error in computing the two integrals of (10) in this way may reach 10 to 15 per cent. To be correct one must choose as auxiliary profile the straight line running from the trailing edge nearly to the center of curvature of the

leading edge and then use a graphical method for the inverse transformation. The best way to do it is to outline the networks consisting of two sets of corresponding circles in the z plane and z' plane (see Fig. 4).

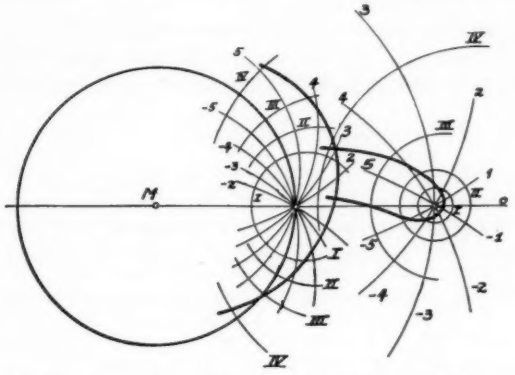

FIG. 4. Conformal transformation of the leading edge of an airfoil.

If the first correction seems to be insufficient, one may perform a second step according to the general formulas (9) given above. In this way any required accuracy can be reached.

4. Systems of Independent Wings

If two or more airfoils sufficiently distant from each other are exposed to the same flow, one may assume to a first approximation that there is no mutual interference between them. To each single wing corresponds a lift force L_ν whose dependence on the angle of attack α is given by a focus F_ν, straight line l_ν°, and vector L_ν°. The resultant of all L_ν is a force depending on α too and the theorem that this force is of the same kind as each single L, will be established, *i.e.*, there is a focus F, straight line l° and vector L° so that for every α the resultant lift L can be deduced from the elements F, l°, L° in the way described in §1.

As to the magnitude and direction of L there is no difficulty. All L for a given angle α are parallel and the resultant force has, of course, the same direction. The lengths L are the projections of the vectors L° in the common direction normal to V. The sum of the projections is obviously the projection of the geometrical or vector sum of $L_1^\circ, L_2^\circ, \ldots L_n^\circ$.

In order to prove the theorem it is only necessary to show that a point F for which the moment of the parallel forces $L_1, L_2, \ldots . L_n$ is independent of α exists. As stated in §1, every individual lift force L_ν can be replaced by a force (of the same magnitude and direction) acting at F_ν plus a moment which is not dependent on α. Therefore, in dealing with F it can be assumed that all the individual lift forces L_ν have the respective foci F_ν as points of application.

Now, the best method to compute the moment is, for present purposes, to use complex numbers. If the force whose components are X_ν and Y_ν is applied to the point $z_\nu = x_\nu + iy_\nu$, then the moment M and the virial N of this force with respect to the point $z = x + iy$ are given by

$$M + Ni = i(z_\nu - z)(X_\nu - iY_\nu) \tag{11}$$

The lift force L_ν has the magnitude $L_\nu^\circ \sin(\alpha + \beta_\nu)$ and its angle with the x axis is $\pi/2 - \alpha$. Hence the expression for $X_\nu + iY_\nu$ becomes

$$X_\nu - iY_\nu = -L_\nu^\circ \sin(\alpha + \beta_\nu) ie^{\alpha i} = -\tfrac{1}{2} L_\nu^\circ [e^{(2\alpha + \beta_\nu)i} - e^{-\beta_\nu i}] \tag{12}$$

If x_ν, y_ν are the coordinates of F_ν, the value $M + Ni$ for the whole system is equal to

$$M + Ni = -\tfrac{1}{2} i \sum (z_\nu - z) L_\nu^\circ [e^{(2\alpha + \beta_\nu)i} - e^{-\beta_\nu i}] \tag{13}$$

This expression is independent of α, if z is chosen in a way such that

$$\sum (z_\nu - z) L_\nu^\circ e^{\beta_\nu i} = 0, \text{ or } z = \frac{\sum z_\nu L_\nu^\circ e^{\beta_\nu i}}{\sum L_\nu^\circ e^{\beta_\nu i}} \tag{14}$$

The point determined by (14) satisfies the conditions of the theorem and so this theorem is proved.

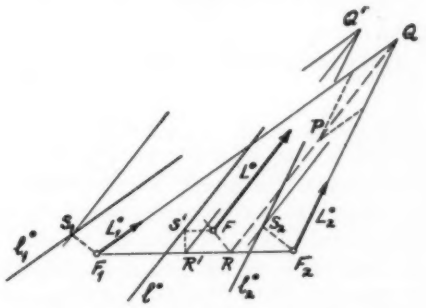

FIG. 5. Composing of two lift force systems.

In quite the same way a second point G exists for which the sum of the virials of all the individual lift forces is constant. As shown in §2, for a single wing such a point G_ν exists. Therefore, if one introduces in Eqs. (13) and (14) for z_ν the coordinates of the G_ν instead of the F_ν, the resultant point will be G.

The figure shows how the resultant elements F, l°, L° can be found, if for two single airfoils the elements F_1, l_1°, L_1°, and F_2, l_2°, L_2°, are given. First the vector L° is found as the vector sum PQ of L_1° and L_2°. Then, by drawing F_1S_1 and F_2S_2 normal to the direction of L° the lines of action of the two air forces are obtained in the case where they are parallel to L°. The resultant of these two forces has l° as line of action. Finally to find F it can be seen that Eq. (14) expresses the fact that F is the Hamilton center of forces of magnitudes L_ν° applied at the points F_ν and acting in directions β_ν. So F must lie on the straight line RF which is symmetrical to the resultant QPR with respect to F_1F_2. On the other hand the line of action of the resultant force L in the case where the

flow is parallel to F_1F_2 can easily be found by taking the intersection of $l_1°$ and $l_2°$ at Q′ and drawing Q′R′$\|$ QR. Then R′S′ $\perp$ F_1F_2 and S′F$\|F_1F_2$ give a second location for F.

If this method is applied to the combination of an airplane wing with an almost plane tail surface, it is easily seen that the resultant metacentric parabola lies above the longitudinal axis. This means that the usual stability condition will be fulfilled as long as the center of gravity does not lie too far above this axis.

5. General Case of Wing Systems

It turns out, even in the general case of several airfoils with mutual interference that the character of the lift force in its dependency on the angle α is the same as for a single wing. The proof of this statement may conclude the present remarks.

As in §3, the complex potential is designated by w and its derivative with respect to z or the reflected velocity vector by w'. Then w is a function of z which at infinity, admits the development

$$w' = A + \frac{B}{z} + \frac{C}{z^2} + \ldots,$$

$$w'^2 = A^2 + \frac{2AB}{z} + \frac{2AC + B^2}{z^2} + \ldots \quad (15)$$

The coefficients $A, B, C, \ldots$ are determined by two conditions: first, that at the boundaries of the given profiles the normal component of the velocity vector vanishes; second, that the velocity at infinity has the given components $V_x = -V\cos\alpha$ and $V_y = V\sin\alpha$. Now the first of these conditions is homogeneous; hence the whole problem (the differential equation for w) is linear. Therefore two solutions for different values of V_x, V_y can be superposed; the resulting solution corresponds to the sums of the respective values of the V_x and of the V_y. It follows that all coefficients $A, B, C, \ldots$ must be *linear* functions of V_x and V_y.

The first coefficient A equals immediately the reflected vector of the velocity at infinity:

$$A = -Ve^{\alpha i} \quad (16)$$

The second coefficient B must be an imaginary number. For, the imaginary part of the integral

$$\oint w'dz = 2\pi iB$$

gives the sum of sources and sinks within the velocity field. But it is assumed that the velocity field is thoroughly regular outside the airfoil profiles. So one has, with real constants b_1, b_2:

$$B = (b_1V_x + b_2V_y)i = V(-b_1\cos\alpha + b_2\sin\alpha)i = -2aiV\sin(\alpha + \beta) \quad (17)$$

with $\sqrt{b_1^2 + b_2^2} = 2a$, $-b_1/b_2 = \tan\beta$

As to the third coefficient, C, there is no restriction except for the fact that it must be a linear function of V_x and V_y or of $Ve^{\alpha i}$ and $Ve^{-\alpha i}$:

$$C = c_1'V_x + c_2'V_y = V(c_1e^{\alpha i} + c_2e^{-\alpha i}) \quad (18)$$

with complex values c_1, c_2.

The hydrodynamic theory shows that the lift components L_x, L_y and the moment M and virial N with respect to a point z_0 can be computed from the formulas

$$L_x - iL_y = {}^1/_2\rho i\cdot\oint w'^2dz$$
$$M + Ni = -{}^1/_2\rho\oint(z - z_0)w'^2dz \quad (19)$$

If the second expression (15) is introduced and use is made of the residue theorem, as above,

$$L_x - iL_y = {}^1/_2\rho i\cdot 2\pi i\cdot 2AB = -4\pi\rho V^2a\sin(\alpha + \beta)ie^{\alpha i} \quad (20)$$

This means that the force with components L_x, I_y is normal to the flow vector and has the magnitude $4\pi\rho V^2a\sin(\alpha + \beta)$.

In the same way

$$M + Ni = -{}^1/_2\rho\cdot 2\pi i(2AC + B^2 - z_0 2AB)$$
$$= 2\pi\rho V^2i[c_1e^{2\alpha i} + c_2 + 2a^2\sin^2(\alpha + \beta) + 2az_0\sin(\alpha + \beta)e^{\alpha i}] \quad (21)$$

The value

$$z_0 = -(c_1/a)e^{-\beta i} \quad (22)$$

is introduced. Then the expression reduces itself by a brief computation to

$$M + Ni = 2\pi\rho V^2i[c_2 + 2a^2\sin^2(\alpha + \beta) + c_1e^{-2\beta i}] \quad (23)$$

Here the real part of $M + Ni$ does not depend on α. This means that in (22) a focus F, *i.e.*, a point with constant moment has been found. On the other hand by using

$$z_0 = -(c_1/a)e^{-\beta i} + ae^{\beta i} \quad (24)$$

the equation (21) for $M + Ni$ becomes

$$M + Ni = 2\pi\rho V^2i[c_2 + a^2i\sin 2(\alpha + \beta) + c_1e^{-2\beta i}] \quad (25)$$

Now the imaginary part of $M + Ni$ is independent of α. In other words the point (24) is the second focus G for which the virial is constant. So the characteristic properties of the force system are deduced without any assumption concerning the shape or the number of airfoil sections involved.

References

[1] von Mises, R., Zeitschr. f. Flugtechnik 1917, pages 157–163; 1920, pages 68–73, 87–89. Zeitschr. f. angew. Mathem. u. Mechanik 1922, pages 71–73.

[2] The essential idea of this approximation method was outlined by Th. v. Kármán and E. Trefftz, Zeitschr. f. Flugtechn. 1918, page 111 and developed by W. Müller, Zeitschr. f. angew. Mathem. u. Mechanik 1926, page 265.

A Simplified Method for Determining Wing Profile Drag in Flight

A. SILVERSTEIN AND S. KATZOFF

National Advisory Committee for Aeronautics

ABSTRACT

The determination of wing profile drag by means of total-pressure and static-pressure measurements in the wing wake provides a technique applicable in flight. The use of the method is difficult, however, outside of a research laboratory without considerable simplification of instruments and calculations; and extensive use by aircraft designers to study effects of wing surface roughness, protuberances, etc., is restricted.

In this paper the design of an instrument to simplify the pressure measurements is presented. It consists of a total-head rake that can be attached to the wing trailing edge to measure the average total pressure in the wing wake. Charts are given to convert the average total pressures into drag coefficients. The calculations on which the instrument design and charts are based are given, together with instructions for practical application.

INTRODUCTION

THE momentum method of determining profile drag by means of pressure measurements in the wake has been an important addition to experimental aerodynamics. The equations that Betz[1] and Jones[2] developed for the practical application of the method have been amply verified.[3] The momentum method is of particular interest for the measurement of profile drag in flight for which no other practicable method exists. It was believed that extensive application of the method in flight by aircraft manufacturers to determine effects of wing roughness, protuberances, etc., would be encouraged by a simplification of the instruments and the calculations required.

Two experimental techniques have been widely used to measure the total and the static pressures in the wake. In one of the techniques, all of the measurements are made simultaneously by means of a rake of total-pressure and static-pressure tubes with connections from each tube leading to a recording or averaging manometer. In the other technique, a mechanically driven pitot tube traverses the wake point by point. The rake method is advantageous in providing simultaneous observations of all the pressures in the wake but is awkward because of the numerous pressure connections and the multitube manometer that must be installed. The traversing system provides excellent results with careful use but is susceptible to errors, owing to changes in flight conditions that may occur during the wake traverse.

This paper describes an instrument in which an attempt has been made to combine the advantages of the rake and the traversing pitot. It consists of a rake of equally spaced total-head tubes that are connected to a common reservoir. A similar instrument has been discussed in reference 4. As will be shown, the drag is a function of the pressure in the reservoir and it is therefore necessary for only a single pressure tube to pass from the rake to the cockpit. In some cases, however, the static pressure in the wake must also be measured. The total-pressure tubes and the reservoir are assembled into a streamline body that is so supported, preferably at about 0.15 to 0.30 chord length behind the trailing edge of the wing (Fig. 1), that the centers of the wake and the rake coincide. The bore of the total-head tubes must be small and, for structural rigidity, they are located concentrically within larger and stiffer tubes. (See *A-A* in Fig. 2.) Two pressure indicators similar to airspeed meters are the only additional equipment required.

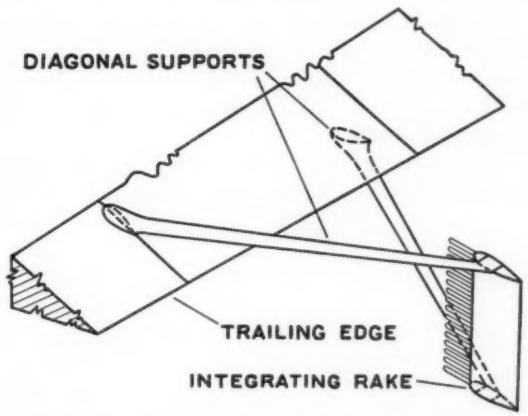

FIG. 1. Isometric view of integrating total-pressure rake.

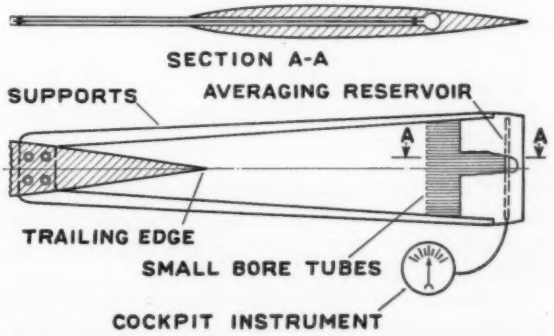

FIG. 2. Two-view drawing of integrating total-pressure rake.

Presented at the Aerodynamics Session, Eighth Annual Meeting, I.Ae.S., New York, January 25, 1940.

The theory underlying this method has been studied in considerable detail. Particular attention has been directed to possible sources and magnitudes of the errors including those due to compressibility and many of the important concepts have been experimentally verified. In order to facilitate application, charts are given to enable the instrument indications to be readily converted into drag coefficients.

Theory of Method

Disregarding slight corrections to be considered later, the flow in each tube is proportional to the difference $H_1 - p_r$ between the stagnation pressure H_1 at its forward opening and the pressure p_r in the reservoir. Thus

$$\bar{u} = \kappa(H_1 - p_r)$$

where κ is a proportionality constant and $\bar{u}$ is the mean velocity in the tube.

At equilibrium, the algebraic sum of the flow through all the tubes is zero:

$$\sum_n \bar{u} = \kappa \sum_n (H_1 - p_r) = \kappa \left[\sum_n H_1 - np_r\right] = 0$$

where n is the number of tubes.

Then $p_r = (1/n) \sum_n H_1$; that is, p_r is the average value of H_1 across the width of the rake.

The difference between this pressure and the free-stream total pressure is the average total-head loss across the width of the rake. The integral of the total-head loss across the wake is found by multiplying this average by the rake width.

This integral is, to a rough approximation, proportional to the drag coefficient; thus,

$$c_{d_0} \cong (1/cq) \int_{wake} (H_0 - H_1) dy$$

or, more precisely,

$$c_{d_0} = \frac{F}{c} \int_{wake} \frac{H_0 - H_1}{H_0 - p_0} dy = F \frac{w}{c} \frac{H_0 - H_{1_{av}}}{H_0 - p_0} \quad (1)$$

where

c_{d_0} = section profile-drag coefficient;
F = a factor, usually about 0.8 to 0.9;
c = wing chord;
H = total pressure;
p = static pressure;
y = vertical distance from wake center;
w = height of rake;

and the subscript 0 represents values pertaining to the free stream; the subscript 1, values pertaining to the plane of measurement; and the subscript av, average values.

The accurate estimation of the factor F then becomes the most important step in the evaluation of the profile drag with this instrument.

Wake Characteristics

The possibility of developing a reasonably simple method of estimating F depends on the fact that the wake characteristics are determined almost solely by the profile-drag coefficient.

The total pressure is a minimum in the center of the wake and increases to free-steam total pressure at the wake edge. The distribution across most of the wake is given with good accuracy by the equation

$$H_0 - H_1 = (H_0 - p_0)\, \eta \cos^2 y\pi/\zeta \quad (2)$$

where

η = (maximum total pressure loss in wake)/$(H_0 - p_0)$. The parameter ζ is designated the wake width although, since Eq. (2) is approximate, the region in which a measurable deficiency of total pressure exists is frequently slightly more than ζ in width.

Equations and curves useful for estimating the values of η and ζ as functions of the drag coefficient and the distance behind the trailing edge are given in Figs. 3 and 4. (See reference 5.)

The static pressure is practically uniform across the wake. Its value increases with wing thickness and decreases with distance from the trailing edge. The wake itself effects a slight decrease in the static pressure, as compared with that for potential flow. In Fig. 5 are shown curves of the static pressure as a function of wing thickness and distance behind the trailing edge. These curves apply for wings that have their maximum thickness $0.3c$ back of the leading edge and represent experimental results and theoretical studies of wings with wakes.[3]

The static-pressure field of the fuselage reduces the static pressures behind the airplane wing below that shown on the curves of Fig. 5 by about 0.01 to 0.04 of the free-stream dynamic pressure q_0 depending on the fineness ratio of the fuselage and on the distance from it. The amount of this correction, as calculated for positions at which wake measurements will normally be made, is shown in Fig. 6.

Calculation of F *at Low Speed*

Assume a wake in which the distribution of total pressure is given by Eq. (2) and in which the static pressure is p_1. By the Jones equation

$$c_{d_0} = \frac{2}{c} \int_{wake} \sqrt{\frac{H_1 - p_1}{H_0 - p_0}} \left(1 - \sqrt{\frac{H_1 - p_0}{H_0 - p_0}}\right) dy \quad (3)$$

or, on substitution from Eq. (2),

$$c_{d_0} = \frac{2}{c} \int_{wake} \sqrt{1 - \frac{p_1 - p_0}{H_0 - p_0} - \eta \cos^2 \frac{\pi y}{\zeta}} \times \left(1 - \sqrt{1 - \eta \cos^2 \frac{\pi y}{\zeta}}\right) dy \quad (4)$$

which may be evaluated for assumed values of η and $(p_1 - p_0)/(H_0 - p_0)$ with reasonable facility. The corresponding value of $\int_{wake}(H_0 - H_1)/(H_0 - p_0)dy$ is $\eta\zeta/2$, which, on substitution in Eq. (1), gives

$$c_{d_0} = F\eta\zeta/2c \qquad (5)$$

Comparison of Eqs. (4) and (5) gives F as a function of η and $(p_1 - p_0)/(H_0 - p_0)$.

Values of F were computed for various values of the two parameters; the results are shown in the chart of Fig. 7. When the chart is used, the value of $(p_1 - p_0)/(H_0 - p_0)$ is either measured or estimated from Figs. 5 and 6. The value of η is estimated from Fig. 3, using a value for c_{d_0} obtained roughly by a system of successive approximations; thus, a preliminary value of η is first determined from an estimated value of c_{d_0}, and the value of c_{d_0} corresponding to this value of η is used to determine a more accurate value of η.

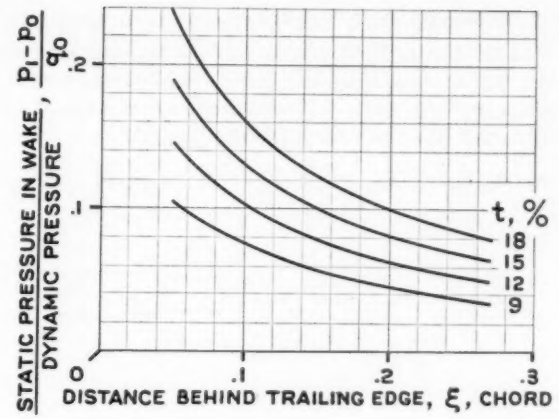

FIG. 5. Variation of static-pressure coefficient with wing thickness and distance from trailing edge (no fuselage).

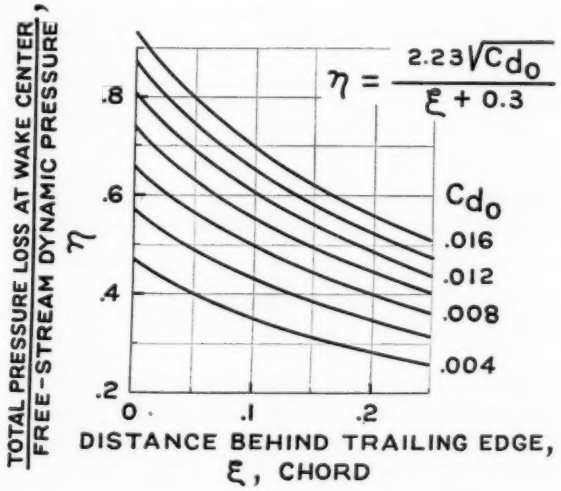

FIG. 3. Variation of η with drag coefficient and distance from trailing edge.

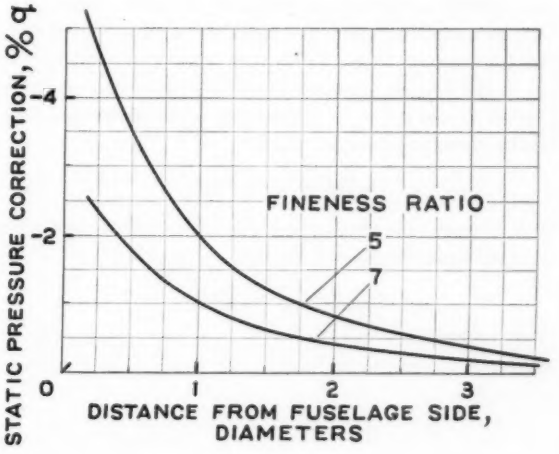

FIG. 6. Effect of the fuselage on the static-pressure coefficient.

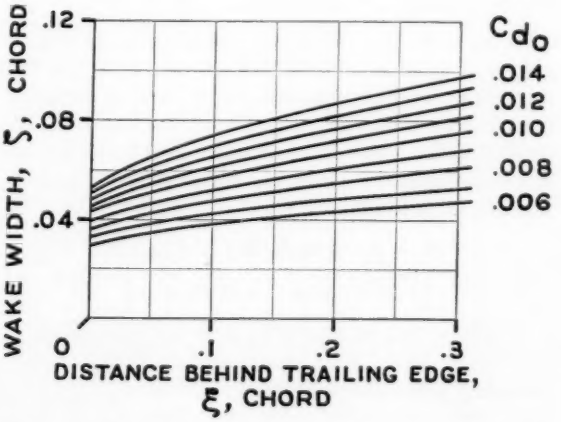

FIG. 4. Variation of wake width ζ with drag coefficient and distance from trailing edge.

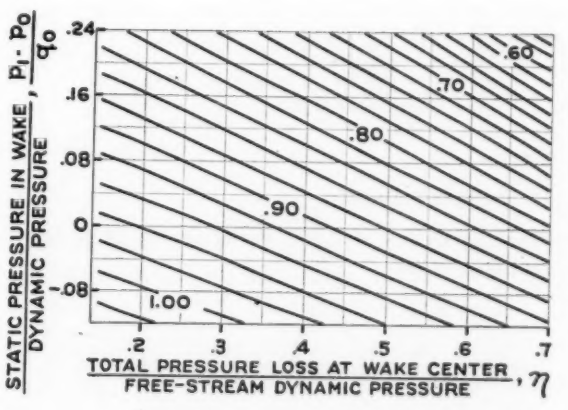

FIG. 7. Contours of F as a function of static-pressure coefficient and η.

Compressibility Correction to F

At the higher flight speeds, Eq. (3) becomes inaccurate due to compressibility and to the increased temperature of the wake. The method of evaluating F at the higher Mach Numbers follows (Fig. 8).

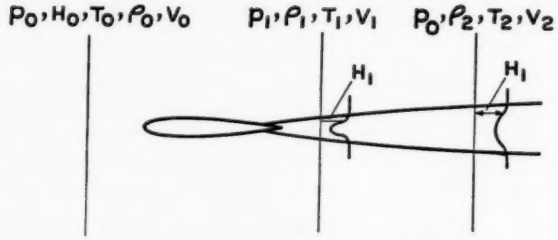

FIG. 8. Description of wake. H and $(T_2 - T_0)/T_0$ are given by $H = p_0[1 + 0.7025(V/V_c)^2 + 0.1756(V/V_c)^4 + 0.0174(V/V_c)^6 + \ldots\ldots]$; $(T_2 - T_0)/T_0 = 0.202(V_0/V_{c_0})^2 \times [1 - (V_2/V_0)^2]$.

Assume a velocity distribution V_2/V_0 in the wake at the rearmost plane corresponding to some value of η. The subscript 2 refers to values for a plane far downstream where $p_2 = p_0$. The drag increment corresponding to the flow in a lamina of width dy_2 (in the rearmost plane) is $\rho_2 V_2(V_0 - V_2)dy_2$, and the corresponding work expended per unit time is

$$\rho_2 V_2 V_0(V_0 - V_2)dy_2$$

The kinetic energy produced in this lamina per unit time by the airplane in flight is

$$\tfrac{1}{2}\rho_2 V_2(V_0 - V_2)^2 dy_2$$

If the difference between the last two expressions is assumed to remain as heat in the lamina, its temperature rise is

$$T_2 - T_0 = [\tfrac{1}{2}\rho_2 V_2(V_0^2 - V_2^2)dy_2]/(c_p \rho_2 V_2 dy_2)$$

where

T = absolute temperature, °C.
c_p = specific heat at constant pressure.

Substitution of the correct units for c_p and division by the equation $T_0 = 0.000231\ V_{c_0}^2$ leads to

$$\frac{T_2 - T_0}{T_0} = 0.202\,\frac{V_0^2}{V_{c_0}^2}\left(1 - \frac{V_2^2}{V_0^2}\right)$$

where

V_c = speed of sound.

Assuming a value of V_0/V_{c_0} the succeeding steps in the computation are

$$\rho_2/\rho_0 = T_0/T_2$$

$$\frac{V_2}{V_{c_2}} = \frac{V_2}{V_0}\,\frac{V_0}{V_{c_0}\sqrt{T_2/T_0}}$$

$$\frac{H_1}{p_0} = \left(1 + \frac{\gamma - 1}{2}\,\frac{V_2^2}{V_{c_2}^2}\right)^{\frac{\gamma}{\gamma - 1}}$$

where

γ = ratio of specific heats of air.

Assume a value of $(p_1 - p_0)/(H_0 - p_0)$ and solve for p_1/p_0

$$\rho_1/\rho_2 = (p_1/p_0)^{1/\gamma}$$

$$\frac{V_1}{V_2} = \left\{1 - \frac{2}{\gamma - 1}\,\frac{V_{c_2}^2}{V_2^2}\left[\left(\frac{p_1}{p_0}\right)^{1 - \frac{1}{\gamma}} - 1\right]\right\}^{1/2}$$

This expression is obtained from the generalized Bernoulli's equation

$$\tfrac{1}{2}V_1^2 + \frac{1}{\gamma - 1}\,\frac{\gamma p_1}{\rho_1} = \tfrac{1}{2}V_2^2 + \frac{1}{\gamma - 1}\,\frac{\gamma p_0}{\rho_2}$$

by dividing by V_2^2 and transforming by the equations

$$\frac{\gamma p_0}{\rho_2} = V_{c_2}^2,\ \frac{\gamma p_1}{\rho_1} = \frac{\gamma p_2}{\rho_2}\,\frac{p_1/p_0}{\rho_1/\rho_2} = V_{c_2}^2\left(\frac{p_1}{p_0}\right)^{1 - \frac{1}{\gamma}}$$

$$dy_1/dy_2 = \rho_2 V_2/\rho_1 V_1$$

The desired factor, F, is

$$\frac{(1/\tfrac{1}{2}\rho_0 V_0^2)\int \rho_2 V_2(V_0 - V_2)dy_2}{\dfrac{1}{H_0 - p_0}\int (H_0 - H_1)dy_1}$$

This expression may be rewritten in the following form, to which the preceding computations are applicable:

$$\frac{2\int (\rho_2 V_2/\rho_0 V_0)(1 - V_2/V_0)dy_2}{\displaystyle\int\left(\frac{H_0 - H_1}{H_0 - p_0}\right)\frac{dy_1}{dy_2}dy_2}$$

Numerical integration was used in order to evaluate this fraction for various values of V_0/V_{c_0}, η, and $(p_1 - p_0)/(H_0 - p_0)$. The results are given, as corrections to the values of Fig. 7, in Table 1 and Fig. 9.

ANALYSIS OF INSTRUMENT ERRORS

Entrance Losses

Owing to the fact that the entrance losses of the tubes vary with $\bar{u}^2$ instead of the average velocity $\bar{u}$, the flow through each tube is not quite proportional to the difference in pressure across its ends and, consequently, the pressure in the reservoir is not quite equal to the average stagnation pressure across the wake width. Thus, for the flow in each tube,[6]

$$H_1 - p_r = (8\mu l\bar{u}/R^2) \pm 2.7\rho\bar{u}^2/2$$

$$(+ \text{ if } H_1 > p_r;\ - \text{ if } H_1 < p_r)$$

$$\sum_n (H_1 - p_r) = (8\mu l/R^2)\sum_n \bar{u} + 2.7\sum_n (\pm\rho\bar{u}^2/2)$$

Since $\sum_n \bar{u} = 0$ at equilibrium,

$$p_r = (1/n)\sum_n H_1 - (2.7/n)\sum_n (\pm\rho\bar{u}^2/2)$$

where

μ = viscosity of air;
l = length of tubes;
$\bar{u}$ = average velocity of flow in tubes;
R = inside radius of tube;
n = number of tubes in rake;

and subscript r refers to the reservoir.
The correction has been obtained as a function of w/ζ and of the tube characteristics (Fig. 10). It will generally be possible to keep the tube diameter so small that the correction will be negligible.

Compressibility Correction

The flow of air through a tube is proportional to the difference of the squares of the pressures, rather than of the first powers, so that the pressure in the reservoir tends to be the root mean square, rather than the average, of the stagnation pressures across the width of the rake.

Thus, assuming laminar flow, with a parabolic velocity distribution across the tube,

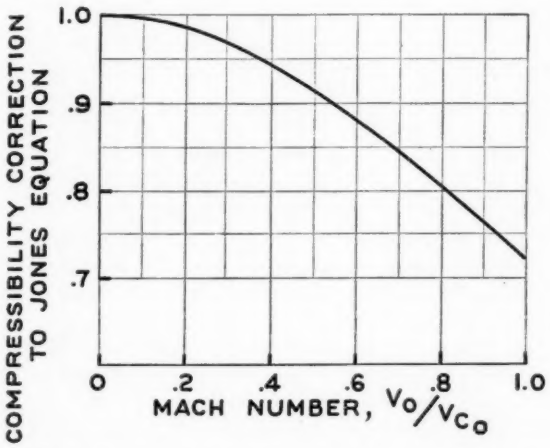

FIG. 9. Compressibility correction to Jones's equation for typical conditions; $\eta = 0.5$, $(p_1 - p_0)/(H_0 - p_0) = 0.1$. Use to multiply uncorrected drag coefficient, $F\frac{w}{c}\frac{H_0 - H_{1_{av}}}{H_0 - p_0}$, in order to obtain corrected drag coefficient.

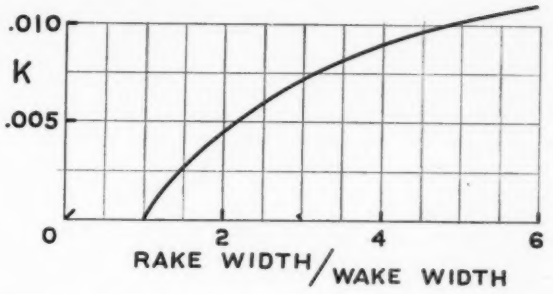

FIG. 10. Entrance loss correction. Increase the observed value of $\frac{H_0 - p_r}{H_0 - p_0}$ by $\frac{k\rho\eta q_0 R^4}{\mu^2 l^2}\frac{(H_0 - p_r)}{H_0 - p_0}$.

$$u = 2\bar{u}(1 - r^2/R^2)$$

where r = distance from center of tube.
The momentum transfer per unit time across a section is $\int_0^R 2\pi r\rho u^2\, dr = \frac{4}{3}\pi\rho R^2\bar{u}^2$. The frictional force per unit length is $2\pi R\mu(du/dr)_{r=R} = 8\pi\mu\bar{u}$. The differential equation of the flow in the tube is then

$$\pi R^2 dp = -8\pi\mu\bar{u}\, dx - \tfrac{4}{3}\pi R^2\, d(\rho\bar{u}^2)$$

where x = distance along tube.
There is practically no net heat effect in the flow of air along a fine uniform tube. Hence, the product $\rho\bar{u}$ is practically constant along the tube and equal to $\rho_r\bar{u}_r$; also $\rho/\rho_r = p/p_r$, where subscript r refers to the reservoir end of the tube. The equation then becomes

$$dp = -(8/R^2)\mu\bar{u}_r(p_r/p)dx + \tfrac{4}{3}\rho_r\bar{u}_r\bar{u}_r p_r dp/p^2$$

which, on integrating between the two ends of the tube, gives

$$H_1^2 - p_r^2 = (16\mu p_r l/R^2)\bar{u}_r + \tfrac{8}{3}\rho_r p_r\bar{u}_r^2 \log H_1/p_r$$

Calculations showed that the last term of this equation is negligible under any conditions for which the entrance loss correction is reasonably small. If it is neglected, it follows that, at equilibrium ($\sum_n \bar{u}_r = 0$), $p_r = [(1/n) \times \sum_n H_1^2]^{1/2}$. The corresponding correction to $H_0 - p_r$ in order to obtain $H_0 - H_{1_{av}}$ is given in Fig. 11.

TABLE 1

Compressibility Correction to Jones's Equation

V_0/V_{c_0} \ $(p_1 - p_0)/(H_0 - p_0)$	$\eta = 0$				$\eta = 0.36$				$\eta = 0.51$				$\eta = 0.64$			
	−0.1	0	0.1	0.2	−0.1	0	0.1	0.2	−0.1	0	0.1	0.2	−0.1	0	0.1	0.2
0	1.000	1.000	1.000	1.000	1.000	1.000	1.000	1.000	1.000	1.000	1.000	1.000	1.000	1.000	1.000	1.000
.4	.923	.931	.937	.943	.936	.941	.945	.948	.938	.943	.945	.945	.941	.947	.945	.944
.6	.842	.856	.868	.883	.863	.873	.882	.889	.869	.879	.885	.901	.875	.884	.884	.885
.8	.744	.767	.790	.811	.777	.797	.813	.824	.786	.803	.815	.818	.798	.811	.814	.789
1.0	.638	.673	.706	.738	.680	.711	.736	.754	.695	.722	.741	.744	.710	.734	.738	.690

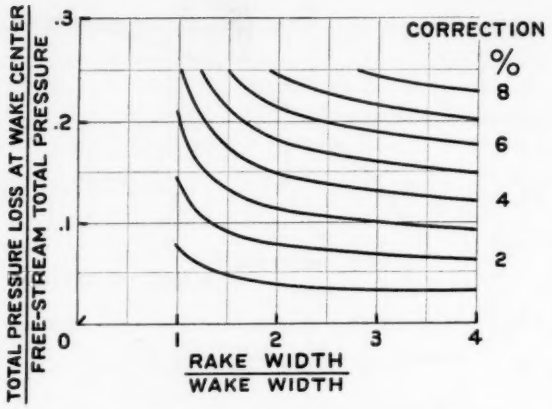

FIG. 11. Correction for the effect of compressibility on the flow in the tubes. Increase the observed value of $(H_0 - p_r)/(H_0 - p_0)$ by the percentage shown. The ordinate is $\eta\ (H_0 - p_0)/H_0$ in which H_0 and p_0 are absolute pressures.

Tube Displacement Correction

When a tube is pointing into a stream in which there is a total-pressure gradient, the effective stagnation pressure on the end of the tube corresponds, not to that at the center of the opening but to a point slightly toward the higher-pressure side of the center. The pressure in the reservoir will therefore be slightly too high, the error being approximately[7]

$$\Delta p_r = 2\eta\delta(H_0 - p_0)/w \qquad (6)$$

in which $\delta = 0.131D_0 + 0.0821D_i$, in which D_0 is the outside and D_i the inside diameter of the tube.

DESIGN AND APPLICATION

Instrument Design

In the design of the rake, its location behind the wing trailing edge must first be decided. The 0.20 chord position is recommended; however, any position from 0.15 to 0.30 of the chord behind the trailing edge may be used with equal accuracy. The number, the size, and the spacing of the total-pressure tubes may then be determined. The distance between centers of the top and the bottom tubes should normally be chosen about twice the wake width given in Fig. 4; where the drag coefficient is not readily predictable, however, as for wings with cooling ducts or large protuberances, it is conservative to use about three times the estimated wake width. It should be noted that, since each tube measures the average stagnation pressure across a width equal to the distance between adjacent tubes, the effective rake width w is n times the distance between adjacent tubes rather than the distance between centers of the top and bottom tubes, which is only $(n - 1)$ times the distance between adjacent tubes.

The rake width is not a critical dimension, but care must be taken that the wake is fully included. The upper limit of the rake width is limited by the fact that, as the ratio of the rake width to the wake width is increased, the pressure in the reservoir, p_r, approaches the free-stream total pressure, H_0, thus reducing the sensitivity of the instrument. The preliminary estimate of the drag coefficient, which is required in using Fig. 4, may be made with sufficient accuracy from published data on similar wings or bodies.

The tube spacing should be chosen so that about 20 tubes lie in the wake proper; an instrument of twice the wake width should therefore have 40 equally spaced total-pressure tubes leading to the reservoir.

The inside diameters of the tubes must be sufficiently small to minimize the corrections of Fig. 10. The correction will not exceed 1 per cent for the following bores:

Speed, M.p.h.	Inside Diameter of Tubes, In.
200	0.024
300	.020
400	.017
500	.015

These bores were computed for a tube length of 6 inches and, if deviation from this length is desired, it should be remembered that the correction varies as the fourth power of the diameter and inversely as the square of the length. Uniformity of the bore is of greatest importance and, for this purpose, it is desirable to use stainless-steel tubes selected if possible for equal internal resistance. The tubes are mounted for protection within larger diameter tubes, as shown in Fig. 2.

The rake may be supported from the wing trailing edge by two streamline arms arranged diagonally (Fig. 1) to minimize interference. The included angle at the rake between the supports should not be less than 40°, to insure that none of the drag of the wing-support juncture is included in the wake measurements. In some cases, the rake may be more conveniently supported from the fuselage. A method of locating the rake center with reference to the wing trailing edge is shown in Fig. 12. At any selected longitudinal position of the rake m locate its center at a distance d measured from a line parallel to the relative wind and passing through the trailing edge of the wing. The vertical

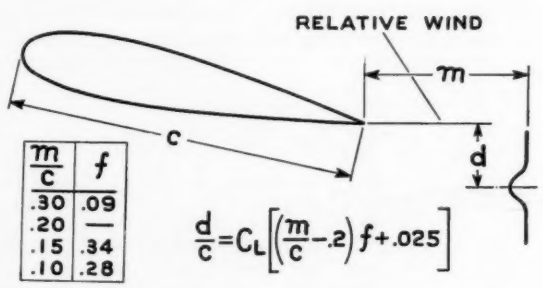

FIG. 12. Chart for locating the center of the rake.

position d/c is, as shown by the equation of Fig. 12, a function of the distance behind the trailing edge, the lift coefficient C_L, and an empirical constant f, which has been derived from investigations of numerous wakes.

The cockpit instruments will normally consist of a meter to indicate the pressure difference $H_0 - p_r$, and the conventional air-speed meter to indicate $H_0 - p_0$. The former may be considerably more sensitive than the latter, and its maximum dial capacity should be about $(\eta\zeta/w)q_0$. The pressure H_0 required for one side of the instrument indicating $H_0 - p_r$ may be obtained by branching from the pressure line to the air-speed head. The usual corrections to the air-speed head, which are required for all flight measurements, should be known. For measurements behind irregular shapes, intersections, wing ducts, large protuberances, etc., the static-pressure difference $p_1 - p_0$ should also be determined on a separate meter with p_1 obtained from a static-pressure tube in the wake and p_0 obtained by branching from the line to the air-speed indicator.

It is suggested that the total-pressure tubes be carefully blown out and checked for leaks before each flight and then covered during the take-off. A rip string or similar device may be used to uncover the tubes just before the observation is made.

The adaptability of the rake for drag measurements behind wings of different chords may be improved by making the rake wide enough to cover the probable useful range. Airtight caps may then be provided for the ends of the tubes that are not in use.

Application of Charts

The following steps are taken to convert the observed pressure readings into drag coefficients:

(1) Correct the value of $(H_0 - p_r)/(H_0 - p_0)$ by adding
   (a) The correction for entrance loss given in Fig. 10.
   (b) The correction for compressibility given in Fig. 11.
   (c) The correction for effective displacement of the tube center given by Eq. (6).

(2) Estimate from Fig. 3 the value of η.

(3) From Figs. 5 and 6 estimate the value of $(p_1 - p_0)/(H_0 - p_0)$ for the chosen position of the rake with reference to the wing and fuselage.

(4) Determine the value of F by substitution of the values of steps 2 and 3 in Fig. 7.

(5) Multiply the factor F by $\left(\frac{H_0 - p_r}{H_0 - p_0}\right)_{corr.} \frac{w}{c}$ and obtain $c_{d_{uncorr.}}$

(6) Determine final value of c_d by multiplying the value from step 5 by the compressibility factor given in Table 1.

The corrections of step 1 are small and may be entirely omitted for flight speeds below 300 m.p.h. with an error of not more than about 1 per cent. For a position of the rake at 0.2 chord behind the trailing edge, and a value of Mach Number $V_0/V_{c_0} = 0.4$ a simplified chart has been prepared and is given in Fig. 13. This chart

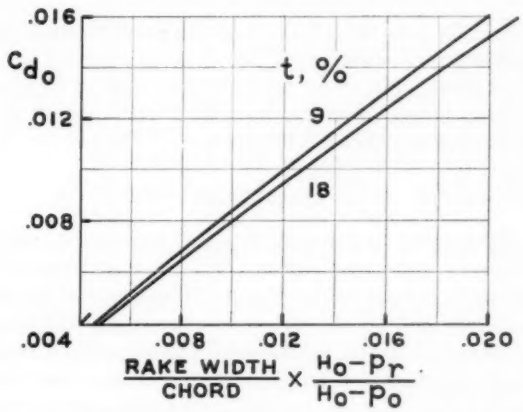

FIG. 13. Simplified chart for the determination of the profile-drag coefficient for flight speeds between 250 and 350 m.p.h.

may be used with practical accuracy to determine the corrected drag coefficients for flight speeds between 250 and 350 m.p.h., assuming average values for rake dimensions and other parameters.

REFERENCES

[1] Betz, A., *A Method for the Direct Determination of Wing Section Drag*, N.A.C.A. Technical Memorandum No. 337, 1925.

[2] The Cambridge University Aeronautics Laboratory (B. Melvill Jones), *The Measurement of Profile Drag by the Pitot-Traverse Method*, British A.R.C. Reports and Memoranda No. 1688, 1936.

[3] Silverstein, Abe, *Wake Characteristics and Determination of Profile Drag by the Momentum Method*, Proceedings of the Fifth International Congress of Applied Mechanics, Cambridge, Massachusetts, John Wiley & Sons, Inc., 1939, pages 403–409.

[4] Doetsch, H., *Profilwiderstandsmessungen im grossen Windkanal der DVL.* Luftfahrtforschung, Bd. 14, Lfg. 4/5, April 20, 1937, pages 173–178.

[5] Silverstein, Abe, Katzoff, S., and Bullivant, W. Kenneth, *Downwash and Wake behind Plain and Flapped Airfoils*, N.A.C.A. Technical Report No. 651, 1939.

[6] Prandtl, L., and Tietjens, O. G., *Applied Hydro- and Aeromechanics*, Ch. III, McGraw-Hill Book Co., Inc., 1934.

[7] Young, A. D., and Maas, J. N., *The Behaviour of a Pitot Tube in a Transverse Total-Pressure Gradient*, British A.R.C. Reports and Memoranda No. 1770, 1937.

Some Economic Aspects of Transport Airplane Performance. Parts II and III*

W. C. MENTZER AND HAL E. NOURSE
United Air Lines Transport Corporation

Part II. Presentation of Airplane Characteristics in Terms of Significant Operating Cost

It is the purpose of Part II of this paper to show, by applying the foregoing cost equations to a related series of airplanes, the effect on significant cost of varying cruising power available, cruising power required, airplane first cost, and trip length.

Block Speed

Block speed is the only airplane performance characteristic appearing directly in the cost equations. It can be defined as the distance from terminal to terminal divided by the time from passenger station to passenger station. An accurate determination of block speed requires the computation of climb, level and descent distances and times as well as the arbitrary establishment of a terminal maneuvering and taxi time. For purposes of simplification in this study the following assumptions are made: (a) flight altitude—14,000 feet; (b) terminal altitudes—sea level; (c) wind velocity—zero; (d) net time lost in climb and descent—0.06 hour; (e) taxi and maneuvering time —0.20 hour. In order to account for inaccuracies in flying, necessary deviations from true course and other contingencies it is further assumed in the computation of block time that the distance is increased 2 per cent. Based on the above assumptions, the equation for block speed can be expressed as

$$V_b = \frac{D}{(1.02D/V) + 0.26} \qquad (17)$$

where:

V_b = Block speed, m.p.h.
V = Level flight speed at altitude, m.p.h.
D = Trip length, miles.

Basic Airplanes

The significant costs of a particular type of transport airplane are investigated. The type of airplane selected is a four-engine, low-wing monoplane sleeper having a supercharged cabin and passenger accommodations somewhat superior to airplanes now in service. The type closely approximates transport airplanes now under construction.

Three basic airplanes differing from each other only in the value selected for f (which is defined as the flat-plate area of unity drag coefficient equivalent to minimum profile and parasite drag) are assumed. These basic airplanes are further assumed to have certain characteristics in common, as given in Table 3.

Table 3

Characteristics Common to the Three Basic Airplanes

Wing area	1430 sq. ft.
Aspect ratio	9.5
Span	116 ft.
Airplane "efficiency factor," e	0.87
Propeller efficiency, η	0.85
Maximum desired cruising speed at 14,000 ft.	225 m.p.h.
Gross weight	50,000 lbs.
Useful load	15,000 lbs.
Wing and nacelle weight	7200 lbs.
Weight empty	35,000 lbs.
Crew weight (3 at 170 lbs. and 2 at 130 lbs.)	770 lbs.
Landing gear weight in per cent of gross weight	7.5 per cent
Engine and propeller weight in terms of cruising b.hp.	2.90 lb./b. hp.
Total take-off b. hp. available	5200 b. hp.
Cruising specific fuel and oil consumption	0.46 lb./hp. hr.
Number of day seats	0.40

The first of the basic airplanes is assumed to be designed according to present standards which results in f being equal to 35 sq. ft. The other two basic airplanes are assumed to be successively cleaner aerodynamically and are arbitrarily assigned values of $f = 27.5$ and $f = 20$. Aerodynamic efficiency is used in this paper to denote the degree of aerodynamic "cleanness." For purposes of convenience the basic airplanes are henceforth designated simply by their f values in sq. ft. All of the basic airplanes have the same take-off power loading and the same wing loading. Consequently their take-off and landing characteristics are almost identical inasmuch as f has little effect on either take-off or landing performance. However, the powers required computed for a level speed of 225 m.p.h. at 14,000 feet are 2600, 2150 and 1730 b.hp. for the f-35, f-27.5, and f-20 airplanes, respectively.

Variation of Cruising Speed

So far only one cruising speed has been determined for each airplane but any cruising speed within reason-

Presented at the Airplane Design Session, Eighth Annual Meeting, I. Ae. S., New York, January 26, 1940.

*Part I, on "Development of Significant Cost Equations" appeared in the April issue of the Journal.

able limits can be obtained by varying the cruising power available. The simplest way to vary cruising power is to assume a specific engine and arbitrarily increase the amount of cruising power that is taken out of it. There is, of course, a limit to what can be done along this line without seriously impairing engine reliability. Existing engines appear to operate with good reliability up to 50 per cent of take-off power, therefore this figure is adopted as the limit of cruising power of any specific engine.

In this study it is desired to investigate speeds higher than those obtainable by using 50 per cent of the take-off power available in the basic airplanes. This necessitates the installation of more powerful engines which in turn increases the take-off power available. If more powerful and consequently heavier engines are installed either the useful load must be decreased or the gross weight increased. The latter alternative, which results in a constant useful load, is believed reasonable within the range of gross weights under consideration for the following reasons: (a) The increase in wing loading is more than offset by the decrease in power loading so that take-off and climb performance should not be impaired. (b) The increased wing loading will increase landing and approach speeds slightly but climb-out performance with the wing flaps set for the approach condition should be improved by the reduced power loading. The increased landing run is at least partially compensated for by the ability of the airplane to climb-out more rapidly in the event of an inaccurate approach to the landing area.

Variation of Weight

If comparable structural integrity is to be obtained, the strength, and consequently the weight, of the wings, engine nacelles, fuselage and tail group must be varied with speed. The determination of the exact variation of structural weight with speed is extremely complex but can be approximated by making several simplifying assumptions, namely: (a) that the weight changes in the fuselage and tail group are small and can be neglected; (b) that the wing and nacelle weight varies directly with the maximum cruising speed; (c) that some arbitrary percentage (75 per cent in this case) of the basic wing and nacelle weight is made up of actual structural material; and (d) that the maximum cruising speed in any particular instance is proportional to the cube root of the maximum cruising power selected. The maximum cruising power selected may be less than but never greater than 50 per cent of the take-off power available. It is assumed that cruising power for level flight or descent will be limited by placard or otherwise to that necessary to obtain the arbitrary maximum cruising speed selected in any instance.

The landing gear is the only variable weight item remaining. As mentioned in Table 3 it is assumed to constitute 7.5 per cent of the gross weight.

Having made the above assumptions it is possible to set up the following approximate equation for variation of gross weight in terms of maximum cruising power bearing in mind that the structural limit speed (so called "never exceed" or "placard" speed) must be varied to suit the maximum cruising speed and power selected in any particular instance.

$$GW = GW_0 + (1 + A)\left[EB + D\left(W\frac{P^{1/3}}{P_0^{1/3}} - W\right)\right] \tag{18}$$

where:

GW = Gross weight in lbs.
A = Landing gear weight in per cent of gross weight expressed as a decimal.
B = Specific engine weight in lbs. per cruising b.hp.
D = Arbitrary ratio of structural to total wing weight.
W = Basic airplane wing and nacelle weight in lbs.
P = Total maximum cruising b.hp.
E = (P − 50 per cent of the basic airplane take-off b.hp.)*

The subscript 0 denotes values pertaining to the basic airplane while no subscript denotes values pertaining to the revised airplane.

Substituting the values previously assumed Eq. (18) becomes

$$GW = 50{,}000 + 1.075\left[2.9\,(P - 2600) + 0.75\left(7200\frac{P^{1/3}}{P_0^{1/3}} - 7200\right)\right] \tag{19}$$

where:

P_0 = 2600 for f-35 airplane.
P_0 = 2150 for f-27.5 airplane.
P_0 = 1730 for f-20 airplane.

The useful load is assumed to be constant and therefore if the engine weight is assumed to be a function of take-off or cruising power the weight of the airplane less engines can easily be determined.

Gross weight, airplane weight less engines, and take-off power are plotted against maximum total cruising power used in Fig. 3. It should be noted that no additional take-off power has been provided to compensate for additional wing, nacelle and landing gear weight. However, the effect of this additional weight on take-off and landing performance is not great and is neglected in the interest of simplicity.

* If E is negative it must be assumed equal to zero in order to maintain take-off performance.

Cruising Power Required

The cruising b.hp. required at 14,000 feet altitude is computed for each of the airplanes at various gross weights by use of the following equation:

$$\text{b.hp. required} = \frac{\frac{\rho f V^3}{1100} + \frac{2W^2}{500\rho\pi e b^2 V}}{\eta} \qquad (20)$$

where:

ρ = Atmospheric density in slugs per cubic foot.
f = Profile and parasite equivalent flat-plate area in sq. ft.
V = Velocity in ft. per sec.
W = Gross weight in lb.
e = Airplane efficiency factor
b = Span
η = Propeller efficiency.

Fuel and Oil Reserves

Before the payload for any flight can be determined it is necessary to establish what reserve fuel and oil is to be carried. Present government requirements state that sufficient fuel must be carried to keep the airplane aloft for 45 minutes after reaching its destination. However, the destination must be the most remote alternate airport set forth in the flight plan for the particular trip. For the purposes of this study, no time reserve is assumed but each airplane is assumed to have enough fuel on board to fly 300 miles at cruising power after reaching its destination. Oil necessary for the trip plus 300 miles, as well as an additional 20 gallons of oil per engine, is also assumed to be on board.

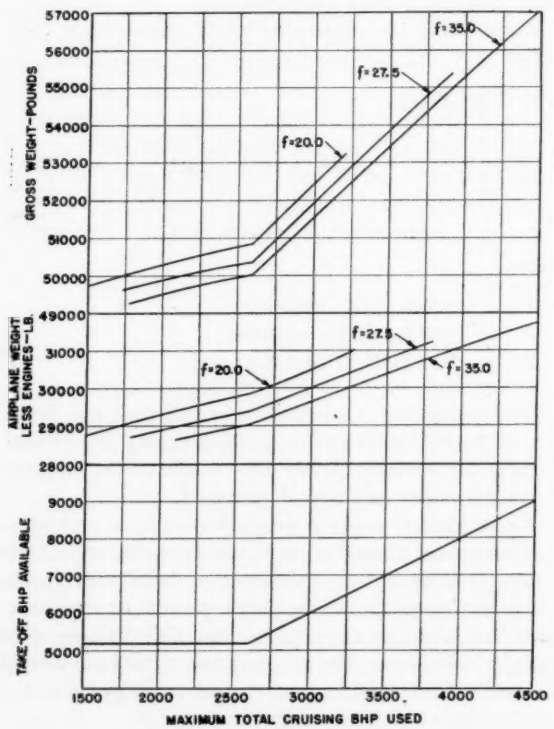

FIG. 3. Gross weight, airplane weight less engines and take-off power available plotted against maximum total cruising power used in accordance with Eq. (19).

Payload

Relationships having been established between true speed and block speed, and between true speed, weight, and power, it is now possible to compute payloads for trips of different lengths when operated at different block speeds. In computing block speeds the approximate average gross weight for the particular length trip being investigated is used. Figs. 4, 5, and 6 show payload plotted against block speed for the three assumed values of f and for trip lengths of 600, 900, and 1200 miles. On the same figure the total cruising b.hp. required is plotted against block speed. These curves show quantitatively the effect of block speed and aerodynamic efficiency on payload. The three curves when considered together show the effect of trip length on payload. They form the basis for the presentation of airplane performance in terms of significant cost.

Weight and Cost Relationships

Before significant costs can be determined certain cost and weight relationships must be established. The symbols defined in Part I are used. Current airplanes of the general type of the f-35 airplane being considered cost approximately \$11.00 per pound of airplane weight less engines but including propellers. Current engines weigh approximately 2.3 lbs. per maximum cruising b.hp. for reasonable reliability, and cost approximately \$9.40 per pound or \$21.60 per cruising b.hp. The above relationships can be written as follows:

$$C_a = 11W_a \qquad (21)$$
$$W_e = 2.3\,P/4 = 0.575P \qquad (22)$$
$$C_e = 21.60\,P/4 = 5.40P \qquad (23)$$
$$C_i = C_a + NC_e = 11W_a + 5.4PN \qquad (24)$$

It should be borne in mind that the symbol P represents the total cruising b.hp. which in this study is the sum of the cruising b.hp. of four engines and that the symbols W_e and C_e represent the weight and cost, respectively, of one engine.

Significant Costs

Relationships have now been established so that all variables appearing in the significant cost equations of Part I can be determined for any block speed selected. For comparing the effect of aerodynamic efficiency, cruising power, and range on significant cost, only the total cost is necessary. However, Figs. 7, 8, and 9 are shown for the three values of f and for a 900

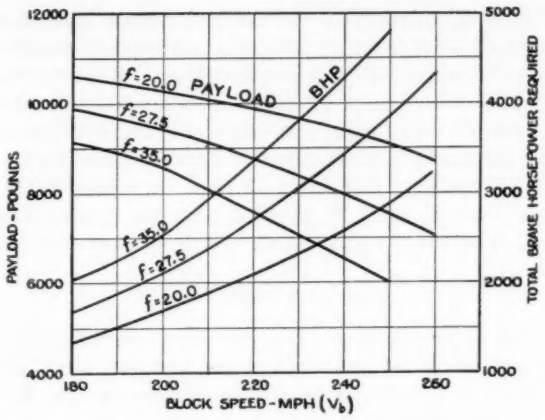

FIG. 4. Payload and total b.hp. required for a trip length of 600 miles plotted against block speed.

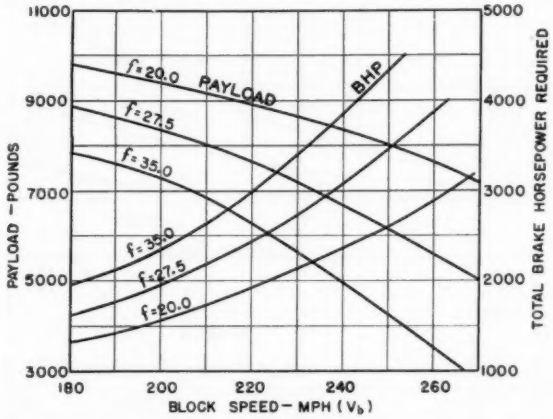

FIG. 5. Payload and total b.hp. required for a trip length of 900 miles plotted against block speed.

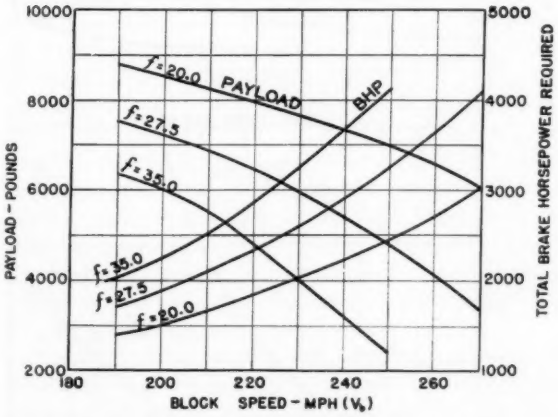

FIG. 6. Payload and total b.hp. required for a trip length of 1200 miles plotted against block speed.

mile trip length to illustrate the relative importance of the individual cost factors. Factors that are more or less related are combined in the interest of simplicity.

The most striking feature of Figs. 7, 8, and 9 is the

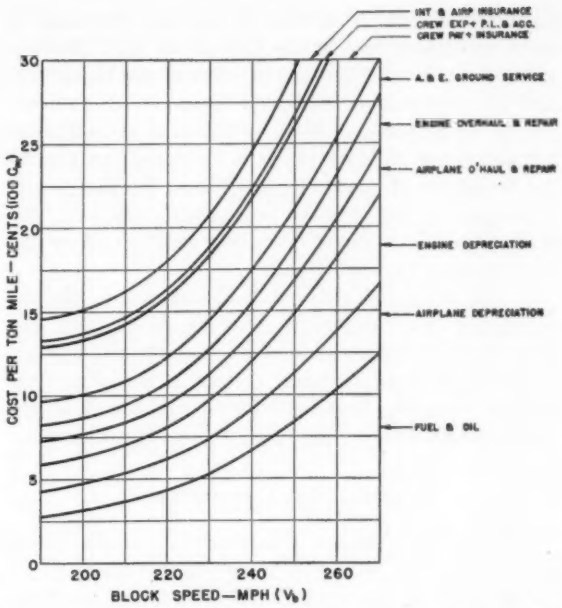
INT. & AIRP. INSURANCE
CREW EXP.+ P.L. & ACC.
CREW PAY + INSURANCE
A. & E. GROUND SERVICE
ENGINE OVERHAUL & REPAIR
AIRPLANE O'HAUL & REPAIR
ENGINE DEPRECIATION
AIRPLANE DEPRECIATION
FUEL & OIL
COST PER TON MILE — CENTS (100 C_m)
BLOCK SPEED — MPH (V_b)

FIG. 7. Significant cost factors *vs.* block speed for 900 mile trip length and $f = 35$ sq.ft.

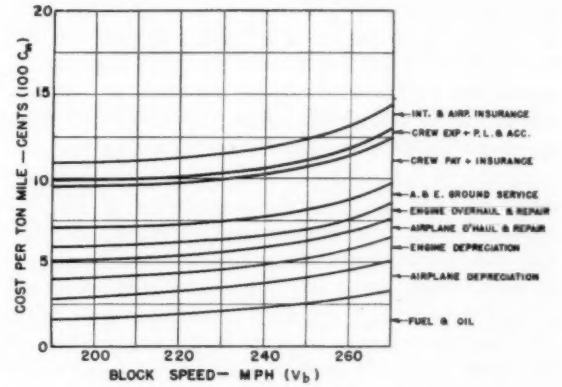
INT. & AIRP. INSURANCE
CREW EXP.+ P.L. & ACC.
CREW PAY + INSURANCE
A. & E. GROUND SERVICE
ENGINE OVERHAUL & REPAIR
AIRPLANE O'HAUL & REPAIR
ENGINE DEPRECIATION
AIRPLANE DEPRECIATION
FUEL & OIL
COST PER TON MILE — CENTS (100 C_m)
BLOCK SPEED — MPH (V_b)

FIG. 8. Significant cost factors *vs.* block speed for 900 mile trip length and $f = 20$ sq.ft.

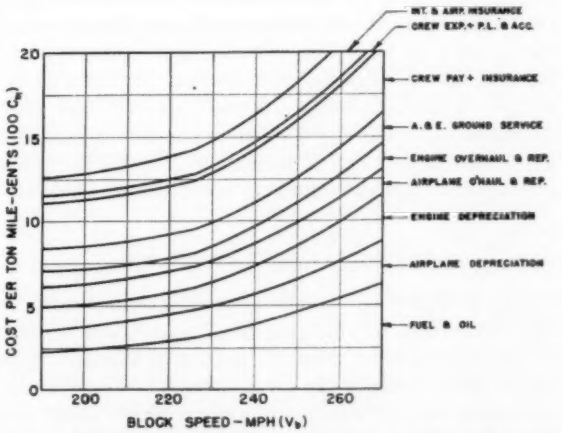
INT. & AIRP. INSURANCE
CREW EXP.+ P.L. & ACC.
CREW PAY + INSURANCE
A. & E. GROUND SERVICE
ENGINE OVERHAUL & REP.
AIRPLANE O'HAUL & REP.
ENGINE DEPRECIATION
AIRPLANE DEPRECIATION
FUEL & OIL
COST PER TON MILE-CENTS (100 C_m)
BLOCK SPEED - MPH (V_b)

FIG. 9. Significant cost factors *vs.* block speed for 900 mile trip length and $f = 27.5$ sq.ft.

rapidity with which significant fuel cost increases as block speed increases in the case of the *f*-35 airplane, and the rapid reduction in the effect of significant fuel cost as aerodynamic efficiency improves. Significant cost is influenced not only by the cost of additional fuel consumed as block speed is increased but also by the reduction of payload necessitated by the greater fuel requirements. As the aerodynamic efficiency improves, the fuel on board becomes a smaller and smaller percentage of the useful load.

It will be noted that payload appears in the denominator of all significant cost equations. For any given airplane the useful load is essentially fixed. Consequently payload is almost entirely a function of the amount of fuel on board and for that reason all significant costs are affected indirectly by fuel requirements.

Specific Fuel Consumption

Although not studied quantitatively in this paper it is obvious that reduction of specific fuel consumption has an effect on cost somewhat similar to but much less important than improvement in aerodynamic efficiency. For instance, if specific fuel consumption were reduced approximately 33 per cent (from 0.45 lb. to 0.30 lb. per b.hp. hr.) on a 900 mile trip operated at a block speed of 209 m.p.h. with the *f*-35 airplane the actual fuel consumed would be the same as that consumed by the *f*-20 airplane when operated at the same speed and for the same distance with a specific fuel consumption of 0.45. However, if the block speed were increased, the specific fuel consumption of the *f*-35 airplane would have to decrease very rapidly to maintain the above relationship. Furthermore, increases in block speed above 209 m.p.h. (for a 900 mile trip length) require more and more powerful engines in the *f*-35 airplane whereas more powerful engines are not required in the *f*-20 airplane until a block speed of 250 m.p.h. (for a 900 mile trip length) is reached. If constant engine specific weight is assumed, more powerful engines affect all of the significant cost factors indirectly through reduction in payload and affect some of them, such as engine overhaul, engine depreciation, interest on investment, and airplane insurance, directly. Therefore, while reduced specific fuel consumption cannot be overlooked as a means of reducing significant cost it is of secondary importance when compared with improvement of aerodynamic efficiency.

Significant Cost Comparison

Fig. 10 is plotted to show directly the effect on total significant cost of changing block speed and aerodynamic efficiency for three different trip lengths. This figure shows directly the great effect that aerodynamic efficiency has on significant cost as block speed and trip length increase. The 260 m.p.h. block speed (which assumed a 15 m.p.h. tail wind) established in Part I as approaching the maximum block speed required for transcontinental service, corresponds roughly to a 240 m.p.h. block speed in still air. Reference to Fig. 10 shows that if the trip lengths are 900 miles the significant cost for the *f*-35 airplane is nearly 25 cents per payload ton-mile while the significant cost for the *f*-20 airplane is just under 12 cents or approximately half that of the *f*-35 airplane. Similar comparisons can be drawn for other block speeds and trip lengths.

Airplane First Cost

All of the previous data presented are arbitrarily based on the assumption that the first cost of all airplanes is $11.00 per pound of airplane weight less

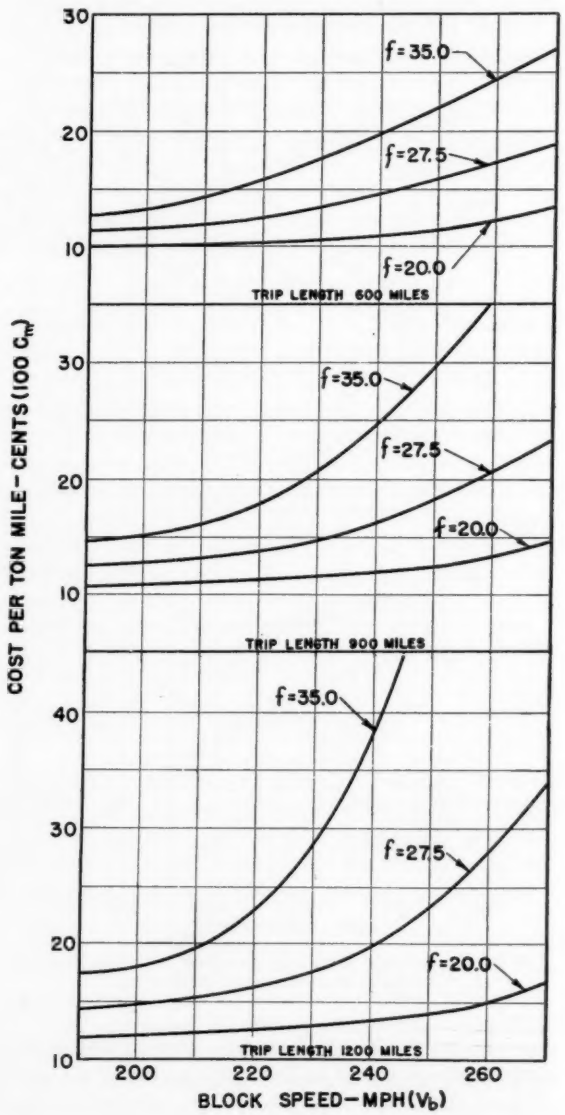

Fig. 10. Significant costs *vs.* block speed for trip lengths of 600, 900, and 1200 miles.

engines, because the rate of change of airplane first cost as aerodynamic efficiency increases is highly indeterminate. It is reasonable to assume, however, that this cost per pound will increase as aerodynamic efficiency increases. In order to show the effect of increasing airplane first cost on significant cost Fig. 11 is presented. In this figure significant cost is plotted

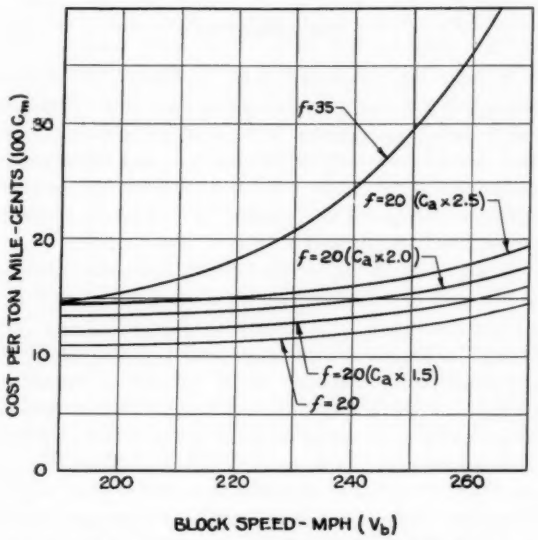

FIG. 11. Significant cost *vs.* block speed for a 900 mile trip length and variable airplane first cost.

against block speed for a trip length of 900 miles and for the *f*-35 airplane assuming the original airplane cost of $11.00 per pound. The same information is plotted for the *f*-20 airplane assuming the original airplane cost of $11.00 per pound and also assuming that this cost is increased successively to $27.50 per pound, that is, to 250 per cent of the original value. It can be seen that even this absurdly high airplane cost is justified theoretically if block speeds above 190 m.p.h. are desired. Of course a value of $f = 20$ for the type of airplane under consideration is not realizable in the present state of the art. The value of f for the cleanest airplane was intentionally made much lower than has been demonstrated on any existing transport airplane in order to emphasize the importance of aerodynamic efficiency and to show that increased airplane first cost is justified in order to obtain cleanness.

The above remarks about airplane first cost must not be interpreted too literally inasmuch as they present only the theoretical cost side of the picture. In Part III of this paper other factors which influence the overall economy of a particular operation are set forth. The possible action of one or all of these factors would undoubtedly make the business risk of investment in airplanes of the type studied which might cost $1,000,000 each, too great for consideration even though the increase in efficiency might be great. However, it does follow that relatively large increases in airplane first cost can be justified if they result in sufficient improvement in aerodynamic efficiency.

TRIP LENGTH

The airplane designer has no control over trip length. The transport operator, however, must choose in many instances between the economy of shorter trips and the greater public appeal resulting from longer trips. Reference to Fig. 10 shows the relatively great effect of trip length on significant cost for the airplanes studied. The short trip is less efficient than the long trip in that a higher true speed is required to make good the same block speed. This is due to the fact that the fixed taxi time, maneuvering time, and net time lost in climb and descent remain constant and therefore represent a larger proportion of the total time on a short trip than on a long one. However, the increased fuel required much more than offsets this inefficiency on trips of reasonable length. Of course if trip lengths are shortened too much the total payload capacity cannot be utilized in most instances because the number of seats is limited.

Obviously the cleaner the airplane the better it is on long trip operation because the fuel required for a given trip represents a smaller proportion of the useful load as the cleanness of the airplane increases.

Part III. Economic Factors Not Associated with Design and Performance

The purpose of Part III of this paper is to point out certain other economic factors of air transportation apart from those pertinent to airplane design and performance.

These outside economic considerations which have been operative during the brief history of air transportation are centered around such factors as:

(1) Interior arrangement and passenger comfort.
(2) State of general public acceptance.
(3) Nature of the competition.
(4) General economic conditions.

The above enumerations may seem quite obvious but it is believed important that they be reviewed just briefly as they have assumed, during the past, the major role in the control of the economic destiny of the various individual air transport companies.

In consideration of factor (1), it might be said that the interior arrangement of an airplane providing berths and the almost simultaneous inauguration of transcontinental sleeper schedules provided real economic stimulus to the air transport industry. Although it is felt the present sleeper transport airplane used by domestic operators does not represent the best as an economic unit, its success as a business getter very definitely has demonstrated the value of proper considerations to interior arrangement and comfort, even at

the expense of a fundamentally less efficient airplane. In other words, the average layman probably does not make the finer engineering distinctions as to fundamental efficiency but his choice for air transportation is more likely to be made on the basis of those things that add most to his personal comfort and enjoyment.

In consideration of factor (2), the following is offered. Air transport history indicates that public acceptance of a new airplane model has been remarkable. It has been so remarkable in fact that an air transport organization which has been able to precede the rest of the field with a new model has insured for itself with the new model immediate economic success. This leadership has continued as long as no new type of airplane is introduced in the field and as long as outside economic conditions have remained satisfactory. This single factor of competition has had a major bearing on the economic destiny of individual companies during the past five years, and is a factor that might well be considered by operators in purchasing new equipment as well as the factor of design efficiency.

Factor (3), or the state of general public acceptance of air transportation, is influenced profoundly by safety records. Air transport market studies indicate that fear and not fare has been the greatest single reason in the retardation of public acceptance of air travel. Lack of public acceptance due to reasons stated therefore has also been a major economic consideration in the air transport industry.

In considering factor (4), until recent years the air transportation industry was in such a stage of infancy that it seemed to create its own trend and was almost entirely immune to the effects of general economic conditions surrounding it. This fact is best illustrated by air transportation's steady growth during the depression years of 1930 through 1933. The number of passenger miles flown doubled during this period. Since about 1935, general business conditions have become a significant economic factor in the air transport picture. There is little doubt but that the industry did share in the benefits derived as a result of the upward trend of the industrial production index in 1936 and the fore part of 1937. Also no doubt the air transport passenger volume increase was retarded during the latter half of 1937 and first half of 1938, during which time the country as a whole suffered a recession in business compared to the previous year.

Conclusions

It may be concluded that variation of airplane utilization has a profound effect on significant operating cost; and that airplane utilization in terms of flying time is fundamentally dependent on trip length, with a secondary dependence on such factors as seasonal schedule changes, block speed, etc. (as block speed increases, utilization decreases).

It may further be concluded that material increases in airplane first cost can be justified if they result in a sufficiently great improvement of aerodynamic efficiency. The study indicates how rapidly significant operating cost increases on a modern conventional airplane as block speed increases when that increase in block speed is obtained only by the addition of power. This is true even if the gross weight is increased enough to offset the additional structural and engine weight. It is also shown that significant cost increases rapidly as trip length increases.

While only one general type of airplane is investigated in this study the method of attack, that is, the idea of expressing certain airplane characteristics in terms of significant cost, is applicable to any type of transport airplane. Further experience with the method will undoubtedly result in simplification and increased accuracy.

In consideration of Part III of this study, it may be concluded that economic factors apart from those pertinent to fundamental design and performance play a major role in the economic outcome of air transportation.

Book Review

Aerosphere 1939, edited by GLENN D. ANGLE; Aircraft Publications, New York, 1940; 1420 pages, $15.00.

This is a monumental work which should prove of great value to the aviation industry. In many respects the book is unique.

The editor deserves great praise for the thoroughness with which he has prepared the material and in particular for the section dealing with engines. This section, comprising 844 pages and 1524 illustrations, is a remarkably complete compilation of aircraft engine development from the earliest days to the present time. The engines of early experimenters, some of whose names are now nearly unknown, except to those whose memories stretch back many years, are described. Histories of manufacturers no longer engaged in the manufacture of aircraft engines form an important part of this section, since it illustrates and lists the various types and models which were produced, with their principal dimensions and ratings. Family histories of current models are easily traced, through the many types which preceded them, by photographs and specifications, while the specifications and ratings of these models themselves are very complete and up to date.

The Modern Aircraft Section, covering 202 pages and 379 illustrations, gives the specifications and performance data on aircraft which were current at the time of publication. While the information on the products of domestic manufacturers is, of course, available from other sources, and foreign aircraft are not covered completely because of wartime restrictions, it is nevertheless very helpful to have the available data collected in a single volume, which deals in addition with so many other features of the aviation industry.

This is followed by a 63-page section dealing with statistics, giving a well-arranged compilation of international and American records, passenger miles flown, engine and plane production, causes of accidents, exports and imports, etc.

A Directory Section, comprising 274 pages, is designed to be an international trade directory. Firms and organizations (both

(Continued on page 310)

Institute Notes

Second Annual Summer Meeting

The Second Annual Summer Meeting of the Institute to be held on June 24, 25, and 26 has met with such an enthusiastic response that arrangements have been made to hold the technical sessions and the banquet at the Hotel Ambassador in Los Angeles. All interested persons are invited to attend the technical sessions. There will be no registration charge.

The Program Committee, consisting of Dr. A. E. Lombard, Jr. (Chairman), W. W. Beman, J. R. Goldstein, E. J. Horkey, Dr. A. L. Klein, R. W. Palmer, E. A. Peterman, and W. C. Rockefeller, has arranged the following Tentative Program. The Final Program will be mailed to members within a few weeks.

Monday, June 24, 2:00 p.m.

W. L. Howland and Carl Beed, Lockheed Aircraft Corporation, **Tests of Pressurized Cabin Structures.**

John C. Mathes, The Dow Chemical Company, **Recent Developments in Magnesium Alloys.**

Symposium: Stability of Aircraft Structures. Prepared notes will be presented by Alfred S. Niles, Stanford University; Louis G. Dunn, California Institute of Technology; N. J. Hoff, Stanford University; John C. Silliman, Pacific Railway Equipment Company; and J. L. Fredrick, California Institute of Technology.

8:00 p.m.

R. L. Thoren and C. L. Johnson, Lockheed Aircraft Corporation, **Effects of Propeller Slipstream and Tail Position on the Vibration Characteristics of the Lockheed "Lodestar."**

Jean Wylie and E. P. Wheaton, Douglas Aircraft Company, **Flutter: A Diagnosis—Its Prevention and Cure.**

W. B. Bergen and Lee Arnold, The Glenn L. Martin Company, **A Graphical Solution of Flutter Instability.**

Tuesday, June 25, 2:00 p.m.

James B. Darragh, Jr., Lockheed Aircraft Corporation, **The General Use of a Magnetic Steel Tape Recorder in Airplane Testing.**

C. S. Draper, J. H. Lancor, and Leighton Davis, Massachusetts Institute of Technology, **The Application of an Electromagnetic Indicator to Internal Combustion Engine Problems.**

M. A. Biot, Columbia University, **Coupled Vibrations of Propeller Crankshaft Systems.**

Fred Foulon, Douglas Aircraft Company, **A New Approach to Bonding and Shielding Requirements for Aircraft.**

8:00 p.m.

W. Randolph Lovelance, II, W. M. Booth, and O. O. Benson, Mayo Clinic, **High Altitude Flight and Its Effect on the Human Body.**

A. D. Tuttle, United Air Lines, **A Proposed Subdivision of the Troposphere for Scientific and Practical Purposes.**

W. H. Hunter, The B. F. Goodrich Company, **Experiments on Drop Impingement.**

Wednesday, June 26, 2:00 p.m.

Ralph H. Upson, Ann Arbor, Michigan, **Performance Dictates Design.**

Louis H. Enos, Curtiss Propeller Division, Curtiss-Wright Corporation, **Some Recent Developments in Propeller Blade Desgin.**

Norton B. Moore, University of California, **Range at Constant Speed.**

7:00 p.m.

Closed Session: Open only to members of the Institute and invited guests.

Banquet: The Fiesta Room, The Ambassador Hotel.

Program: "Some Startling New Developments in Aircraft Design and Flight Testing."

Institute Session at A.A.A.S. Summer Meeting

As announced in the April issue of the Journal, the Institute will hold a one-day meeting on Transoceanic and High Altitude problems on Friday, June 21st, at the University of Washington in Seattle, in connection with the Summer Meeting of the American Association for the Advancement of Science. An interesting program is being arranged and all who are interested in the problems being discussed are urged to attend. Programs will be sent to members later this month.

A banquet, at which Robert J. Minshall will be awarded the Musick Memorial Trophy, will be held in the large ballroom of the Masonic Hall. P. G. Johnson, President of the Boeing Aircraft Company, will be toastmaster. The speakers will be prominent officials and leaders in aviation.

Dr. Petterssen to Give Wright Brothers Lecture

The Wright Brothers Lecture for 1940 will be delivered by Dr. Sverre Petterssen, Professor of Meteorology at the Massachusetts Institute of Technology. Dr. Petterssen is a graduate of the University of Oslo and was formerly Chief of the Weather Bureau for western Norway. Since 1934 he has been a member of the International Meteorological Organization and was elected President of the Commission for Maritime Meteorology in 1939.

Dr. Petterssen is well known to aeronautical meteorologists in this country. In 1935 he came here under the auspices of the U.S. Navy to lecture to the personnel of its meteorological services. He also lectured at several of the universities. His many contributions to dynamic and synoptic meteorology have played a prominent part in facilitating more detailed forecasts of weather phenomena.

The Wright Brothers Lecture, which is given on December 17th, the anniversary of the first flight of the Wright Brothers, has an endowment of $17,000 provided by Mr. Edmund C. Lynch in 1938 in memory of his brother, Vernon C. Lynch. The selection of the lecturer is made by a committee composed of Americans who have delivered the Wilbur Wright Memorial Lecture before the Royal Aeronautical Society in London.

Gifts to the Aeronautical Archives

The most important addition to the Aeronautical Archives during April has been the loan of Mr. Harry Guggenheim's exceptionally interesting collection of prints and engravings. It includes many of the best prints of early aeronautics and is particularly complete in portraits of famous persons whose names are well known in aeronautical history. Mr. Guggenheim has placed the collection in the Archives for an indefinite period, where it will be on exhibition.

Mr. Grover Loening, who contributed the furnishings of the Institute when it opened its offices in 1930, has had several of the settees and chairs re-upholstered.

Mrs. Bella C. Landauer is continually adding to the collection of the Archives by sending more aeronautical music, interesting trade cards, and books.

A large collection of books and photographs has been presented by Mr. William Wait, Jr.

The Misses Octavia and Elizabeth Chanute, daughters of Octave Chanute, have presented the Archives with a copy of *Progress in Flying Machines* and a photograph of their father, both autographed.

Col. Charles A. Lindbergh sent the manuscript of Mrs. Lindbergh's book, *Flying Around the North Atlantic.*

Dr. William C. Geer presented the book, *The Chemistry and Technology of Rubber,* and a collection of articles on aeronautical uses of rubber.

Dr. Michael Watter sent several books and pamphlets on early aviation.

Two large packing cases of early aeronautical magazines have been received from Mr. Waldo Waterman.

A bound volume of *Popular Aviation* was presented by Mr. Max Karant.

Mrs. Jacqueline Walker sent a copy of her book, *Equator South Equator North.*

The appreciation of the Institute is expressed to the New York Museum of Science and Industry for the design and construction of an exhibit case for models, medallions, stamps, etc.

The Stevens Institute of Technology presented copies of Technical Memorandums Nos. 32, 40, 47, 67, and 87. These give test results from various investigations in the Experimental Towing Tank at the Stevens Institute.

Conferences on Friction and Surface Finish

Conferences on Friction and Surface Finish will be held by the Departments of Mechanical Engineering and Metallurgy at the Massachusetts Institute of Technology, June 5, 6, and 7, consisting of all-day meetings devoted to the subjects of friction and surface finish. The program will include formal technical papers in the morning of each day, to be followed by informal discussions in the afternoons.

The purpose of the conferences is to bring before engineers, associated with the many industries concerned with machinery, a summary of present knowledge regarding friction and surface finish, in the hope of bringing out by discussion an appreciation of what new information is needed and an indication of the most promising directions for future research in this and allied fields of wear, seizure, lubrication, and so on.

Papers will be presented by A. F. Underwood, General Motors Research Laboratories; John Wulff, Massachusetts Institute of Technology; D. A. Wallace, Chrysler Corporation; Stewart Way, Westinghouse Research Laboratories; Hans Ernst, Cincinnati Milling Machine Company; G. B. Karelitz, Columbia University; Otto Beeck, Shell Development Company; J. C. Geniesse and R. Simard, Atlantic Refining Company; R. W. Dayton, Battelle Memorial Institute; and A. R. Stevenson, General Electric Company.

Further particulars may be had by communicating with Prof. J. C. Hunsaker, Department of Mechanical Engineering, Massachusetts Institute of Technology, Cambridge, Mass.

Personnel Opportunities

Available

An experienced University graduate aeronautical engineer with a personality for sales and consultant work seeks a connection with a responsible and well known company dealing with or in the aircraft industry. At present engaged in a responsible position in the engineering department of a major aircraft company. Address reply to Box 100, Institute of the Aeronautical Sciences.

Necrology

Johann Schütte

Dr. Ing. Johann Schütte, a Fellow of the Institute, died at his home in Dresden, Germany, on April 1, 1940, at the age of 67.

Dr. Schütte is best known for his pioneering work on airship design. Along with Karl Lanz he designed the Schütte-Lanz type of airship, of which 22 were built during the years 1911 to 1918. His factory also produced more than 1000 airplanes during the first World War.

In 1919 Dr. Schütte became President of the Wissenschaftliche Gesellschaft fur Luftfahrt and, at the time of his death, was President of the Schiffbautechnische Gesellschaft e.v. He was awarded a Dr. Ing. degree by the Technische Hochschule, Berlin, and was appointed Ordtl. Professor at that institution.

Robert Moffatt Losey

Captain Robert Moffatt Losey, a Technical Member of the Institute, assistant Military Attaché for Air to the U.S. Legation in Norway, was killed during an air raid at Dombaas, Norway, on April 22, 1940.

Born on May 27, 1908, in Andrews, Iowa, Captain Losey was graduated from West Point in 1929. After brief duty with the field artillery he was transferred to the Air Corps and was graduated from the Air Corps Advanced Flying school at Kelly Field, Texas, in 1930. In 1934 he was assigned to do graduate work at the California Institute of Technology, where he received a Master of Science degree in Meteorology in 1935. Between 1935 and 1940 he was, successively, meteorological officer at March Field, California, and on duty with the Training and Operations Section of the Chief of the Air Corps at Washington, D. C. In January, 1940, he was assigned as assistant Military Attaché for Air to the U.S. Legation in Finland. On January 17, 1940, he was transferred to Norway.

Book Review

(*Continued from page 308*)

foreign and domestic) affiliated with aviation, their addresses, personnel, branch offices, products, etc., are first listed alphabetically, then are included under a "Products" listing. While there are some omissions in the list of institutions having wind tunnels, the coverage in the commercial fields seems remarkably complete.

Considering the encyclopaedic scope of the book and its excellent makeup the price is quite reasonable. Much of the information given is of vital importance in many aeronautical activities, notably manufacturing, the work of government agencies and universities, advertising, banking, etc., and the volume should enjoy a wide distribution.

J. M. Coburn, New York University

Aeronautical Reviews

These brief reviews of recent articles on aviation subjects are published by the Army Air Corps for the information of its officers, and are printed here each month by permission of the Chief of the Air Corps

Aerodynamics

The Influence of Reynolds Number on High Mach Numbers. A. Eula. Drag of a sphere and of cylinders has been measured in the supersonic field at different Reynolds Numbers. First results of the measurements are explained, and it is deduced that, in the field explored, the influence of Reynolds Number on drag is zero. Experimental results in the supersonic range, research at Guidonia, experimental results on the sphere, cylinder, and flat plate, and practical importance of the research are discussed. *L'Aerotecnica*, January, 1940, pages 20–29, 7 illus.

Aircraft Design

Diving Air-Brakes for Sailplanes and Aeroplanes. H. Jacobs and A. Wanner. Technique which was developed for the safety of sailplanes when flying through clouds has been applied to reduce the terminal velocity of dive bombers. Evolution of the dive-brake used on German sailplanes, and tests on the Focke-Wulf Fw.56 Stoesser airplane are described in great detail. Tests of air-brakes on the Rhoensperber sailplane, flying trials, installations on the Rhoenadler, Minimoa, and Reiher, and points to be considered in the design of air-brakes of the D.F.S. type are discussed.

In regard to tests on the Focke-Wulf Fw.56 Stoesser monoplane, the arrangement on the airplane, brake position, effect of slots, test arrangements, analysis of airstream, drag coefficients, and effect of different arrangements on stalling and spinning are covered. Translated from the German "Jahrbuch 1938 der Deutschen Luftfahrtforschung." *Aeroplane*, February 23, 1940, pages 253–257, 21 illus.

Military Development. "The present War, if it lasts long enough, may bring us big fighters and little bombers." The bigger fighter, which has greater range, more guns, and more ammunition for each, is advocated as an escort for bombers. Large four-engine bombers are criticized, and it is said that a small bomber carrying a big load at high speed, with the aid of assisted take-off, would not be nearly so vulnerable, even though comparatively lightly armed. Such an airplane might be designed to cruise at 400 m.p.h. Trend of fighters probably bears first toward airplanes armed with still greater numbers of machine guns (than the present eight guns on fighters) and then logically toward fighters armed with multi-cannon. Short discussion. *Aeroplane*, February 16, 1940, page 221.

Contribution to the Theory of the Two-Dimensional Potential Flows around Tail-Surface Profiles. F. L. Loesch. Introduction to the four succeeding articles describing investigations of the theory of the two-dimensional flows around tail-surface profiles. Purposes of these investigations are discussed and symbols used are listed and explained. *Luftfahrtforschung*, January 20, 1940, pages 1–2, 2 equations, 1 table.

Lift and Moment of Tail-Surface Profiles of Finite Thickness with Diminishing Slots. W. Weinberger. Theory of two-dimensional potential flow around the tail-surface profiles of diminishing thickness without slot, calculated mainly by H. Glauert from the method of the vortex covered distance, does not yield values for the aerodynamic coefficients of profiles which conform satisfactorily with measured results obtained on flapped airfoils with practical slot effect missing. The three D.V.L. investigations described were made to determine how far the results of the potential theory are affected by the consideration of thickness and thickness distribution of profiles.

Effect of maximum thickness and thickness distribution of a tail-surface profile on the values of lift, moment, normal component of force on the control surface, and control-surface moment, calculated according to the theory of the two-dimensional potential flows under limitation of a linear theory pertaining to angle of attack and control-surface angle, was investigated on profiles which can be reproduced in a simple manner conforming to the circle. Only the effect of maximum thickness on the coefficient of the control-surface moment was proved of importance. Report of the D.V.L. *Luftfahrtforschung*, January 20, 1940, pages 3–11, 16 illus., 20 equations.

Velocity Field in the Vicinity of a Tail-Surface Profile of Finite Thickness with Diminishing Slot. H. Menzel-Rogner. Two-dimensional flow about an infinitely thin, flapped airfoil can be computed in a simple manner from Birnbaum's method of the vortex covered distance. In order that an indication of the effect of profile thickness on field of flow may be obtained, the velocity field of the two-dimensional potential flow around a profile of finite thickness is investigated. The profile conforms approximately to a Joukowsky profile divided into a fixed plane and mechanically deflected control surface. D.V.L. report. *Luftfahrtforschung*, January 20, 1940, pages 11–17, 7 illus., 6 tables, 10 equations.

Lift and Moment of the Angular Plate with Slot. H. Soehngen. Procedure for the calculation of lift and moment coefficients as well as the pressure distributions of the symmetrical double-section airfoil is established on the Birnbaum theory of the lifting vortex sheet and from the solution of an integral equation system. The various solution values are given in explicit form and are exact within the meaning of a linear theory for the flow angles. For the four control-surface thickness ratios, 0, 1/9, 2/9, 3/9, the coefficients of lift and moments, as well as the lever arm of the normal force on the control surface when the angle between the fixed surface and control surface equals zero, are shown in diagrams which should be sufficient for obtaining intermediate values of control-surface thickness ratios by interpolation. D.V.L. report. *Luftfahrtforschung*, January 20, 1940, pages 17–22, 8 illus., 8 equations.

Lift and Moment of an Unsymmetrical Double-Section Airfoil. F. Loesch. Two-dimensional potential flow about an unsymmetrical double-section airfoil is calculated by means of conformal representations. The fixed plane and control surface of the airfoil are Joukowsky-Betz profiles similar to each other. Under the limitation of small control-surface angle, the following are determined and shown in diagrams: pressure distribution over fixed plane and control surface, lift and moment of the double-section airfoil, normal force on the control surface, and control-surface moment. D.V.L. report. *Luftfahrtforschung*, January 20, 1940, pages 22–32, 15 illus., 13 tables, 24 equations.

Correlation of Wind-Tunnel and Flight-Test Results. W. W. Symington, Jr., Glenn L. Martin Co. Method proposed first assigns definite values to all of the miscellaneous drag items, uses full-scale static propeller whirl-test results, and uses wind-tunnel results obtained under fully turbulent conditions, logically extended to full-scale Reynolds Number. Fully turbulent condition is obtained by running the tests at a high enough speed or by placing a screen in front of the model thus mechanically inducing turbulence. When the transition region has thus been eliminated, it is possible to extend the results to full-scale Reynolds Number by use of the formulas given.

Table giving a summary of coordination data for three airplanes follows the recommended procedure and includes general dimensions, wind-tunnel test results, additional items not included in the wind-tunnel results (such as drag coefficients due to surface irregularities, to antenna mast and wires, to engine cooling-air flow, and to total airplane drag), and flight test results. The three major variables having great influence in determining the final performance of an airplane, namely, engine power, propeller, and drag are discussed in great detail. *S.A.E. Preprint for Annual Meeting*, January 15 to 19, 1940, 11 pages, 9 illus., 1 table, 1 equation.

Design and Production. E. Ritter. A German production engineer's views on desirable coordination to be achieved between the design and production departments of an aircraft factory, and suggestions for its attainment. Discussion covers: cooperation between designer and engineer beginning at the start of the design stage; basic requirements to be borne in mind when planning new designs; use of mockups using genuine wiring and pipes; selection of materials and use of semifinished materials; coordination in development of parts and accessories (such as beaded flanges, branch boxes, detachable wing panel, airplane door, and control column); fuselage construction; cooperation in drawing up tolerances to form a compromise between aerodynamic requirements and economy of production of wing sections; final assembly of the fuselage and fitting of pipes and of electrical and radio equipment; collaboration of designer and production engineer in making an airplane accessible for maintenance and repair; organization necessary for collaboration; the human factor in coordination; and apprenticeship, advanced training, and exchange of experience.

Among the photographs are shown a power-plant mockup with genuine wiring and pipes and sheet fairing and upper and lower fuselage shells for a Junkers Ju.87 two-seater dive bomber. Translated from "Jahrbuch 1938 der Deutschen Luftfahrtforschung." *Aircraft Engineering*, February, 1940, pages 35–39, 11 illus., 2 tables.

Rigorous Performance Prediction without Drudgery. E. G. Reid. New graphical method of predicting airplane performance has been evolved by utilizing the unique properties of Eiffel's logarithmic propeller chart. Method is particularly convenient when constant-speed propellers are involved, and yields performance characteristics for altitudes below, as well as above, the critical ones for supercharged engines.

Principal departure characterizing the new method is the adaptation of Eiffel's logarithmic propeller chart to the construction of available power curves. Use of "indicated airspeed" ($\sigma^{1/2} V$) and the analogous quantity "indicated power" ($\sigma^{1/2}$ hp.) as coordinates causes a single curve to represent power requirements for level flight at all altitudes. Other simplifications arising from recognition of certain engine characteristics, utilization of the unique properties of the Eiffel chart, and development of a convenient method for evaluating the excess available power (from logarithmic curves) make it possible to eliminate a large portion of the labor previously required for rigorous performance prediction. Recent Institute of Aeronautical Sciences paper. *Royal Aeronautical Soc., Jour.*, February, 1940, pages 176–194, 17 illus.

Rotary-Wing Aircraft. J. A. J. Bennett. Vertical descent of rotary-wing aircraft without power is discussed. Analysis given shows that, when profile drag is sufficiently small, only part of the rotor is in the "windmill brake" state. This part receives more torque from the air than can be expended in profile drag and therefore the rotaplane rotor at zero torque must be partly a propeller in the "vortex ring" state. The vortex theory of propellers is inapplicable to the vortex ring state and adjacent part of the windmill brake state, but Glauert and Lock have determined, by analysis of propeller experimental data, the form of the characteristic curve connecting two non-dimensional parameters f and F in the region where the vortex theory breaks down. To define the state of working of the rotor blade elements, the author uses an empirical relationship between f and F suggested by the Glauert-Lock analysis. Continued. *Aircraft Engineering*, February, 1940, pages 40–44, 12 illus., 3 tables, 23 equations.

Stress Analysis and Structures

The Control of Vibration in Aircraft. H. H. Bruderlin. Aircraft vibration is explained, and excitation originating directly from the engine and from the propeller is considered. An engine-propeller vibration anaysis chart is illustrated and discussed. To be continued. *Aviation*, January, 1940, pages 40–41, 3 illus.

The Control of Vibration in Aircraft. H. H. Bruderlin. As a general rule, excessive amplitude in the main structural members is caused by resonance; that occurring in non-structural parts or in auxiliary structures is forced and should not be stiffened. Stiffening by reinforcement is often resorted to when parts begin to disintegrate unaccountably, and may be the wrong thing to do as often as the right. If affected parts are actually resonant and are vibrating sympathetically with the engines or some other driving force, stiffening correctly applied may well serve to move them out of the resonant range. Decreasing the stiffness serves the same purpose and damping may be a simpler remedy. If the part is actually being forced to deflect with a fixed amplitude, a reinforcement will usually increase the unit fiber stress and cause failure to occur more rapidly, particularly when there are discontinuities in the stressed part, as when a reinforcing member carries across only part of it and causes a concentration of stress to occur at its points of attachment as in the case of fillets, gussets, and cowl sheets. Design of shock mountings is discussed.

Phenomena of resonance are explained and curves are given to illustrate the responses of a vibrating system to constant excitation varying frequency and to excitation proportional to frequency, as well as the effect of damping on a resonant system. A simple relation between the natural frequency of a shock-mounted object and its deflection on the shock mounts due to its own weight is shown in a curve (natural frequency *versus* static deflection),

which is said to be useful in determining what type of suspension should be used. Another curve gives the reduction obtainable for a given ratio of resonant frequency to forcing frequency for the condition of no damping in the mounts, which is approximated in the usual types of shock mount at frequencies far from resonance. Concluded. *Aviation*, March, 1940, pages 38–39, 117, 119, 5 illus.

Principal Conceptions of the New Regulations for the Acceptance of Airplanes in Regard to Strength. Ten. Gen. GARI A Fiore. Informative criterions are explained which have guided the Director General of Aeronautical Construction in the Italian Air Ministry in fixing the new regulations recently published for the acceptance of modern aircraft in regard to strength. *L'Aerotecnica*, January, 1940, pages 3–10, 4 illus., equations.

Air Forces on Radial Air-Cooled Engine Cowling as Determined from Pressure Distribution Tests. R. R. Higginbotham, Republic Aviation Corp. Factors influencing engine-cowl surface pressures are discussed, and results of pressure tests on one cowl model in the wind tunnel and on three representative cowl designs in flight are presented and analyzed. Methods of applying pressure-distribution data to the stress analysis of other cowls are suggested.

Theoretical considerations dealt with cover: airfoil pressure distribution; engine-cowl flow equations; pressure distribution at zero angle of attack; unsymmetrical pressure distribution; effects of Reynolds Number, engine conductivity, and flaps; comparability of pressure curves; and propeller effects. Flight and wind-tunnel test procedures are described, and results of both tests are discussed in detail. Cowl forces are computed from pressure data, with a discussion of the following: forces to be determined; determination of worst flight condition; construction of average loading curves; integration of average pressure curves; conservative approximate methods; and calculated loads on flight test cowls. Long paper. *S.A.E. Preprint for Annual Meeting*, January 15 to 19, 1940, 67 pages, 24 illus., 2 tables, 14 equations.

Aerofoil Sections and Torsion. F. David. Geometrical properties of symmetrical N.A.C.A. airfoils for use in torsional calculations. While the chart illustrated refers to symmetrical airfoils of the N.A.C.A. family, ordinary magnitude of the mean camber will have no practical influence on the results if it is also used for nonsymmetrical airfoils. Calculation of the required area and perimeter of the box between 11 per cent and 67 per cent behind the leading edge of N.A.C.A. Section 2412 is presented as an example. *Aircraft Engineering*, February, 1940, page 44, 3 illus., equations.

Aircraft Accessories

Problems of Ancillary Services for Aircraft. R. H. Chaplin and F. Nixon. Replies of the authors to discussions on the paper presented before the Royal Aeronautical Society are given, which deal with: hydraulics *versus* electrics; low pressures for gun turrets; arcing risks in electrical systems; question of main or auxiliary engines; scope for both systems; and American experience.

"Moreover, had the Douglas engineers," in the design of the DC-4, "had the benefit of the latest British hydraulic practice it is doubtful whether the auxiliary engine would have shown itself superior to the hydraulic drive." Compact way in which the accessories are arranged at the back of the 890-hp. Rolls-Royce Peregrine engine is illustrated in a photograph. *Aeroplane*, February 16, 1940, pages 222–224, 2 illus.

Aircraft Manufacture

Interesting Development by Glenn L. Martin Company. First metal stretching press to be built and operated in the United States recently has been completed in the Glenn Martin plant. Sheet of metal to be stretched is placed over the form and clamped tightly in both rows of jaws. Pressure is then applied on the hydraulic cylinders, causing the platen to move up and stretching the sheet tightly over the form. Thickness of the material is reduced only from 5 to 7 per cent in the stretching process. Few details. *U. S. Air Services*, March, 1940, page 20.

Loft Layout Method Developed by Northrop. Northrop method of layout of body-plan lines promises to speed up new aircraft production by cutting down time required between design and fabrication stages. Northrop loft has been using Alclad. The sheet was painted white and the preliminary work was drawn in pencil. After final approval, the lines were scrieved in with a regular scrieve knife. The knife cut (about 0.01 in. wide by 0.005 in. deep) was smoother than a cut in wood, and the knife edge stayed sharp for at least as much cutting. Experiments seem to indicate that several metals may be scrieved in this manner. However, the light weight of aluminum is of decided advantage for layouts. Brief note. *Aero Digest*, March, 1940, page 252.

Manufacturers of Airplanes. Alphabetical directory of American aircraft and engine manufacturing companies as well as their executive personnel, department heads, and export representatives. *Aero Digest*, March, 1940, pages 58, 60.

Production of the Messerschmitt Me.109 at the Erla Shadow Factory. Journalists taken on a tour of this plant were impressed with the fact that more than 25,000 rivets are required for one wing, and that women workers perform this job with great accuracy and skill, using either electric or hydraulic riveting machines. After the top skin of the wing is fixed the electric wiring is installed before the bottom skin is put on. "In the first stage of the assembly, a point mentioned especially was the installation of the armament—two shell guns, one on each wing, and two Rheinmetal-Borsig synchronized machine guns mounted in the cowling in front of the pilot. A casual remark suggests that the Luftwaffe is considering the equipment of the present type of Me.109 with three 20-mm. shell guns." Subcontracting in Germany, and layout of the plant are discussed. *Aeroplane*, March 1, 1940, pages 278–280, 5 illus.

Process Control of Spot Welding. C. L. Hibert. First issue—Requirements of spot-welding equipment to meet its most severe test in aircraft manufacture are discussed, including: the welding variables, time of current dwell, diameter and shape of electrodes, pressure on electrodes, contact resistance, and current intensity necessary to weld the gages of aluminum alloys required in aircraft. Recommended welding data for various aircraft materials are given in a table.

Second issue—Data on design of spot-welded parts; equipment necessary; personnel; and inspection procedure for welds. *Iron Age*, March 7 and 14, 1940, pages 43–47 and 31–34, 5 illus., 3 tables.

Refinements of Fine Measurements. Principle of the Electrolimit gage for measuring diameters is that of mechanical contact measurement magnified many times through an electric circuit. It is possible to measure to one-millionth part of an inch with the gage. Two types are provided for measuring external and internal diameters, respectively. The Alignment Telescope was produced initially for aircraft assembly work and is used to check the alignment of large jigs for assembly. It is capable of showing want of parallelism amounting to one part in 20,000 on bearings or surfaces as widely separated as 80 ft. Collimator projects a fine true column of light upon scales and a special kind of telescope is placed at the other end of the work through which the scales can be read. The Profile Projector projects a much magnified profile of the image of the particular object upon a screen where the magnified image of the profile may be measured. The Section Projector deals with work which cannot otherwise be measured with the degree of accuracy necessary in modern production and illuminated section is photographed by means of a special camera.

Descriptions and illustrations of these Taylor, Taylor and Hobson devices. *Flight*, March 7, 1940, pages 208f–208g, 8 illus.

Steel-Faced Cast-Iron Dies for Drop Hammer Work. J. H. Engel. Dies developed by Engel Aircraft Specialties for use in conjunction with lead dies. Combination steel-faced cast-iron dies have been used for making stampings from light-gage aluminum alloys to chrome-molybdenum (X4130) sheets 0.094 in. thick. Wrinkles in the sheet are said to be avoided by the use of slippage controlling plates made of boiler steel. Other methods of controlling wrinkles are discussed. *Iron Age*, March 21, 1940, pages 46–48, 3 illus.

Welding Aluminum Aircraft Alloys. M. Sciaky. Perfect consistency of welds and welds free from cracks are the claims of the French-English Sciaky Company of Paris for its system of electric resistance welding. Stored energy and variable-pressure cycle are the two principles on which the welding machine is based. The reactor is charged with electromagnetic energy from a three-phase mercury-arc rectifier. Pressure at the electrodes is obtained by a differential air cylinder. Douglas, Consolidated, and other aircraft companies have purchased machines, and Southern California Edison and Philadelphia Navy Yard have been testing them out. Description of system and results obtained. *Iron Age*, March 21, 1940, pages 33–35, 5 illus.

Lofting Speeds Production for Consolidated. T. J. Coughlin. Lofting procedure adopted by the Consolidated Aircraft Corporation is described. Lofting as applied to aircraft production follows the practice used in ship building which applies to laying out of hull or fuselage bulkheads, belt frames, and other parts, on the full-size scale. In addition, aircraft lofting is applied to the wing, tail, furnishings, and armament groups. *Aviation*, January, 1940, pages 34–35, 88, 2 illus.

They Stand on Their Own Feet. F. A. Hoffman. New types of jigs and fixtures developed by Harlow Aircraft Company for use in the manufacture of metal airplanes. Forming operations are held to a minimum and attention has been concentrated on the assembly jig as the major production tool. *Aviation*, January, 1940, pages 36–37, 90, 7 illus.

Welding Technique in Aircraft Construction. K. Queitsch. Translation of another portion of the German Air Force welding handbook. The examples on the welding of fittings and sub-assemblies given have been taken from the actual manufacturing practice of the German airplane industry, and serve to illustrate to the welder how to make intelligent use of the working methods and rules discussed in the previous articles. Examples include: sheet fairings and tubular structures; construction of a simple spar fitting; construction of a control column; undercarriage fitting; tubular strut for an undercarriage cover; tubular cross bracing of an undercarriage; bearing bracket for a hydraulic jack cylinder; manufacture of highly stressed spar and bulkhead fittings; and struts and miscellaneous fittings and parts. Among the drawings and photographs are included the following: spar fitting in a jig; glider control shaft and method of welding it; Dornier undercarriage strut and fittings and welding jigs; Heinkel foot rest in its welding jig; Heinkel main-wing spar joints and stages in construction; glider main spar and bulkhead fitting; Junkers welded joints (from the F.13, Ju.52, and Ju.34); and Junkers welding jigs and fixtures. Continued. *Aircraft Engineering*, February, 1940, pages 56–59, 29 illus.

Aircraft

Military Aircraft. H. F. King. International practices in the design, construction, armament, equipment, and, to a lesser degree, operation, of bombers, fighters, army-cooperation, ship-borne aircraft, shore-based marine aircraft, coast-defense landplanes, trainers, and military transports, are covered in great detail in separate articles to which this is the introduction. Many of the machines discussed and illustrated are prototypes only. *Flight*, March 14, 1940, page 221.

Bombers. International practice in the design of bombers including multi-purpose aircraft suitable for reconnaissance and ground attack, as well as modern bombing and dive-bombing tecaniques, is discussed in great detail.

Various types of bombers of many countries, some new prototypes, are referred to in the text and are illustrated. Performance, dimensions, disposable load, engines, typical armament, and progress (prototype, or in or out of production) are shown in tables. *Flight*, March 14, 1940, pages 222–233, 246, 45 illus., 4 tables.

Fighters. Fighters are being provided with still more power, armament, and armor, and some now attain 400 m.p.h. New twin-engine designs are included in the discussion on international practice in the design of fighters.

Dimensions, disposable load, engine, performance, armament, and progress (prototype, or in or out of production) are given in tables for single- and twin-engine monoplane and single-engine biplane single-seater fighters, and single- and twin-engine two-seater fighters of various countries. *Flight*, March 14, 1940, pages 234, 234a–234l, 51 illus., 2 tables.

Army Cooperation. New tactics may result in further specialization of army-cooperation aircraft. Wide speed ranges required, the problem of visibility, and the use of rotating-wing aircraft are discussed in this consideration of international practice in the design of army-cooperation aircraft. Various types of various countries are illustrated in photographs and referred to in the text. Dimensions, disposable load, engine, performance, progress (prototype, or in or out of production), and armament are given for one British, one French, one American, two German, two Bohemia-Moravian, one Polish, two Italian, and one Rumanian army-cooperation aircraft. *Flight*, March 14, 1940, pages 234m–234o, 16 illus., 1 table.

Ship-Borne Aircraft. Special requirements for naval operation, catapultable and deck landing machines, maintenance requirements, and dimensional restrictions are considered in this discussion of international practice in the design of ship-borne aircraft. Types produced in various countries are illustrated by photographs and referred to in the text. *Flight*, March 14, 1940, pages 234p, 235–236, 17 illus.

Shore-Based Marine Aircraft and Coast-Defense Landplanes. Aircraft capable of operating far out to sea and based on shore, including large flying boats and floatplanes (or amphibians) for bombing, torpedo-dropping, possibly mine-laying, reconnaissance, naval-cooperation, patrol, and convoy missions are covered in a discussion of international practice in the design of such aircraft. Different types produced in various countries are illustrated and referred to in the text. Dimensions, disposable load, engine,

performance, armament, and progress (prototype, or in or out of production) are presented in a table for one British, one American, three German, two Italian marine aircraft, and one French, one Italian, and one Dutch torpedo-carrying aircraft. *Flight*, March 14, 1940, pages 237–238, 12 illus., 1 table.

Trainers. International practice in the design of trainers is discussed, and different types of various countries are illustrated in photographs. Use of elaborate equipment for "crew" trainers is emphasized. *Flight*, March 14, 1940, pages 239–240, 10 illus.

Military Transports. International practice in the design of military transports is briefly discussed with reference to British, American, and German practice. *Flight*, March 14, 1940, page 240, 2 illus.

Germany's Fastest Fighter. Top speed of the Focke-Wulf Fw.198 single-seater single-engine pusher fighter is considered to be about 370 m.p.h. at 19,000 ft., lower than originally rumored. It is believed to be powered by the latest Daimler-Benz D.B.601 engine, supercharged to give 1360 hp. for take-off and 1175 hp. at 16,400 ft. Armament is reputed to be two cannon in the wings in the line of each tailboom, and four machine guns in the nose of the nacelle. Wing loading is said to be 28 lb./sq.ft. which is unusually low for a German fighter.

From further information and a general description of the machine an estimate of the performance is made giving the following: with the armament quoted and 110 gal. of fuel, all-up weight not less than 7200 lb.; wetted area approximately 832 sq.ft.; rate of climb about 2750 ft./min.; duration on 110 gal. about two hours at 295 m.p.h. on 50 per cent of power; and ceiling about 34,500 ft. Disadvantages of the pusher design are pointed out. It is said that one reason why the Messerschmitt Me.109 and Heinkel He.112 single-seater fighters have not been completely successful is that they are too highly loaded compared with their original designs. Reference is made to the Hurricane and Spitfire in comparison with the German airplanes. *Aeroplane*, March 1, 1940, pages 276–277, 1 illus., 1 table.

The Junkers Ju.87 Dive Bomber. Junkers Ju.87 single-engine two-seater dive-bomber monoplanes, having proved their worth in Spain, were used in great numbers with much success in the campaign against Poland. They are not particularly fast, latest version having a top speed of 242 m.p.h. at 13,780 ft., nor are they heavily armed. Airplane is immensely strong, flies well, and is especially designed for ease of maintenance in the field. Design has been kept as simple as possible and it does not have a retractable undercarriage.

Evolution from the Swedish-built Junkers K-47 of 1932 down to the Ju.87B, is traced, and construction of the Ju.87, its fuselage, empennage, 1200-hp. Junkers 211 gasoline-injection engine, accommodation, and action in two wars are described in great detail. Dimensions, weights, loadings, and performance of the Ju.87B are presented, and photographs and a cut-away drawing showing location of equipment are given. Span 45 ft. 4 in. Wing loading 27 lb./sq.ft. Disposable load 3200 lb. Range 498 miles at 186 m.p.h. Climb to 14,750 ft., 10 min. Service ceiling 27,900 ft. *Aeroplane*, February 23, 1940, pages 248–252, 8 illus., 1 table.

GREAT BRITAIN

Aeroplanes of the Bomber Command. Three views of a new Vickers-Armstrong Wellington long-range bomber on its acceptance trials before delivery to the R.A.F. are illustrated. The Handley-Page Hampden (two 1000-hp. Bristol Pegasus XVIII engines), Armstrong-Whitworth Whitley IV, Bristol Blenheim IV, Bristol Bombay, Fairey Battle, Vickers-Armstrong Wellington I, and Saunders-Roe Lerwick flying boat (two 1375-hp. Bristol Hercules II engines) in flight are shown on four two-page supplementary sheets of composite photographs. *Aeroplane*, March 8, 1940, page 316, 3 illus. and 4 on suppl. sheets.

Dynamic Similarity. Latest firm to build a flying scale model is Saunders-Roe. Model created a very favorable impression in flight tests, not only being fast and very maneuverable in the air, but showing good sea qualities, clean running, and absence of porpoising. Overall length is 42 ft. 8¼ in. and wing span 50 ft. The four 90-hp. Pobjoy engines come very close to being a scale model of modern radials, having reduction gearing for its propeller. Few details and photographs are given, and the necessity for building flying scale models of a large aircraft which departs considerably from previous models is pointed out. *Flight*, March 14, 1940, page 251, 3 illus.

The 1940 Flamingo. New DeHavilland Flamingo (DH 95) passenger liner has two of the later-type Bristol Perseus XVI sleeve-type engines which have greater power rating at altitude (maximum power in level flight for five minutes 905 hp. at 6500 ft.) than the Perseus XIIc fitted to earlier models. Use of DeHavilland Hydromatic feathering propellers involves an increase in propeller weight of 100 lb., but the better performance due to increased engine power has allowed the loaded weight to be increased by 600 lb., so giving an increase in disposable load of 500 lb. Wing loading 27.0 lb./sq.ft. Loaded weight 17,600 lb. Maximum speed 239 m.p.h. at 6500 ft. Payload 3244 lb. Range in still air 1210 miles at 65 per cent power and 1345 miles at 50 per cent of continuous emergency power. Description, weights, engine ratings, and performance. *Flight*, March 14, 1940, pages 241, 242, 2 illus.

THE NETHERLANDS

Hundred Octane. Comparative figures are presented for performances of the Koolhoven Fk.59 two-seater reconnaissance bomber biplane with the Bristol Mercury XV engine when using 87 and 100 octane fuel, respectively, and for performances of the engine itself on these two fuels. Maximum speeds at 2750 ft. are given as 236 m.p.h. and 260 m.p.h., respectively. Production of 100 octane fuel in the United States is mentioned. *Flight*, February 22, 1940, 2 tables.

An Engineer's Close-Up of the Curtiss-Wright Transport. G. A. Page. An engineer's eye-view of how a few of the salient features of the new 36-passenger Substratosphere Transport were worked out. Safety features have been designed and built into the ship both structurally and aerodynamically, one being the provision against wing-tip stall. The means used has been the gradual alteration in airfoil section from root to tip, coupled with the use of moderate washout of angle of attack. Fuselage, wings, wing flaps, cowling, and power boost controls are covered in a detailed description.

A second article by C. W. France, entitled "Maintenance at a Profit," describes, also in great detail, how the Substratosphere Transport has been designed to keep maintenance costs to a minimum. *Aviation*, March, 1940, pages 46–50, 53–55, 57, 112, 15 illus.

Private and Commercial Aircraft Manufactured under Approved Type Certificates. Outline scale drawings are shown for 62 American basic models of commercial airplanes, and a photograph, specifications, performance, construction, engines, standard equipment, and instruments are given for each. Data are included on variations of several types. *Aero Digest*, March, 1940, pages 62–108 (alternate pages), 134 illus.

Private and Commercial Aircraft without Approved Type Certificates. Outline scale drawings are shown for 23 basic types of American commercial and private aircraft which have not been granted Civil Aeronautics Authority Approved Type Certificates at the time the issue went to press. Some airplanes are experimental, some are restricted, while others, pending completion of tests, are awaiting Government approval. *Aero Digest*, March, 1940, pages 110–124 (alternate pages), 46 illus.

Unveiling the Airacobra. R. J. Woods. Long detailed description by the designer of the airplane. *Aviation*, March, 1940, pages 40–41, 104, 5 illus.

U.S.S.R.

Soviet Airplanes Employed against Finland. The pursuit squadrons appear to be better supplied than the bombardment squadrons which are equipped with the light bomber S.B.2 "Katiouska" derived from the Martin 139 midwing airplane. A few details only are given. Reference is made to foreign airplanes for which the Soviets have acquired licenses. Illustrations shown are from Aircraft Engineering. *Les Ailes*, February 8, 1940, page 4, 5 illus.

Dornier 24 Reconnaissance Flying Boat. A. Frachet. Dornier Do.24, 14-ton, three-engine flying boat is designed for exploration over the high seas, for reconnoitering the route for battleships and commercial ships, and for the refuelling of submarines at sea. It is capable of landing on and taking off from the high seas. It weighs 8400 kg. empty and will carry a load of 5600 kg. of which the 1500 kg. of bombs can be replaced by an equivalent weight of men or material. Armament consists of three stations of fire under transparent cupolas, one at the prow, the second in the center of the hull, and the third in the stern, each being armed either with machine guns or a 20-mm. Oerlikon cannon. Holland has received a license for construction. Some Do.24s designed for the German Navy will be powered by Daimler Benz or Junkers 1200-hp. engines, but performance with these engines is not known. With three 875-hp. B.M.W. 132-Dc engines normal range is 3000 km. Announced maximum speed 350 km./hr. Cruising speed 320 km./hr. Minimum speed 95 km./hr. Climb to 1000 meters 3 min. 5 sec. Short description. *Les Ailes*, January 4, 1940, page 3, 2 illus.

Heinkel 114 Coastal Seaplane. A. Frachet. German coastal reconnaissance units have been equipped since 1938 with Heinkel He.114 two-seater twin-float sesquiplanes for cooperation with the Navy but this has been kept secret. However, the He.114 is not in any way extraordinary and its performances are simply normal. Powered by a B.M.W.-132K engine, the He.114 has a cruising speed of only 248 km./hr., and its ceiling does not exceed 5200 meters. Powered by the B.M.W.-132N engine, it has a maximum sea-level speed of 280 km./hr., and, at 3500 meters, 335 km./hr. Range is 1000 km. at 270 km./hr. The He.114 has two machine guns, one fixed in front and one movable and firing to the rear. Load of munitions carried is 45 kg. Description. *Les Ailes*, February 1, 1940, page 3, 2 illus.

U.S.A.

American Planes and Engines. Annual directory consists of: photographs and three-view drawings with abridged specifications for 30 American military aircraft (domestic and export) and 66 other aircraft; photographs of 12 engines; tables of characteristics and performances for 135 aircraft engines, 132 civil aircraft, and 68 military aircraft; directory of aircraft and aircraft-engine manufacturers and key personnel; and an accessory directory for aircraft, engine and airport accessories, materials, parts and assemblies.

The magazine's "Sketch Book of Design Detail" which is included contains drawings of structures of interesting parts or cutaway drawings of whole airplanes showing structure of the wing and fuselage and location of equipment. *Aviation*, February, 1940, pages 36–98, 209 illus.

Air Transportation

T.A.C.A.—Jungle Air Freighter. R. Hancock. Transportation of freight by the Transportes Aereos Centro Americanos in the Central Americas is described. This airline is said to have hauled more freight than any other single airline in the world. Account of activities, conditions encountered, and kind of freight carried. *Aviation*, January, 1940, pages 30–31, 88, 5 illus.

Trends in Air Transportation. T. P. Wright. Rapid acceleration of air transportation, growth of the airplane in weight, size, and number of engines, and improvement in airplane characteristics, comfort and safety are discussed and illustrated in curves for the period 1924–40. Predictions are made for air transportation's future. Factors causing increases of airplane cruising speeds for the past ten years, and possibilities of improving each factor in the next ten years are listed and discussed. Ten years' advance in aerodynamic cleanness is shown in a table. *Aviation*, March, 1940, pages 36–37, 115, 117, 16 illus., 3 tables.

Gliding

The Case for Gliding. N. H. Sharpe. The case presented rests on the three main claims of assistance to aerodynamical development and research, advanced training for airplane pilots, and elementary training in pilotage and airmanship. It is considered that the whole future existence of gliding, and not only its suspension in Britain during the war, probably depends on the British decision which should be made now about its future. *Aeroplane*, February 16, 1940, page 230.

Propellers

Variable-Pitch Propellers. P. A. Richard. Results of calculations and tests concerning propellers with variable parameters are presented, and forces which are exerted on the blade of a propeller in operation are derived. Different types of propellers with controllable blades are described, including: propellers with automatic or semiautomatic operation to two positions (Hamilton, Ratier with automatic control by compressed air, Levasseur, Ratier with control by wind vanes); automatic propellers with a complete series of variation of pitch; and propellers with mechanical control of the variation of incidence (Ratier with electric control, Curtiss with electric control, and Hele-Shaw with hydraulic control). *L'Aérophile*, December, 1939, pages 267–270, equations.

Miscellaneous

Light Plane Roundup. Forecasts of the immediate future are given by the heads of five of the leading companies manufacturing light airplanes as follows: "1800 Cubs a Record," W. T. Piper; "New Trainer—New Plant," C. Friendlander; "Factory Still Growing," C. G. Taylor; "Winter Production Up," J. H. Torrens; and "Big Six Months," W. A. Mara. *Aviation*, February, 1940, pages 31–33, 7 illus.

Light Seaplane Pointers. K. Baetz. Recommendations regarding taxiing into the wind, downwind, crosswind, turning into the wind, turning downwind, sailing, take-off, and landing. *Western Flying*, March, 1940, pages 14–16, 24, 8 illus.

Acoustics

Application of Piezoelectric Vibration Pick-Ups to Measurement of Acceleration, Velocity and Displacement. B. Baumzweiger. Inertia-type piezoelectric vibration pick-up, and control circuits which produce output potentials corresponding to either of the three characteristics of vibration are described. Instrument plugs into the microphone receptacle of a General Radio type 759-A sound level meter for direct determination of the average level of vibration. Together with a wave analyzer it permits analysis of the great majority of vibration problems encountered in industrial work.

Direct measurement of velocity or displacement of vibration necessitates establishment of a stationary body to serve as a reference frame against which these functions may be determined. Acceleration is measured directly in terms of inertia reaction forces developed in the vibration pick-up. These forces are converted into electrical potentials by means of a piezoelectric crystal, and integrating networks may be used to obtain velocity and displacement of vibration. Calibration procedure is also discussed. *Acoustical Soc. Am., Jour.*, February, 1940, pages 303–307, 5 illus., equations.

Noise and Vibration Isolation. H. A. Leedy. A solution is offered for the problem of reducing the noise and vibration in vibrating machinery by means of reducing the transmission of the machine vibrations to the base on which the machine is mounted. It is shown that the force transmissibility curves are not applicable to determination of vibration reduction where the base cannot be considered as immovable. An equation which is developed and the amplitude transmissibility curves drawn therefrom indicate under what conditions the force transmissibility curve is applicable. For cases in which the mass of the base is comparable to, or less than, the mass of the machine, it is very important that this equation or the curves be used in order to obtain the magnitude of the reduction of transmitted vibrations.

Curves show that it is generally desirable to have the mass of the base as large as possible with respect to the mass of the vibrating machine, since under these conditions the resilient support is more effective in reducing transmitted vibrations. *Acoustical Soc. Am., Jour.*, January, 1940, pages 341–345, 10 illus., 4 equations.

Vibratory Characteristics of Vibrafram. L. B. Ham and H. T. Darracott. Acoustical absorption in the Heerwagon acoustical tiles, or Vibrafram, is definitely associated with the magnitude of vibration of the tile and is thought of as due to internal mechanical friction. Material itself offers but little absorption of sound, but when mounted with an air pocket behind it, the tile becomes a very good absorber of sound over a wide frequency band. Material appears to be of less importance than the shape, form and thickness of the material. Theory, experiments, and results are described. *Acoustical Soc. Am., Jour.*, January, 1940, pages 333–340, 9 illus.

Aircraft Instruments and Navigation

Martin Flight Recorder. Airspeed, altitude, air temperature, manifold pressure, and engine speed for two or four engines are recorded simultaneously in the system developed by Glenn L. Martin Company for the purpose of simplifying flight-test measurements. One instrument, which records airspeed, altitude, and free-air temperature, was made from a standard 0–5 milliampere Esterline-Angus recording milliameter. Manifold pressure and engine r.p.m. of two engines are recorded on a modified Friez Flight Analyzer incorporating four Autosyn motor units, each operating a single pen. Short note. *Aviation*, March, 1940, page 93.

Single Gyroscopic Flight Devices and Their Behavior in Flight. S. Wintergerst. The single gyroscopic devices used today in general flight, with gyroscope supported at the center of gravity, are not independent in their construction of the earth's rotation and motions in flight. Therefore they are often provided with arrangements which compensate for a deviation of the gyroscopes from their desired position at any time. Magnitude of the compensating movement which is the determining factor, and the practical form for such correcting arrangements are described, including: rate of deviation of the gyroscope in regard to rotation of the earth, flight motion and overlapping of both motions, and production of the corrections. *V.D.I.*, January 13, 1940, pages 35–38, 8 illus., 33 equations.

Turn and Bank Installation. R. Snyder. Correct installation of the turn and bank indicator is described. *Aviation*, March, 1940, page 75, 1 illus.

Acceleration-Free Pendulum Having a Degree of Freedom on a Small Circular Path. E. Schmid. Oscillation period of the accleration-free physical pendulums having a degree of freedom, has generally been assumed as 84 minutes, but it is demonstrated that the period has a different value. Stability of the equilibrium positions of these pendulums is investigated when the axis with uniform velocity as tangent of a small circular path is brought into the gravitational field of the earth. Report of the D.V.L. Institute for Instruments and Navigation. *Luftfahrtforschung*, January 20, 1940, pages 32–36, 4 illus., many equations.

Ideal and Real Navigation. W. Immer. Fundamentals of navigation for aviation are surveyed, including: navigation as applied mathematics; navigation based on physical measurements; problem of the technique; the compass as an oscillating system; the gyroscope; artificial horizon as a measuring basis; influence of the medium; level and astronomical navigation; errors of radio direction finding; meteorological navigation; necessity of recognizing errors; accuracy of terrestrial navigation; effect of winds; terrestrial error circle; necessity for other navigating methods; course deflection in radio direction finding; error quadrangle of radio orientation; error of astronomical navigation; causes of level variations; the sun compass; and navigation as requiring far-reaching stabilization. Photograph of the instrument board of the Heinkel He.116 long-distance transport, and drawings illustrating errors of compass, and radio and altitude parallel are included. *Luftwissen*, January, 1940, pages 3–9, 10 illus.

Electrical Equipment

Remarks on the Structural Specifications for Aircraft. E. A. Reussner. Development of German specifications for electrical equipment of aircraft, distributed November, 1939, setup of specifications, and contents are discussed. *Luftwissen*, January, 1940, pages 13–14.

Fire Prevention

Fire and What Is Being Done About It. C. Froesch. The Civil Aeronautics Authority and the Air Transportation Association of America have joined forces to investigate the cause and cure of fires on board aircraft, and an elaborate test rig which is described and illustrated has been set up at the Bureau of Standards. What has been done in this investigation and what the project is designed to accomplish is discussed. *Aviation*, January, 1940, pages 38–39, 92, 2 illus.

Fuel Tanks

Aluminum Aircraft Fuel Tanks. E. H. Dix, Jr., and R. B. Mears, Aluminum Research Laboratories. Characteristics of aluminum alloys used in fuel tanks are considered, including the nonheat-treatable alloys, heat-treatable alloys, and Alclad sheets. Corrosion considerations in regard to tanks are discussed, including: service experience; operating practice; composition of accumulated water in tanks; effect of different types of fuels on composition of the sump water; effect of flux when it is not thoroughly removed after the welding operation; causes and mechanism of corrosion; methods of protection against corrosion; advantages of Alclad sheet; service results obtained in using various alloys and coatings; and means for preventing corrosion caused by water lying in the bottom of the tanks for extended periods. *S.A.E. Preprint for Annual Meeting*, January 15 to 19, 1940, 14 pages, 2 tables.

Miscellaneous Equipment

Outwitting the Wind. J. D. Mountain. By the new addition to the Link Trainer, vital factors of wind direction and velocity may be added to instrument training methods. When the wind simulator which was designed and constructed by Transcontinental and Western Air, is used in connection with the Link Trainer, direction and velocity of the wind may be set once and for all. Then the instrument automatically sets the correct drift and the correct ground speed, no matter what the heading of the Trainer. Wind speeds from zero to 100 m.p.h. may be set on the machine, and direction of the wind may be from any point in the circle, being changeable at will during progress of a problem. Associated with the wind similator is a loop direction finder simulator providing means for accurately simulating the use of the loop direction finder in aircraft navigation. New use for the direction finder is that of determining one's position and heading without recourse to the magnetic heading of the airplane. *Aviation*, March, 1940, pages 34–35, 112, 7 illus.

Testing Apparatus

Precision Optical Apparatus. "Electrolimit" gage for mass production inspection measures by mechanical contact, the readings being electrically magnified and is adjustable for large magnification. Profile projector has a horizontal screen which can be swung in a horizontal plane through an angle of 10° on either side of normal to provide a means of locating the template. An alignment telescope for setting up of assembly jigs of large airplane wings, and lining up of bearings and long shafts, consists of telescope and collimator. Section projector was designed to obtain sections of work which cannot be projected with the normal profile projector, such as an axial section of a screw thread having a large helix angle, a worm wheel, or a helical bevel gear. Description of this equipment being made at the works of Taylor, Taylor and Hobson, Ltd. *Engineer*, January 26, 1940, pages 92–93, 5 illus.

Materials

New Developments in Automotive Materials. Properties of the new air-hardening tool steel, developed by Bethlehem Steel Company to replace steels requiring liquid quenching to develop the characteristics essential in dies, punches, and similar tools, are described in detail. Shorter descriptions are given for the following: Paisley protective compound for stainless steel; Stewart-Warner Alemite rubber lubricant and preservative; Durez 1900 Black easily preformed high-impact phenolic molding material; General Malleable Holcroft furnace which shortens annealing cycle; Allegheny-Ludlum Plurameltt steel-making process; Detroit Macoid extrusion process for molding Eastman cellulose acetate butyrate Tenite II; and Phelps improved copper plastically converted by tremendous pressure in a reducing atmosphere at elevated temperature into smooth dense copper bar, rod, or strip. *Automotive Industries*, March 15, 1940, pages 274–277, 6 illus., 3 tables.

Fuels and Lubricants

Aviation Gasoline Assuming Increasing Importance. H. S. Norman. Gasoline and oil consumed by Government and civil aircraft by years (1932–38 and estimated for 1939), and number of civil airplanes of the United States (scheduled air carriers and private airplanes) for 1929 to 1939 are shown in tables. Present position and future of the aviation gasoline field are discussed. *Oil & Gas Jour.*, March 14, 1940, pages 21–22, 2 illus., 2 tables.

Alkylation as a Source of Safety Fuels. R. Haskell, Texas Co. Sulphuric acid alkylation plant is illustrated and described. Straight reactions and possible cross reactions to obtain safety fuels are explained. Properties of a typical 300°–400°F. cut are shown. Engine tests, quantity available, and cost are discussed. *S.A.E. Preprint for Annual Meeting*, January 15 to 19, 1940, 7 illus.

Safety Fuels by Catalysis. W. M. Holaday. A fuel manufacturer's opinions on the availability and cost of producing partially aromatic safety fuels by catalytic cracking. Method is now available which will provide for the large-scale production of the aromatic-type safety fuel having an octane number above 85. Use of this base fuel with addition of 3 c.c. of tetraethyl lead per gallon makes available fuels having an octane number in excess of 85, and by blending with paraffinic-type safety fuels and tetraethyl lead, higher octane numbers can be obtained. Heat of combustion and engine performance are considered. Inspection tests of a catalytically-cracked safety fuel and composition are shown in a table. *S.A.E. Preprint for Annual Meeting*, January 15 to 19, 1940, 7 pages, 2 tables.

Metals

Hot Pressing of Metal Powders. W. D. Jones. Very good tensile and elongation figures are possible in copper-base alloys manufactured by hot pressing powders in air, and results described justify a much closer and extended attention to the subject. It is necessary to try to ascertain the basic principles of the sintering process involved. Perfect non-porous alloys can be manufactured. Process is very much less sensitive to composition, particle size distribution, or particle shape than the cold-pressing method. Oxide inclusion does not appear to play the same role as it does in eastalloys, and in some cases is not detrimental to tensile strength or elongation.

Over the range of alloys examined, working with mixed powders gives better results than working with powdered alloy. Success of results with simple brasses and bronzes using mixed powders is possibly in a measure due to the fact that the zinc and tin are, for a period at least, molten during the heat treatment which may facilitate in dislodging of oxide films and permit of easier sintering. *Metal Industry*, March 8, 1940, pages 225–228, 1 illus.

Laboratory and Workshop Notes. "Note on the Protection of Thin Metal Films against Oxidation," W. Ehrenberg. "The Deviation Produced by a Biprism," C. M. Focken. *Jour. Scientific Instruments*, February, 1940, pages 41–42.

Iron and Steel

Heat Resisting Steels. W. H. Hatfield. History of the development of heat resisting steels, and some of the types of steels now available and their service characteristics. Scaling and creep of steels with increasing chromium content are given in a table indicating that as the chromium content increases so does the resistance to scaling. A steel containing 30 per cent chromium shows great resistance to scaling at very high temperatures. If chromium content be increased, the actual strength at 1292°F. is not increased. Scaling and creep of a series of heat-resisting alloys used in the industrial world are given in another table. Steel containing about 23 per cent chromium, 12 per cent nickel, and 3 per cent tungsten possesses great strength at high temperatures as well as resistance to scaling. Notes of a recent lecture before the Midland (British) Metallurgical Societies. *Iron Age*, March 14, 1940, pages 35–37, 2 tables.

Progress in Steel Metallurgy during the Last Ten Years. W. H. Hatfield. Application of general science to metallurgical problems, and improvements in materials required for industrial and scientific plants and applications. From "Metallurgia," December, 1939. *Heat Treating and Forging*, February, 1940, pages 78–80.

"18 and 8" and Related Stainless Steels. W. M. Mitchell. Proper heat treatment, thermal properties, endurance limit, fatigue and stress corrosion, and properties at high temperatures are discussed. Continued. *Metals & Alloys*, February, 1940, pages 60–64, 4 illus., 2 tables.

Nonferrous Alloys

Aluminum-Bronze Gravity Die Casting. A. Street. Effect of added elements; mold for gravity die casting; best working temperature for the die; and solidity of aluminum-bronze die castings. Table gives mechanical properties of cast aluminum bronzes. Concluded. *Engineering*, February 23, 1940, pages 190–191.

Corrosion of Aluminum Alloys under Static Stress. G. Forrest. Stress-time curves for the four aluminum alloys under static stress corrosion indicate a steep drop at high stresses and a tendency to approach the horizontal at lower stresses. They do not appear to reach the horizontal up to maximum time tested and further considerable change of direction of curves is observed, *i.e.*, comparison on a short-time (or very high-stress) basis may prove misleading. Progressive reduction of strength with time is not due only to corrosive influence since the effect of prolonged loading in causing failure at stresses lower than the ultimate strength, quite apart from corrosion, must be taken into account. From the appearance of the particular samples under test, none of the materials appeared to be susceptible to intercrystalline corrosion. *Metal Industry*, March 8, 1940, pages 229–230, 1 illus., 3 tables.

Aluminum-Bronze Gravity Die Casting. A. Street. Properties and constitution of aluminum bronze. Tables show corrosion of nonferrous alloys (aluminum bronze, manganese bronze, brass, phosphor bronze, and gun metal) in aerated solutions at 60°F.; effect of quenching on Brinell hardness numbers of aluminum bronze; effect of quenching from various temperatures on tensile strength, elongation, and notched-bar impact strength of aluminum bronze containing 9.77 per cent aluminum; and mechanical properties of aluminum-bronze rod after quenching and tempering. To be continued. *Engineering*, February 16, 1940, pages 159–160, 7 illus., 4 tables.

Failure of Aluminum Subjected to Combined Stresses. J. Marin and R. L. Stanley. Tests on aluminum-alloy tubes subjected to torsion combined with axial tension, and test apparatus used are described. Such a loading condition produces biaxial principal stresses of opposite sign. Various ratios of the principal stresses were considered by varying the ratio of the torsion to axial tension. Failure was in this way determined for various ratios of the principal stresses, and a comparison is made with theories of failure. Material tested was a common unheat-treated aluminum alloy designated between 3S-$^1/_4$H and 3S-H alloy.

Experimental investigation gives further support to recent tests on ductile metals in showing that, for the aluminum alloy tested, the distortion energy theory is a good approximation. Formulas for equivalent proof stresses for the case of biaxial stresses and the case of torsion are developed in the appendices. In the introduction the maximum-stress, maximum-shear, and maximum-distortion theories and their use in design are briefly reviewed, and results of previous experiments in combined stresses are briefly discussed. *Welding Jour., Welding Res. Sup.*, February, 1940, pages 74s–80s, 12 illus., 2 tables, 24 equations.

Testing of Metals

The Bending-Tensile Test, a New Test Method for Metallic Materials. E. Mohr. The simplified bending-tensile test is being used successfully as the material-testing technique for the determination of the uniformity of sheets, strip, and wire. By the nature of the forces attained on the test pieces at the reflection, even the slightest differences in the sheet at load application in different directions can be determined.

Characteristic of the bending-tensile test is that material-test pieces of like dimensions are bent back and forth at a small angle over cylinders under simultaneous application of a static load up to fracture, whereby this force varies from bar to bar, and loads from the very smallest up to breaking loads are selected. Bending tensile diagrams are recorded which give the number of bendings back and forth, causing the fracture, as a function of the corresponding static tension σ. These curves show a turning or sometimes almost a buckling point which is especially distinct when the abscissas are plotted on logarithmic scale. *V.D.I.*, January 27, 1940, pages 49–52, 10 illus., 2 tables.

High-Speed Tension Machine. Templin improved type of precision testing and metal working equipment described is capable of exerting a force of 3,000,000 lb. in compression and 1,000,000 lb. in tension, and can exert maximum compression and tension at speeds up to 36 in./min. In addition to testing, the machine can be used as an extrusion, forging, or forming press, and is provided with auxiliary equipment which will permit defining, within close limits, the relationships existing between the various forces involved in the plastic flow of aluminum throughout a wide range of conditions. Short description of machine installed in research laboratories of the Aluminum Company of America. *Iron Age*, March 7, 1940, page 63, 1 illus.

Industrial Radiography. R. G. Tobey. First issue—Latest advances in equipment for industrial radiography, technique of continuous and planar inspection, types of protection necessary for personnel and photographic materials, and use of a penetrameter to indicate that a suitable exposure technique has been employed are discussed. Metallic shot technique for masking round bars is illustrated.

Second issue—Use of low-voltage radiation, flexible calcium tungstate intensifying screens, and new types of developing solutions are discussed. Industrial stereo-vision is described, and a mirror stereoscope incorporated in the X-ray stereometer is illustrated. *Iron Age*, February 29 and March 7, 1940, pages 27–30 and 64–67, 6 illus.

A New Method of Determining Damping Coefficients. J. Geiger. New apparatus and resonance method for the experimental determination of damping coefficients of materials (in this case cast iron) for high-speed crankshafts under conditions of resonant (constant-amplitude) vibration. The usual method of determining the damping factors of materials is not in accordance with conditions under which damping takes place when a crankshaft is vibrating torsionally at a critical speed, and therefore the author devised the new apparatus in which these conditions are more closely simulated.

Test specimen in the form of a cylindrical torsion bar is rigidly clamped in a bearing at its right end, while at the opposite end it carries an inertia disc and is supported by a ball bearing. Both supports are rigidly mounted on the baseplate. At one end of the inertia disc a shaft is mounted which carries an eccentric inertia mass and is connected to an electric motor through very flexible rubber coupling. When shaft is rotated a rotating centrifugal force is set up which may be resolved into a radial and tangential component.

Apparatus is described in detail and results obtained with cast-iron torsion-bar specimens are discussed. Damping coefficient curves for eight grades of cast iron and two grades of steel are illustrated. From *A.T.Z.*, December 25. *Automotive Industries*, March 1, 1940, pages 252–255, 263, 3 illus., equations.

Notes Regarding Spectrographic and X-Ray Tests of Metals Used in Modern Industrial Welding Practice. W. M. Cohn. Some practical applications of spectrographic and X-ray tests in the plant. *Welding Jour.*, February, 1940, pages 138–141, 5 illus.

Welding

Spot Welding of Light Alloys. Light alloys must be welded with light electrode pressures to obtain regularity and to avoid rapid deterioration of the electrodes. Quantity of heat supplied to the weld must be very carefully controlled and this can only be done satisfactorily with an electronic "interrupter" or by an accurate and efficient storage device. Since charge of storage condenser machines is limited automatically to a given value according to peak voltage of the supply, they are very convenient in operation.

Welding at very high speeds (less than 1/100 sec.) offers no advantage and can give rise to metal projections between the work pieces. Problems of spot welding light alloys considered in a recent publication issued by Philips Industrial (Philips Lamps, Ltd.). *Engineer*, February 23, 1940, pages 189–190, 2 illus.

Strength Behavior of Tube Welds in the Case of Continuous Load. E. Siebel and K. Wellinger. By means of endurance tests with test bars of welded Cr-Mo-steel tubes, it was demonstrated that the curve for resistance to deformation with time in welds which have undergone no annealing treatment is much more unfavorable than in welds with subsequent heat treatment by annealing or tempering. Whereas the last named welded connections fail beyond the welds in welds of tubular material, the fracture in the unannealed test pieces in the case of longer load duration always runs in the welded seam. *V.D.I.*, January 27, 1940, pages 57–59, 15 illus., 2 tables.

Investigation of the Fatigue Strength of Weld Metal and Welded Butt Joints in the As-Welded and Stress-Relieved Conditions. L. B. Durant and J. F. Ennis. Fatigue strength of weld metal deposited by the Unionmelt process in mild steel plate was found to be higher in the as-welded condition than in the stress-relieved condition, the endurance limits being 35,300 psi and 30,700 psi, respectively. Both values are comparable to the endurance limit of the unwelded plate which is probably 30,000 to 32,000 psi. Endurance limit of weld metal in both the as-welded and the stress-relieved conditions was approximately 50 per cent of the tensile strength. Endurance limit of the welded joint was found to be 26,400 psi for both the as-welded and stress-relieved conditions, which is considerably below that of the weld metal itself. Weakest part of the joint was found to be in the base metal at the junction of the grain-refined zone and unaffected base metal. Tests and results are described. *Welding Jour., Welding Res. Sup.*, February, 1940, pages 61s–65s, 12 illus., 2 tables.

Torsional Fatigue Strength of Fillet Welds. A. Thum and A. Erker. Torsional fatigue strength of fillet welds, which is important in the design of welded machinery such as gears and pulleys, was investigated on mild, high-tensile and cast steels. Fracture occurred through the throat of the fillet in all specimens, the crack starting at the root and spreading at 45° through the throat section. Cast-steel welds were inferior. Higher endurance limits for the intermittent fillets, compared with continuous fillets, are surprising, shaft and flange being far more rigid and deformation extremely small. An explanation is furnished for the higher endurance limit, and microstructure of the weld is discussed. Torsion fatigue tests are described and results given. Long abstract from Elektroschweissung, November, 1939. *Welding Jour., Welding Res. Sup.*, February, 1940, pages 71s–73s, 4 illus., 1 table.

Paint

Airplane Dopes. F. W. Reinhart and G. M. Kline. Relation of tautening and weathering qualities to composition. Exposure tests on experimental dopes are described, formulas for which were presented in a previous report, being selected on the basis of effect of plastic, plasticizer, solvent, and diluent components on shrinkage and flexibility of dope films.

Hydroxyl content of cellulose mixed esters is especially critical in determining their suitability for use in airplane dopes. Solvent combinations and plasticizers which yield optimum tautness, resistance to slackening in wet weather, and least variation in tautness during exposure are indicated for various cellulose derivatives. Close correlation is shown to exist between properties of the unsupported films and behavior of doped fabrics. Research undertaken at the Bureau of Standards for the Bureau of Aeronautics. *Industrial and Engineering Chemistry, Ind. Ed.*, February, 1940, pages 185–193, 8 illus., 7 tables.

Plastics

Effect of Petroleum Products on Neoprene Vulcanizates. D. P. Fraser. When immersed in commercial lubricating oils, neoprene vulcanizates reach

equilibria with respect to swelling or volume increase. Time necessary to reach equilibrium depends upon the immersion temperature and the chemical characteristics of the oil. It is shown that the volume increase of a neoprene compound in lubricating oils is a logarithmic function of the viscosity-gravity constants (or a direct function of the gravity indices). Volume increase appears to be independent of the refractive and viscosity indices of the oils. *Industrial and Engineering Chemistry, Ind. Ed.*, March, 1940, pages 320–323, 8 illus., 1 table.

Plastics and Their Uses in the Automotive Industry. G. M. Kline, National Bureau of Standards. Chronological survey of the development of plastics in this country is presented, and special properties which characterized each new material and which, in many instances, were there by design and not by mere chance alone are outlined. Important uses which have been made of these various plastics in the automobile and airplane industries are referred to. Plastics discussed include: cellulose-nitrate, shellac, bitumen, phenolic-molding, laminated phenolic, casein, cellulose-acetate, urea-formaldehyde, cast phenolic, vinyl-resin, styrene, acrylic-resin, cellulose mixed-ester, ethylcellulose, and lignin plastics, and alkyd resins. Compression, injection, transfer, extrusion, and direct hydraulic methods of molding are described. *S.A.E. Preprint for Annual Meeting*, January 15 to 19, 1940, 26 pages.

What Plastic to Use. Data prepared recently by C. W. Blount of Bakelite Corporation to assist engineers in determining which plastic will best suit a particular need. *Iron Age*, March 21, 1940, pages 36–38, 1 table.

Elasticity of Phenolic Compounds. A. F. Shepard and L. A. Sontag. Flexural properties of a phenolic resin compounded with various fillers are given in a table. Curves indicate the effect of variation in moisture content (before molding) of three standard grades of phenolic compound on the flexural strength and transverse deflection. Type of resin used has considerable influence on deflection value. Field experience has shown that certain grades of molding compound with improved elastic properties have remedied a number of obstinate cases of cracking around inserts. *Modern Plastics*, February, 1940, pages 48, 78, 80, 1 illus., 1 table.

Meteorology

Relative Humidity Gradient and the Form of Cloud Bases. C. E. Deppermann. No matter what the temperature gradient, it is shown that the condition for flat cloud bases is a certain definite relative humidity gradient with respect to barometric pressure. If relative humidity gradient is less steep than the critical one for flat cloud bases, there will be a tendency for cloud bases curved convex downward. If relative humidity gradient is more steep than the critical one, then there will be a tendency for cloud bases curved concave downward. Relations presented cover lifting with dry adiabatic lapse rate (equal specific humidity, specific humidity decreasing and relative humidity increasing, with height, relative humidity high and almost constant, specific humidity increasing with height and relative humidity increasing even more rapidly, and relative humidity decreasing with height), and lifting at other than dry adiabatic lapse rates.

A second article by the same author, entitled "Some Interesting Types of Manila Clouds," deals with altocumulus duplicatus, altocumulus polygons, vortices, and mammato.

Résumés of papers presented before the International Union of Geodesy and Geophysics. *Am. Meteorological Soc., Bul.*, February, 1940, pages 43–46.

Engine Design and Research

Britain Favors High-Octane Fuels for Aircraft. F. R. Banks, Associated Ethyl Co., London. British Air Ministry has encouraged development of engines designed to use 100 octane fuel but they are still in the experimental stage. Large American radial engines with two valves in head are more sensitive to differences in fuel characteristics than similar British engines having four valves per cylinder. New developments in spark plugs are described in some detail, especially the use of insulators of sintered aluminum oxide. Use of German "Sinterkorund," is expected to eliminate the troubles of pinholing or puncturing of the mica insulation and excessive lead deposition on the mica insulators which occurs in engines of military aircraft. All the newer British engines use 14-mm. plugs and gas-tightness is a very important requirement. Point erosion and increase in gap width are greatly reduced by the interference suppressor incorporated in the shielding-cable elbow attached to the plug. Electrode materials used are also briefly reviewed.

Advantages of the German system of direct gasoline injection into the engine cylinder are pointed out. An advantage from the military point of view concerns engine behavior when idling in the case of "silent-approach" tactics, where bombers glide from a high altitude without engine in approaching their target. There will be no 'loading" of the distribution system with "wet fuel" and the engine should pick up immediately when opening the throttle again. A high degree of valve overlap has been found beneficial in conjunction with timed injection from points of view of complete scavenging, cooling of exhaust valve, and power increase.

Composition and properties of a number of fuels specially prepared for use in record-breaking liquid-cooled engines of high specific power used in racing aircraft are shown in a table and discussed. Comments are also given on European aircraft engines in regard to number of valves per head. British practice in valve cooling and coating, valve steels, and differential angles for valves and seats. Photographs show two views of the supercharged test engine used in high-octane fuel research at the Ethyl Laboratories in Detroit. *Automotive Industries*, March 15, 1940, pages 268–271, 4 illus., 2 tables.

Ceramic Insulators for Spark Plugs. F. H. Riddle. Materials and properties of the ceramic insulators employed in spark plugs are discussed, including: clays, quartz, feldspar, porcelain, spark-plug porcelain, glaze, processing, properties of insulators, density and refractoriness, mechanical strength, thermal expansion, electrical resistance, thermal conductivity, resistance to thermal shock, and resistance to chemical agencies. Contribution from the Research Laboratories of the Champion Spark Plug Company, Ceramic Division. *S.A.E. Preprint for Annual Meeting*, January 15 to 19, 1940, 15 pages, 5 illus., 5 tables.

Ceramic Spark Plugs Re-enter Aviation. A. L. Beall, Wright Aeronautical Corporation. Undesirable effects of the leakage or separation of washers of the mica "exposure" are pointed out, and the advantages of a ceramic insulator as a substitute for mica are discussed. Two designs of British spark plugs are illustrated which employ a bulky core insulator with a center spindle fired in place. The insulating material is described as an aluminum oxide of the sintered type. No American-made ceramic-insulated spark plug examined by the author has demonstrated performance in endurance tests equal to a British-made plug with a 14-mm. thread. *S.A.E. Preprint for Annual Meeting*, January 15 to 19, 1940, 9 pages, 3 illus.

The Control of Smoke in the Automotive Diesel. W. W. Manville, G. H. Cloud, A. J. Blackwood, W. J. Sweeney, Standard Oil Devel. Co. Methods of rating smoke; effect of equilibrium and dynamic operating conditions; relation of fuel characteristics to smoking (effects of fuel volatility, viscosity, A.P.I. gravity, and engine design and condition); correlation of laboratory and road-test data; and control of smoking as shown in the test results. *S.A.E. Preprint for Annual Meeting*, January 15 to 19, 1940, 27 pages, 14 illus., 2 tables.

Effect of the Viscosity of the Fuel Oil on the Injection Equipment for Oil Engines. G. W. Baierlein, American Bosch Corp. Of the various effects of the viscosity of the fuel on supply and injection system between supply tank and spray nozzle, the filtering system is affected to the greatest extent by the viscosity, all other effects being entirely negligible in comparison. Filtering system is the link in the injection equipment setup which determines the limit of viscosity of the fuel used. Normally this limit lies at approximately 200 Seconds S.U. With this limitation, no difficulties are expected as far as supply pump, injection pump, and nozzle are concerned, the more so since in actual operation on the hot engine, viscosity of the fuel is generally lower.

Effect of viscosity of the fuel handled by the injection equipment on its lapped parts, such as plungers and barrels, delivery valves, and spray nozzles, is negligible as exhaustive endurance tests conducted in the laboratory as well as in the field have definitely demonstrated. There is increased wear when using a 35 Seconds S.U. fuel as compared with that of a 40 Seconds S.U. fuel and there is a still greater wear with a 30 Seconds S.U. fuel. Effects of fine abrasives or solids suspended in the fuel and not held back by the filtering system used by far outweigh the effect of the viscosity itself on the wear of the lapped parts such as plunger and barrel, discharge valve and spray nozzle. Material such as zinc soaps which may be picked up from galvanized fuel tanks, or such small percentages of iron oxide as may be gathered up from rust caused by contamination inside the fuel tank as well as the corrosive agents the fuel may contain have greater effect on wear than viscosity. *S.A.E. Preprint for Annual Meeting*, January 15 to 19, 1940, 18 pages, 10 illus.

German Supercharger Tests. P. F. Martinuzzi. Important tests which were directed to find the most suitable type of impeller are described after a long detailed interpretation of German methods of calculation which differ considerably from those used in England. Use of H_{AD} for pressure head permits a very easy calculation of number of stages required for very high altitude work. All D.V.L. research seems to assume 65,000 ft. as the practical ceiling.

Different types of impellers tested at the D.V.L. are illustrated in drawings and described, including the Junkers closed-box type still used and the completely closed radial web type developed by the D.V.L. Curves show: number of stages required to maintain ground power at altitudes up to 20,000 meters; influence of axial gap between impeller and casing for both star-type and web-type impellers; comparative test results of closed impeller and web-type impeller with different axial gap; and comparative test results on a purely radial impeller, probably of closed D.V.L. type, with and without the auxiliary inlet fan. Stationary air wedges between the boxes of the Junkers impeller are stated to cause losses, and type is also bad from a structural point of view owing to the large central opening. However, it is still used on Junkers engines.

"The D.V.L. closed type impeller is the apple of the D.V.L. eyes, and their only original development of any importance. . . . Great importance is given to the absence of axial thrust, more particularly for multistage blowers, which the Germans are obviously developing as fast as they can. . . . no special effort seems to have been made to study the supercharger needs of the very large engine, all work being apparently done on blowers suitable for engines of about 1000 hp. The largest supercharger mentioned in the German publications is not a D.V.L. development, but a type that the Bramo people were trying to develop; even then the flow was only about 3 lb./sec."

Discussion of a series of tests on auxiliary inlet fans is started in this issue. Americans are said to have written excellent papers but generally give only the results. The Germans give also comparative data of highest interest. To be continued. *Flight, Aircraft Engr. Sup.*, February 29, 1940, pages 5–8, 6 illus., equations.

High Output Aircraft Engines. E. W. Hives and F. L. Smith, Rolls Royce, Ltd. Aspects of the problem of increasing performance of the power plant, both by increasing propeller output and reducing installation losses. Limitations to engine performance are discussed in regard to detonation, effects of supercharger efficiency and intercooling on engine output, and introduction of water into the charge. Few of the mechanical problems which are limiting performance, and the way in which they are being tackled at Rolls Royce are described including bearings, exhaust valves and sleeve valves, failures due to cyclical temperature variations in the engine, and thermostatic control of coolant temperature.

Installation development for increased performance is considered which includes pressure cooling of engines and ejector-type exhaust manifolds, with reference to the ejector-type exhaust system patented by Rolls Royce. In the latter exhaust gases are discharged rearwards at high velocity through restricted outlets. Their kinetic energy is utilized to give a propulsive effect which actually adds to the airplane's speed. Advantages of the interchangeability scheme from a national and aircraft constructor's point of view are also discussed. Arrangement of streamline exhaust manifold is illustrated in a drawing. Discussions by F. R. Banks, F. Nixon, J. M. Lessels, and S. D. Heron included *S.A.E. Jour.* (*Trans.*), March, 1940, pages 106–118, 18 illus., 2 tables.

The Kadenacy Engine. Simplicity of the Kadenacy system is proved by the fact that it can be employed on the majority of existing designs without the necessity for basic alterations. A number of such conversions have been made in the Slough research laboratories of Messrs. Armstrong Whitworth Securities Company, with striking results, but best results have been secured with engines designed "ab initio" to operate on the system.

A single-cylinder prototype, recently built and tested, is described in detail and illustrated. This engine was designed for general industrial purposes. Brake m.e.p. compared with that of four-stroke engines is considered remarkable. Two six-cylinder engines of the two-cycle type and operating on the Kadenacy system which have been built by this Armstrong company are also described and illustrated. *Engineering*, February 23, 1940, pages 195–197, 18 illus. (7 on suppl. plate), 2 tables.

A New Dynamic Vibration Damper for Crankshafts. H. Bosse. New type of dynamic vibration damper for crankshafts and a new method of calibrating the damper (or tuning it to the crankshaft assembly for which it is intended) are described. Damper is of dynamic type and in the critical speed range vibrates at the same frequency as the end of the crankshaft upon which it is mounted. It consists of a metal hub to which is vulcanized an annulus of rubber forming a web, and to the latter is vulcanized a sort of flywheel rim or tuning ring of leaded rubber (rubber having a large proportion of litharge incorporated in it, which has a specific gravity of approximately five). Tuning ring may be made of ordinary rubber and have steel wire screen incorporated in it. New calibrating or tuning apparatus con-

sists of a frame with bearings supporting a shaft on which the dynamic damper is mounted. Shaft and damper are not rotated but merely oscillated around their axis by means of a mechanism. From A.T.Z., August 10, 1939. *Automotive Industries*, March 15, 1940, page 289, 2 illus.

Observations on the Cranking of Diesel Engines. L. E. Lighton and H. C. Riggs, Electric Storage Battery Co. Problems of supplying adequate storage batteries for starting high-speed Diesel engines under a wide range of temperature and operating conditions are discussed including engine, starting-motor, and storage-battery problems. *S.A.E. Preprint for Annual Meeting*, January 15 to 19, 1940, 24 pages, 14 illus.

An Oil Engine Research Laboratory. A two-cylinder 125-b.hp. Petters supercavenge engine, opposed-piston Junkers-type engine, six-cylinder Armstrong-Kadenacy 120-b.hp. engine, Burmeister and Wain auxiliary 120-b.hp. engine, and a single-cylinder Armstrong-Kadenacy 5-b.hp. engine are described. Special research for further development of the original work of M. M. Kadenacy on exhausting and recharging processes of internal-combustion engines, particularly those operating on the two-stroke principle, undertaken in the Armstrong-Whitworth Securities Laboratories, is discussed. Kadenacy principle is based on the phenomenon that immediately on opening rapidly the exhaust ports of a two-stroke engine, at the end of the expansion stroke, there is within the first interval of a few thousandths of a second an urge or impulse in the body of gases to escape as a whole very rapidly from the cylinder. Resistance offered to the outgoing mass of burnt gases is reduced to a minimum, and mass of gas is kept moving in an outward direction a sufficiently long time in order to enable the cylinder to be recharged with incoming air. *Engineering*, March 8, 1940, pages 235–236, 3 illus.

The Performance of Modern Aircraft Diesels. P. H. Wilkinson. Development of aircraft Diesel engines in various countries is outlined, and characteristics and performances of aircraft Diesels are compared with those of gasoline aircraft engines as follows: the Guiberson A-1020 (S), Pratt and Whitney Wasp S3H1, N.A.C.A. development, and Wright Whirlwind R-975-E3 medium-powered air-cooled engines; B.M.W.-Lanova development, Twin Wasp SC3-G, Wright Cyclone 102A, and Twin Wasp S1C3-G high-powered air-cooled engines; and Junkers Jumo 207, Allison V 1710 C6, Roll -Royce Merlin X, and Hispano-Suiza 12-Y high-performance liquid-cooled engines.

Advantages of the aircraft Diesel are pointed out. Tables show comparison between exhaust-gas temperature and exhaust-manifold temperatures of Diesel and gasoline aircraft engines, and between spontaneous ignition temperatures of Diesel fuel, gasoline, and lubricating oil of aviation grade. Specific fuel operating costs of a Diesel and gasoline aircraft engines, based on specific fuel costs and specific fuel consumptions in civil aviation, are also compared. Table also shows mileage and hours flown with Junkers Jumo 204 and 205 Diesel aircraft engines on regular scheduled flights of civil aircraft from 1931 to 1938. *S.A.E. Preprint for Annual Meeting*, January 15 to 19, 1940, 15 pages, 4 illus., 6 tables.

Processes in Injection Systems of Oil Engines. S. F. Davies and E. Giffen. General conditions affecting injection systems, analytical treatment of simple systems, experimental results with open nozzles, general conditions regarding spring-loaded nozzle valves, general mathematical treatment of fuel injection systems, and experimental work on systems with spring-loaded nozzle valves are discussed.

Concerning the injection systems of the common type consisting of pump, delivery valve, pipe, and spring-loaded nozzle valve: order of residual pressure prevailing in the pipe between injections relatively to the nozzle-valve opening pressure is of vital importance; opening and closing pressures are generally in proportion to effective area of the open nozzle valve and area exposed to oil pressure when valve is closed; action of volumes of oil in the pump and at the nozzle, in addition to that in the pipe is to modify considerably the pressure diagram calculated from simple reflections in the piping; injection lag may consist of three periods (passage of disturbance along the pipe, building up of pressure at the nozzle, and opening of the valve); leakage from the system causes a fall of residual pressure between injections thus affecting nozzle lag; increase of pump speed increases injection angle, increases maximum nozzle pressures, modifies total injection lag, increases valve lift, and gives a sharper cut-off; rough running caused by alternating injection characteristics is common and pump and injection setting for normal running should avoid such instability. *S.A.E. Jour.* (*Trans.*), March, 1940, pages 119–136, 25 illus., equations.

Recent Opinions on Varnish in Engines. F. F. Kishline. Compilation of information and experiences as submitted as a result of questionnaire sent out by the Passenger Car Committee to various manufacturers. *S.A.E. Preprint for Annual Meeting*, January 15 to 19, 1940, 23 pages.

The Shortcomings of Mica as an Insulating Material in Aviation Spark Plugs. V. Cronstedt, Pratt & Whitney Aircraft Division. Difficulties leading to abandonment of porcelain spark plugs and adoption of mica plugs, difficulties encountered with the latter, various design features of an up-to-date mica spark plug, and sources of failure are discussed. With proper substitution of an insulating material more suited to the operating condition than the present one, which is the only shortcoming of the present plug in present engines, one may look forward to a situation where the plug is left in a cylinder between overhauls. *S.A.E. Preprint for Annual Meeting*, January 15 to 19, 1940, 7 pages, 1 illus.

Supercharging High Speed, Four Cycle Diesel Engines. R. P. Ramsey, National Supply Co. Development of high-speed four-cycle Diesel engines which has been directly supervised by the author during the past six years is discussed. Engine developed as a result of tests on a vane-type blower built in England, as well as a four-cylinder engine with a Roots-type supercharger and an aircooler between supercharger and engine are described. Bore and stroke were $4^1/_2 \times 5^3/_4$ in., r.p.m. 2400, hp. rating 160. From the author's experience, it seems likely that 200 lb. b.m.e.p. four cycle may ultimately be obtained in a commercial engine. The aircraft situation is said to present different governing factors than the commercial industrial marine or automotive engine with which the article is concerned, but many things can be learned from aircraft technique in engine structures, which may be applicable to the heavier design class. *S.A.E. Preprint for Annual Meeting*, January 15 to 19, 1940, 34 pages.

The Use of Journal Bearing Friction and Temperature Data in Establishing Criteria for Safe Operation. S. A. McKee, National Bureau of Standards. Method is suggested for the application of friction and heat-dissipation data to the determination of the load-carrying capacity of a journal bearing when operating with a lubricant of known characteristics. Method may be used to estimate the effects upon the operating characteristics of the bearing of changes in a number of the various factors involved, and also provides a means for correlation of data in bearing installations where conditions are such that factors affecting bearing operation cannot readily be determined. Two fundamental concepts upon which the method is based are the establishment of a minimum safe limit for the generalized operating variable ZN/P (product of lubricant viscosity and speed of the journal divided by load per unit projected area) and a maximum safe limit for the operating temperature. Data available at the present time will provide only an approximate measure of bearing capacity.

Discussion covers: equation for thermal equilibrium; method for determination of load-carrying capacity; operating characteristics in the stable region; effect of viscosity characteristics of the oil used; effects of changes in critical ZN/P value; effects of changes in ambient temperature; effects of changes in heat-dissipation characteristics; comparison with pressure-speed (PV) relation; and application of method to automotive engine bearings. *S.A.E. Preprint for Annual Meeting*, January 15 to 19, 1940, 19 pages, 11 illus., 1 table, 10 equations.

The Wear of Crankshafts with "Lead-Bronze" Bearings. C. G. Williams and H. Ludicke. Relative wearing properties of various crankshaft materials when running against a typical copper-lead alloy, at a bearing temperature of 212°F. were determined in the tests described. Tests were carried out with nickel-chrome-steel crankpins and results suggested that variations in composition of the copper-lead bearings do not have a marked effect on the wear obtained. Plain carbon and alloy steels, three cast materials, and chromium-plated and case-hardened crankpins were tested. *S.A.E. Jour.* (*Trans.*), March, 1940, pages 93–99, 20 illus., 3 tables.

What's Ahead in Light Plane Engines. C. T. Doman, Aircooled Motors Corp. Those features of light aircraft engines which have been taken from the high-powered aircraft engines have invariably resulted in a much higher frequency of service complaints, but where features tried and proved in automotive practice have been adopted, service complaints have been reduced to a minimum.

Objectionable features of modern light airplane engines, and possibilities of correcting them are considered, including: hand cranking; excessive piston slap; valve, gear, and exhaust noises; carburetors; and provision of a larger number of cylinders of smaller displacement for smoother running. Practices which have been found most satisfactory in building Franklin air-cooled engines for aircraft are discussed. Specification "for aircraft use" is, with few exceptions, merely an excuse for a higher cost price. Practice in cylinders, valves, valve seats and guides, spark plugs, spring locks to hold piston pins, magnetos, bearings, and testing of engines are dealt with. *Aero Digest*, March, 1940, pages 49–51, 260, 5 illus.

Combustion. L. Mantell. Critical survey of certain current concepts of combustion including optimum exhaust-valve area, and exact nature of flame-controlling factors and entity of the agency which automatically correlated inflammatory speed to r.p.m. It is not suggested that turbulence is non-actinic on flame movements, but rather that its effects thereon are different from those commonly attributed to it. Further research is called for to define more exactly the nature of the agency which synchronizes the general rate of flame spread with engine r.p.m. Definite identification is of prime importance in that it will serve to determine more definitely the most promising direction to follow in head design. Suggestions are made for design of cylinder heads and the Vauxhall "controlled flame" combustion chamber and Aspin cylinder head are shown in drawings. *Automobile Engineer*, February, 1940, pages 41–43, 6 illus.

Fatigue Cracks. A. Thum and E. Bruder. Results of investigation which demonstrated that ball bearings undoubtedly reduce the fatigue strength of a plain shaft. A form of shaft is suggested and illustrated in which all edge pressure is avoided by means of a groove 0.1 mm. deep with a fillet radius as large as possible. In regard to high surface pressures, bearings with an increased width of inner ring are recommended. Another series of tests were carried out in which the fillet or groove was cold worked by means of a roller. By applying a pressure of 515 kg. (say 1130 lb.) the fatigue strength of the VCN-15 material (nickel-chrome steel) could be increased about 69 per cent, or to a strength nearly equaling that of the unloaded material. Short abstract from "Dauerbruchgefahr an Hohlkehlen von Wellen und Achsen und ihre Verminderung," Deutsche Kraftfahrtforschung, Heft 11, 1938. *Automobile Engineer*, February, 1940, page 64, 2 illus.

The Prospects of C. I. Engines. A. W. Morley. Criticism from L. Keuleyan, a French engineer, in regard to an article in the October issue by the above author and dealing with prospects of the compression-ignition engine. Performance improvements attained by the Junkers two-cycle compression-ignition engines are shown in a table of characteristics and performances for the Jumo 204, 205-C, E, F, 206 of 1937, and the 2000-hp. four-crank Jumo of 1938, and these improvements are analyzed.

The French correspondent advocates the two-stroke cycle as being the type which can compete favorably with the modern gasoline aircraft engine. He points out that Morley seems to ignore all the tests carried out in England and the United States, and the remarkable practical results obtained in Germany, and he reviews the results of these tests. *Aircraft Engineering*, February, 1940, pages 43, 48, 1 table.

Some Factors Controlling the Development of Electrical Ignition of Aero Engines. G. E. Bairsto. Difficulties encountered in designing ignition equipment for use on aero engines. Conditions in which ignition has to operate; effect of electrical leakage on performance of a magneto; effect of reduced available space for installation of magnetos; effect of air temperature and reduced density in which system has to operate; standard density test for R.A.F. magnetos; coil ignition systems; development of specialized coil systems; self-regulating generator; interference suppressors; other types of ignition systems; spark plugs; erosion of spark plug electrodes; effect of electrode material; effect of variation of initial plug size; effect of capacity of cables and nature of spark discharge; effect of distributed nature of capacity; use of series resistance; comparative tests of erosion with magnetos and coil systems; effect of electrode shape and material on erosion; bonding and screening; braided and harness high-tension cables for high temperature conditions (effects of heat, oil, gasoline, ozone, and alternative materials to rubber); molded insulation for high-temperature use. Test data quoted were obtained on the Rolls-Royce Kestrel X engine. *Royal Aeronautical Soc., Jour.*, February, 1940, pages 119–162 and (disc.) 162–175, 41 illus., 7 tables, equations.

Engine Manufacture

Modern Precision Grinding Methods. R. Brulé. Finishing operations carried out in the production of aircraft engines in the Hispano Suiza plant are described, including: truing up a grinding wheel; method of attack of a grinding wheel; external grinding between centers and on centerless grinding machines; principle of the centerless machines; driving wheels; methods of supporting the work for grinding in series, plunge-cut grinding, end grinding, grinding by shaped grinding wheels, and internal grinding; plane or surface grinding; thread cutting and the forming of threads by grinding; and machining of elastic cylinder joints. Long detailed description. *Aircraft Engineering*, February, 1940, pages 49–55, 29 illus.

Engine, Fuel and Lubricant Testing

Fuel Distribution in Multicylinder Engines and its Effect on Knocking and Performance. H. J. Gibson and C. Walcutt, Ethyl Gasoline Corp. Difference between the air-fuel ratios of individual cylinders during full-throttle acceleration may be quite large, depending on conditions of engine operation. Mixture heating reduces the spread between individual cylinder air-fuel ratios under accelerating conditions and causes all individual cylinder air-fuel ratios to become richer at low speeds. During the beginning of full-throttle acceleration from a low speed the average of the fuel-air mixtures in the cylinders is leaner than that at the carburetor, becomes richer than the carburetor mixture as the speed increases and finally becomes equal to it. Mixture heating reduces the speed during acceleration at which the average of the fuel-air mixtures in the cylinders become richer than the carburetor mixture and reduces somewhat the extremes of leanness and richness. Mixture heating had no effect on low speed acceleration ability but substantially reduced car performance at high speed. At low speed and with the standard manifold, C.F.R. fuel No. 5, having its antiknock value concentrated in the lighter fractions, was between 5 and 6 octane numbers better than C.F.R. fuel No. 6, having its antiknock value concentrated in the heavier fractions, whereas at the higher speeds fuel No. 6 was better.

Intake manifold having one-third the cross-sectional area of the standard manifold, fitted with the standard carburetor and heat box, gave, at the speed of maximum knock, substantially the same fuel-air mixtures in all cylinders supplied by a common manifold and average cylinder fuel-air mixtures closely approaching the carburetor mixtures, increased the knocking tendency of all fuels, reversed the ratings of C.F.R. fuels Nos. 5 and 6 at the speed of maximum knock, improved low-speed acceleration and reduced high-speed acceleration. Results of research. *S.A.E. Preprint for Annual Meeting*, January 15 to 19, 1940, 12 pages, 6 illus.

Investigation of Detonating Noise in Gasoline Engines with Electro-Acoustic Measuring Devices. A. W. Schmidt. Octane numbers of three different fuels are compared which were determined by the C.F.R. method in the single-cylinder gasoline engine, by road test, and by the electro-acoustic method with different fuel jets. Higher octane numbers were obtained with the electro-acoustic method in each case. Oscillograms of noise of a six-cylinder engine with various fuel jets and operating at 1240 r.p.m. with preignition at 25° before T.D.C. are illustrated. Test results are discussed. *V.D.I.*, January 27, 1940, page 48, 1 illus., 1 table.

Road and Laboratory Fuel Testing. "C.F.R. Motor Survey Report, 1939," D. B. Brooks, National Bureau of Standards. "Description of a Road Test Knockmeter," A. E. Traver and C. E. Habermann, Socony-Vacuum Oil Company. "Engine and Fuel Variables," (a study of behavior of four C.F.R. road-test gasolines when operating a current model six-cylinder engine) W. E. Drinkard, Chrysler Corporation. "The Effect of Milage or Car Use on the Road Anti-Knock Value of Different Fuels, 1939 C.F.R. Road Tests," T. H. Risk, Pure Oil Company. "The Effect of Volatility on Correlation of Road and Laboratory Ratings," A. E. Becker and G. H. B. Davis, Standard Oil Development Company. "Progressive Change of Octane Number Requirements with Milage," C. S. Bruce, National Bureau of Standards. "The Effect of Variations of Air-Fuel Ratio on Octane Number Ratings Obtained on 1939 C.F.R. Road Test Fuels," H. M. Trimble, K. C. Bottenberg, and L. A. McReynolds. *S.A.E. Preprints for Annual Meeting*, January 15 to 19, 1940, many pages, illus. and tables.

Testing Equipment Feeds Progress of Hayes Industries in Development of New Automotive Parts. Testing equipment used in research on fans and mufflers for automobiles. A sound-insulated test chamber contains a wind tunnel for fan tests and a dynamometer. Muffler laboratory contains a chassis dynamometer. *Automotive Industries*, March 15, 1940, pages 272–273, 306, 2 illus.

Aircraft Industries Modernize Testing Facilities. M. F. Behar. Wright Aeronautical control station for engine test stand used in production-engine testing, and equipment used to determine fuel metering characteristics of a carburetor under any set of conditions of air pressure and flow; United Aircraft control stand; and Glenn L. Martin special multipen recorders for flight testing. Photographs and brief explanations only. *Instruments*, February, 1940, pages 50–51, 7 illus.

Free Discharge of Fluids through Small Circular Orifices. H. L. Roy and N. K. Sen-Gupta. Study of the rate of flow with fluids widely varying in their physical properties (water, vacuum oil, D. T. E. heavy medium, Vactra oil heavy X, castor oil, and super cylinder oil 600 W). Curves show coefficients for sharp-edged orifices with free discharge, and data are given in tables. *Industrial and Engineering Chemistry, Ind. Ed.*, February, 1940, pages 288–290, 2 illus., 5 tables.

Knocking Characteristics of Individual Hydrocarbons as an Aid in the Interpretation of the Behavior of Gasolines in Engines. J. M. Campbell, General Motors Research Laboratories. Characteristic types of behavior of individual hydrocarbons, which are given in the experimental data discussed, show why it is difficult, if not impossible, by present methods of attack, to assign a definite antiknock rating to a given fuel which will be valid in different engines under different conditions of operation. Data indicate that pure hydrocarbons are represented by a wide range of critical compression ratios, and that relative knocking tendencies of pure hydrocarbons are enormously affected by changes in engine conditions. Different fuels show a widely different degree of response to changes in engine speed and operating temperature. At low speed and at low operating temperatures, di-isobutylene could be burned without knock at a compression ratio 3.8 units above that at which iso-octane began to knock. Di-isobutylene knocked more when the speed was increased; iso-octane knocked less. In the design of engines for high-octane fuels these characteristics will have to be taken into account. Behavior of pure hydrocarbons is compared with that of gasoline.

Data obtained during development of a procedure for use in conjunction with a project for hydrocarbon research under sponsorship of the American Petroleum Institute. *S.A.E. Preprint for Annual Meeting*, January 15 to 19, 1940, 7 pages, 1 illus., 1 table.

On the Geometry of Optical Indicators. K. J. DeJuhasz. Representative types of optical indicators are critically examined with drawings of each, including the mirror galvanometer, and optical engine indicators of the N.A.C.A., Burstall, Midgley, Hopkinson, Société Genevoise, and DeJuhasz.

Major part of the article deals with the principles of optical indication and covers: advantages of the optical lever as a magnifying and recording element; classification of optical indicators; the optical lever; kinematic considerations; optical levers with one degree of freedom of rotation; application of theorem of the transposed cone to particular cases; effects of deviations from the assumed conditions; non-spherical screens; convergent light beam; and mirror support with beam of uniform cross-section and for beam of uniform strength. *Franklin Inst., Jour.*, January, 1940, pages 53–80, 21 illus., many equations.

Sensitive Paints. F. Penzig. Use of thermocolor paints in the visual examination of temperature fields, especially on air-cooled aircraft-engine cylinders is discussed, including: requirements to be fulfilled by the paint indicator; non-reverting thermocolors which have proved to be of practical use; paints with several critical temperatures; accuracy of the critical change; application of paints; effect of paint on heat transfer to the air; care to be taken that indications of cooler regions on an air-cooled cylinder are not falsified by subsequent heat conduction from the hot zones; tests of a B.M.W.132 cylinder suitably cowled; results obtained in the cases of no guide vanes for airflow, rectangular guide with small exit at the rear, and the latter except that constant clearance is maintained at the rear; piston-temperature measurement; commercial application; and uses of the paint in other than engine fields for indicating dangerous temperature conditions. British Air Ministry translation from V.D.I., Vol. 83, No. 3. *Automobile Engineer*, February, 1940, pages 47–49, 8 illus.

The Theory and Application of Extended Surface Thermocouples. H. Emmons. In the extended-surface thermocouple, one of the junctions is so extensive that appreciable temperature differences occur between various parts of that surface. Theories of the response of rectangular thermocouple junctions (both short-wide and long-narrow), and of response of other junction shapes and varying sections are presented by means of equations.

It is concluded that for long narrow thermocouple junctions only the portion of the junction included between the wires to the cold junction and potentiometer have any effect on indicated temperature. If lead wires are attached opposite each other on the junction, only junction temperature at that point is read. Temperature at discontinuities of resistance have special weighting depending upon magnitude of resistance change. For junctions of uniform resistance, a weighted average of temperatures at the points of attachment of the lead wires is recorded. A junction can be designed to read any desired weighted average of temperature along the junction. Experimental verifications are described. *Franklin Inst., Jour.*, January, 1940, pages 29–52, 17 illus., 1 table, 50 equations.

Engines

American Aircraft Engines. Cylinder data, ratings, type of propeller drive, weight, type of carburetor, ignition system, starting, installation dimensions, height above engine bed, and diameter of mounting ring are given for the following aircraft engines: one Akron-Funk, one Allison, seven Continental, five Franklin, 12 Jacobs, six Kinner, one Lambert, four Lenape, 20 Lycoming, six Menasco (including the Unitwin), 18 Pratt-Whitney, seven Ranger, one Rover, one Sky, four Warner, and 22 Wright engines. *Automotive Industries*, March 1, 1940, pages 216–217, 1 table.

Aircraft Engines Manufactured under Approved Type Certificates. Photograph, specifications, construction, and accessories are given for 57 basic types of American aircraft engines which are currently in production and available for private, military, or commercial aircraft.

A second article presents similar data for 13 basic types of American aircraft engines which had not yet been awarded an Approved Type Certificate. *Aero Digest*, March, 1940, pages 176–212 (alternate pages), 70 illus.

Aircraft Radio

The Impetus which Aviation Has Given to the Application of Ultra-High Frequencies. W. E. Jackson. Ultra-high-frequency radio range, a short-wave counterpart of the conventional long-wave radio range which now provides directional guidance along the Federal Airways, is described. Direct comparison is made between the two by means of graphs based on signal recordings made during flight tests of a standard long-wave range and an ultra-high-frequency range operating under the same conditions and at the same location near Pittsburgh, Pa. Advantages over low frequencies are shown. *Inst. Radio Engrs., Proc.*, February, 1940, pages 49–51, 8 illus.

A Simplified Approach to Frequency Modulation. H. W. Roberts. Engineering advantages of frequency modulation and its possible application to aircraft radio navigation and communication are considered. Such conclusions as to its immediate import in aeronautics as may appear warranted at this time are indicated. Adaptation of frequency modulation equipment to aeronautical needs presents some interesting possibilities especially in radio-range navigation, if suitable frequency modulation ranges could be devised. Problems of generating frequency-modulation radio-range signals are reviewed and a novel omni-directional frequency-modulation beacon proposed by E. N. Dingley, Jr., U.S. Navy, in the January issue of "Communications" is described. The most promising field in aircraft radio where frequency modulation might be used with minimum delay for experimental work is considered to be that of aircraft communications. *Aero Digest*, March, 1940, pages 52, 54, 2 illus.

Free Space Propagation Measurements at 75 Megacycles. G. L. Haller, Wright Field. In the study of radiation characteristics of aircraft antennas in which the principle of similitude is being used with scale models, one of the major problems was devising a system of free space propagation measurements in order to eliminate the error caused by the proximity to ground. Original work was done at a frequency of 75 megacycles and at a height of approximately one-half wavelength (2 meters), and serious errors were noted. Preliminary study and some of the results obtained with a tower system, which was built to make free space measurements with little error due to ground effect, are discussed, including calculation of errors due to ground reflection, measuring equipment and tower, and propagation measurements.

Recorded values for both horizontal and vertical polarization taken on the tower follow very closely the theoretical free-space curve. Error is greater than that predicted by calculation of ground reflection errors and can probably be charged to the tower structure itself, but it is well within the limits of experimental error in this type of measurements. *Franklin Inst., Jour.*, February, 1940, pages 165–180, 13 illus., 20 equations.

Television in the Air. C. G. Grey. Experiments in the use of television by the Fleet Air Arm, presumably carried on for some time, have not been successful, even if they have not been complete failures, according to Lord Chatfield. The television apparatus could not be got into an airplane. Mr. Grey's comments on a newspaper account of the work of Lee DeForest, and on R. Denny's gasoline-powered models controlled by radio. *Aeroplane*, February 9, 1940, page 163.

U.H.F. W. E. Jackson. Brief history and general description of the development and progress of the application of ultra-short waves in air navigation in the United States, including: four-course radio range; two-course radio range with station and sector identification; zone marker; and fan marker. To be concluded. Paper prepared for presentation before the Lilienthal Gesellschaft meeting at Vienna in October, 1939. *Aviation*, January, 1940, pages 42–43, 94, 96, 7 illus.